7-15-2008

Bioanalytical Applications of Intramolecular H-Complexes of Near Infrared Bis(Heptamethine Cyanine) Dyes

Junseok Kim

BIOANALYTICAL APPLICATIONS OF INTRAMOLECULAR H-COMPLEXES OF NEAR INFRARED BIS(HEPTAMETHINE CYANINE) DYES

by

Jun Seok Kim

Under the Direction of Gabor Patonay, Ph.D.

ABSTRACT

This dissertation describes the advantages and feasibility of newly synthesized near-infrared (NIR) bis-heptamethine cyanine (BHmC) dyes for non-covalent labeling schemes. The NIR BHmCs were synthesized for biomolecule assay. The advantages of NIR BHmCs for biomolecule labeling and the instrumental advantages of the near-infrared region are also demonstrated.

Chapter 1 introduces the theory and applications of dye chemistry. For bioanalysis, this chapter presents covalent and non-covalent labeling. The covalent labeling depends on the functionality of amino acids and the non-covalent labeling relies on the binding site of a protein. Due to the complicated binding process in non-covalent labeling, this chapter also discusses the binding equilibria in spectroscopic and chromatographic analyses. Chapter 2 and 3 evaluate the novel BHmCs for non-covalent labeling with human serum albumin (HSA) and report the influence of micro-environment on BHmCs. The interesting character

of BHmCs in aqueous solutions is that the dyes exhibit non- or low-fluorescence compared to their monomer counterpart, RK780. It is due to their H-type closed clam-shell form in the solutions. The addition of HSA or organic solvents opens up the clam-shell form and enhances fluorescence. The binding equilibria are also examed. Chapter 4 provides a brief introduction that summaries the use of capillary electrophoresis (CE), and offers a detailed instrumentation that discusses the importance and advantage of a detector in NIR region for CE separation. Chapter 5 focuses on the use of NIR cyanine dyes with capillary electrcophoresis with near-infrared laser induce fluorescence (CE-NIR-LIF) detection. The NIR dyes with different functional groups show that RK780 is a suitable NIR dye for HSA labeling. The use of BHmCs with CE-NIR-LIF reduces signal noises that are commonly caused by the interaction between NIR cyanine dyes and negatively charged capillary wall. In addition, bovine carbonic anhydrase II (BCA II) is applied to study the influence of hydrophobicity on non-covalent labeling. Finally, chapter 6 presents the conformational dependency of BHmCs on the mobility in capillary and evaluates the further possibility of BHmCs for small molecule detection. Acridine orange (AO) is used as a sample and it breaks up the aggregate and enhances fluorescence. The inserted AO into BHmC changes the mobility in capillary, owing to the conformational changes by AO.

INDEX WORDS: Near-infrared (NIR), Bis-heptamethine Cyanine (BHmC), Non-covalent Labeling, Covalent Labeling, Binding Equilibria, Human Serum Albumin (HSA), Clam-shell Form, Capillary Electrophoresis (CE), Laser Induce Fluorescence (LIF), Bovine Carbonic Anhydrase II (BCA II), Acridine Orange (AO).

BIOANALYTICAL APPLICATIONS OF INTRAMOLECULAR H-COMPLEXES OF NEAR INFRARED BIS(HEPTAMETHINE CYANINE) DYES

by

Jun Seok Kim

A Dissertation Submitted in Partial Fulfillment of the Requirements for the Degree of

Doctor of Philosophy
in the College of Arts and Sciences
Georgia State University

2008

BIOANALYTICAL APPLICATIONS OF INTRAMOLECULAR H-COMPLEXES OF NEAR INFRARED BIS(HEPTAMETHINE CYANINE) DYES

by

Jun Seok Kim

Committee Chair: Dr. Gabor Patonay

Committtee: Dr. Stuart Allison
Dr. Gangli Wang

Electronic Version Approved:

Office of Graduate Studies
College of Arts and Sciences
Georgia State University
August 2008

Dedicated to my parents and my family

Acknowledgements

I would like to thank the following people who encouraged me to fulfill my dream as a chemist. Without their support, the completion of my degree would not have been possible.

I would like to express my gratitude to my research advisor, Dr. Gabor Patonay, who has taught me how to apply fluorescent spectroscopy to bioanalytical chemistry. He has been my advisor as well as my mentor for past 5 years. His advice, motivation and encouragement have given me the strength to pursue and complete my Ph.D degree. It has been my honor to be his student. I will never forget his guidance and support. I would also like to thank Dr. Lucjan Strekowski who has given me an opportunity to study dye chemistry and helped me to learn heterocyclic chemistry. There are also many other professors who have given me lots of advices; Dr. Dabney Dixon, Dr. David Hamilton, Dr. Stuart Allison, Dr. Gangli Wang and many other professors, thank you.

Also, I would like to express my gratitude to my lab mates who ever worked with; Dr. Ravikumar Kodagahally who gave me a chance to work with the first bis-dyes, Dr. Jozef Salon, Dr. Martial Medou, Dr. Martial Say, Dr. Ewa Wolinska, Dr. Mariusz Mojzych, and Dr. Aldona who provided me many bis-dyes that they synthesized. Thanks to other lab mates; especially Amy Watson and Diem Nguyen who helped me when I first joined our lab. And thanks to Dr. Maged Henary for his help regarding organic chemistry. Finally, I would like to say “Thank you so much” to my parents, Jae Wook Kim and Kab Leoy Lee, and my family for their support and patience for last 5 years.

Table of Contents

Dedication……iv

Acknowledgements…….……v

List of Tables…….……ix

List of Figures…….....x

Chapter 1. Introduction to Near Infrared (NIR) Carbocyanine Dyes …..…….……1

1.1. Background …….…….....2

1.2. Near Infrared Carbocyanine Dyes …….……..3

1.3. Protein labeling with NIR dyes ……...5

1.3.1. Covalent labeling ……...6

1.3.2. Noncovalent labeling …….....9

1.4. Non-covalent labeling for protein analysis …….…….....9

1.4.1. Dye Aggregation in Solution …….....9

1.4.2. Binding stoichiometry and equilibria in non-covalent labeling ……...14

1.5. Summary ……23

Chapter 2. Spectroscopic study of a novel bis(heptamethine cyanine) dye and its interaction with human serum albumin …….…….……32

2.1. Introduction …….…...33

2.2. Experimental Section …….35

2.3. Results and Discussion …….…..36

2.4. Conclusions …….…...46

Chapter 3. A study of intramolecular H-complexes of novel bis(heptamethine cyanine)

dyes …….52

3.1. Introduction …….…….....53

3.2. Experimental Section …….54

3.3. Results and Discussion ……..55

3.4. Conclusions …….....68

Chapter 4. Capillary electrophoresis for dye applications ……72

4.1. Introduction …….....73

4.2. Capillary electrophoresis (CE) …….……..73

4.3. Separation parameters …….....77

4.4. Mode of capillary electrophoresis …….……78

4.5. Detection Methods …….81

4.6. Capillary electrophoresis with near-infrared laser induced fluorescence (CE-NIR-LIF) detection ……84

Chapter 5. Investigation of Noncovalent Human serum albumin labeling with Near-infrared Bis(heptamethine cyanine) Dyes by Capillary electrophoresis with near-infrared laser induced fluorescence detection ……..……..90

5.1. Introduction …….....91

5.2. Experimental Section …….....92

5.3. Results and Discussion …….……..93

5.4. Conclusions …….….104

Chapter 6. A Study of Distinct Conformations of Bis-Cyanine Dyes and Their Efficient

Separation via Capillary Electrophoresis …….108

6.1. Introduction ……..…….109

6.2. Experimental Section ……...111

6.3. Results and Discussion ……..……114

6.4. Conclusions ……..…….128

List of Tables

Table 1.1. Comparison of near infrared (NIR) and visible (VIS) lasers. ……...……...4

Table 1.2. Noise comparison of NIR and Visible region. ……...……..5

Table. 1.3. Comparison of covalent and non-covalent labeling. ……...……...9

Table 1.4. Comparison of five binding analysis methods with capillary electrophoresis. The similarity of their experimental set-ups and analytical methods is demonstrated. ……..21

Table 4.1. Mode of Capillary Electrophoresis for Different Classes of Analytes. ……..79

Table 4.2. Methods of detection in CE. ……..83

Table 5.1. Spectral properties of NIR dyes in different solvents. ……..…..94

Table 5.2. LODs and binding constants of NIR dyes with HSA. ……..….99

Table 6.1. The comparison of migration time and relative peak areas. ……...126

List of Figures

Figure 1.1. Near infrared (NIR) spectrum separated form native fluorescence in visible region. Inset spectrum shows absorbance and fluorescence of RK780 in methanol. ……...4

Figure 1.2. Covalent label of amine and thiol groups of proteins and peptides. ……..…7

Figure 1. 3. Covalent NIR dye-Ab labeling for immunoassay. ……..…...7

Figure 1.4. Delocalization of NIR cyanine dye. Delocalization results in resonance stabilization and is energetically favorable. ……..…...10

Figure 1.5. Representative models of cyanine dye aggregates in solution: Dye aggregates with brickwork (a), ladder (b), and staircase (c) molecular arrays; α is the angle of slippage. Aggregate models drawn after ref. 38. ……..…..11

Figure 1.6. The low or non-fluorescent spectra of Bis-dyes caused by the H-characters in fluorescent spectroscopy. Fluorescence spectra of RK780 (**1**) and BHmCs (**2-19**) in 20 nM phosphate, pH 7.2. BHmCs exhibit negligible fluorescence compared to their monomer counterpart, **1**. ……..……13

Figure 1.7. Dye **1** shows H-aggregates in spectrum and non-fluorescence in CE-LIF without a target molecule. Noncovalent labeling of human serum albumin (HSA) with CE-LIF detection. Different functional groups of heptamethine cyanine dyes influence the complexation of dye and protein. Dye **1** (RK780) shows stronger binding property to the protein relative to the other negatively charged dyes, **20** and **21**. ……...……14

Figure 1.8. Representative cooperative pathway. Protein-dye stoichiometry is 1:2 in this figure. Two different pathways show how a binding site influences another binding site. The first bound dye weakens or strengthens the second bound dyes. Also, the second one influences the first one during complexation. Thus, marcro-binding constants, K_1 and K_2, are dependent on four micro-binding constants, k_1, k_2, k_3 and k_4. Hill's plot is used for the assay. More detailed examples and explanations are found in ref. 40. ….....15

Figure 1.9. Illustration of a) affinity capillary electrophoresis (ACE) and b) vacancy affinity capillary electrophoresis (VACE). The mobility of free and bound ligand is used to find binding constant and stoichiometry. ……18

Figure 1.10. Illustration of a) Hummel-dreyer (HD), b) vacancy peak (VP) and c) frontal analysis methods. Peak areas or heights of free and bound ligand are used to find binding constant and stoichiometry. Redrawn after Hummel-Dreyer method. ……..…..19

Figure 2.1. Chemical structure of bis-heptamethin cyanine dye linked with decamethylene chain. ……..……..34

Figure 2.2. Concentration effect on aggregation of BHmC-10 in methanol. Normalized absorption spectra were taken at three different concentrations: 0.1 μM (dotted line), 1 μM

(dashed line), and 10 μM (solid line). ……...……..38

Figure 2.3. Normalized absorption spectra of RK780 (dotted line) and BHmC-10 (solid line) in phosphate buffer at 10 μM dye concentration. ……..……...38

Figure 2.4. Absorption spectra of BHmC-10 in methanol (top) and methanol-phosphate buffer mixture (bottom) at room temperature. ……39

Figure 2.5. Absorption of BHmC-10 (10 μM) in the presence of HSA: (a) 100, (b) 70, (c) 50, (d) 30, (e) 10, (f) 5, (g) 1, (h) 0.5, (i) 0.1, and (j) 0 μM. The arrows indicate the spectral changes of H-, D-, and M-band. ……..……..…40

Figure 2.6. Fluorescence emission spectra of RK780 (dotted line) and BHmC-10 (solid line) in phosphate buffer at 10 μM dye concentration. ……..…...41

Figure 2.7. Fluorescence emission spectra of BHmC-10 (10 μM) in various solvent systems, at room temperature. a, 25% (v/v) methanol in water; b, 25% (v/v) methanol in PB; c, 50% (v/v) methanol in water; d, 1 : 1 ratio, 20 μM total cons., of dye 7-HSA complex in 1% (v/v) methanol in PB; e, 50% (v/v) methanol in PB; f, 100% methanol. ……42

Figure 2.8. Fluorescence emission spectra of BHmC-10 (10 μM) in the presence of HSA: (a) 70, (b) 50, (c) 30, (d) 10, (e) 1, and (f) 0.1 μM. ……..43

Figure 2.9. Saturable binding curve as a function of increasing HSA concentration. The concentration of BHmC-10 was constant at 10 μM, and the fluorescence was measured at 800 nm. …….....44

Figure 2.10. Job's plot to determine the stoichiometry of dye-HSA complex at 800 nm. The total concentration of the complex was $2x10^{-5}$ M. ……..45

Figure 3.1. Absorption spectra of RK780 (dotted line) and BHmCs (solid lines) in methanol: (A), concentration effect on the aggregation of BHmCs at three different concentration, at 0.1 μM, 1 μM, and 10 μM. Normalized absorption spectra were taken.; (B), spectral response comparison (λ_{max} at 780 nm) of RK780 and BHmCs at 10 μM. …….56

Figure 3.2. Spectral comparison of RK780 (dotted line) and BHmCs (solid lines) in phosphate buffer, pH 7.2, at 10 μM dye concentration. (A): Normalized absorption spectra. (B) and (C): Fluorescence emission spectra. ……..…….59

Figure 3.3. A. Absorption of BHmCs (10 μM) in the absence (dotted line) and the presence (solid line) of HSA (0.1 to 100 uM). Upper; BHmC-4, bottom; BHmC-6. ……61

Figure 3.3. B. Absorption of BHmCs (10 μM) in the absence (dotted line) and the presence (solid line) of HSA (0.1 to 100 uM). Upper; BHmC-8, bottom; BHmC-12. ……..62

Figure 3.4. A. Fluorescence emission spectra of BHmCs (10 μM) in the absence (dotted line) and the presence (solid line) of HSA (0.1 to 100 uM). Upper; BHmC-4, bottom; BHmC-6. ……..65

Figure 3.4. B. Fluorescence emission spectra of BHmCs (10 μM) in the absence (dotted line) and the presence (solid line) of HSA (0.1 to 100 uM). Upper; BHmC-8, bottom; BHmC-12. ……...……...66

Figure 3.5. Spectral comparison of BHmCs (10 μM) regarding their complexes in the presence of HSA (10 μM). ……..67

Figure 4.1. Basic configuration of capillary electrophoresis and representation of electroosmotic flow in CE. …….……74

Figrue 4.2. Comparison of electroosmotic flow (CE) and pressure driven flow profiles (HPLC), and differential solute migration in capillary zone electrophoresis. ……..…75

Figure 4.3. Micellar electrokinetic capillary chromatography (MEKC) and Capillary gel electrophoresis (CGE). …….…...80

Figure 4.4. Capillary isoelectric focusing (CIEF) and capillary isotachophoresis (CITP). ...81

Figure 4.5. Schematic of CE-NIR-LIF detection. ……..86

Figure 5.1. Use of three types of heptamethine cyanine dyes for HSA labeling. 5 uM for each dye was injected in upper-left electropherogram. Prior to sample loading, 5 uM dyes with various concentration of HSA in 100 mM borate at pH 9.0 were mixed and injected for 1s. Three dyes with different substitutes and charges are shown in the table. Instrument condition: capillary; 50 cm to detector and 57 cm to outlet, 30kVs, runbuffer; 100mM borate pH 9.0, pressure; 0.5 psi. ……...……..95

Figure 5.2. Indirect fluorescent detection of HSA. CE conditions: 40 cm x 47 cm, 50 um, 20 kV, 3s injection time. Run buffer contains dye 3 (12.8 uM containing 2 % methanol), and DI water and HSA were injected. ……...…..96

Figure 5.3. Non-covalent dye labeling to HSA. CE conditions: 40 cm x 47 cm, 50 um, 20 kV, 3s injection time. Runbuffers contain different dyes, concentrations having (a, b and d) 0 and (c) 30 min incubation time. a; 0.1 uM Dye 4, b and c; 10 uM dye 4, d; 10 uM BHmC-12. Applied protein concentration was 0.15 uM. ……...…96

Figure 5.4. a) Spectral properties of Dye 1 (left) and BHmC-12 (right) in different solvents at room temperature. 10 uM dye concentrations were used in (•) H_2O at 0 min, (*) 100 mM borate at pH 9.0 at 0 min and (◦) 100 mM borate ate pH 9.0 after 30 min. b) Tim-dependent fluorescent spectral property of Dye 1 in borate at room temperature. Inset shows (◦) Dye 1 at 0 min, (•) at 30 min and (*) BHmC-12 at 0 min. Dye 1 exhibits low fluorescence after 30 min. ……...…...97

Figure 5.5. Low limit of detection due to intra-H-type dimers and/or aggregates of BHmCs. From top to bottom, 10 uM of RK780 and 5 uM of RK780, BHmC-12, -10, -8, -6 and -4. Left: 1s injection of dyes in MeOH, Right: 1 s injection dyes and 0.312 uM HSA mixture containing 1% MeOH in 100 mM borate pH 9.0. Instrument condition: capillary; 50 cm to

detector and 57 cm to outlet, 30kVs, runbuffer; 100mM borate pH 9.0, pressure; 0.5 psi. ……..99

Figure 5.6. Non-covalent labeling HSA with dyes. Dye-HSA mixtures were prepared in 100 mM borate pH 9.0 containing 1 % methanol. Various concentrations, 0.312, 0.625, 1.25, 2.50, 5.0, 10, 20 uM, of HSA were prepared with constant dye concentrations, 5 uM. Experiment conditions were same as in Figure 5. Left-upper: linear calibration curves, y = 4E+06x - 1.2009, R2 = 0.9884 (RK780), y = 2E+06x + 0.2154, R2 = 0.9901 (BHmC-4), y = 2E+06x + 0.3752, R2 = 0.9934 (BHmC-6), y = 2E+06x + 0.4616, R2 = 0.9865 (BHmC-8), y = 1E+06x + 1.0449, R2 = 0.9809 (BHmC-10), y = 4E+06x + 0.746, R2 = 0.9931 (BHmC-12). Dye 3 was used as an internal standard to correct the peak areas of the complex. …….……101

Figure 5.7. Modification of bovine carbonic anhydrase II (BCAII) with acetic anhydride. The number of modified lysines in BCAII appears on electropherogram (charge ladder). CE condition: 25 kV, 70 cm to detector, 77 cm to outlet, 10 sec injection for Uv detection at 214 nm, Tris-Glycine (25mM-192mM, at pH 8.4), 0.5 psi injection pressure. ……..……102

Figure 5.8. Charge ladders with acetic anhydride (AA) and succinic anhydride (SA). Left: various concentration of anhydrides (Uv detection at 218 nm). CE condition: 25 kV, at 214 nm, Right: modified proteins with dye-1 (LIF detection). Picture: from left to right, 5.04 mM AA, 1.21 mM AA, 0.039 mM AA, 0 mM AA, No BCAII (dye-1 was added to the solutions). ……..……103

Figure 5.9. Temperature effect on RK780-BCAII complex. The measurement performed at 23 ~ 40 °C at different concentration of anhydrides mixed with RK780 (10 uM). Experimental condition is same as figure 5.8. ……..……104

Figure 6.1. Sample handling scheme. For convenience, BHmC-O_3 drew as a regular single molecule, not open or closed clamshell form. a): BHmC-O_3, b): HSA or AO and c): complex of a) and b). Injection times for each sample are 3 s (a) and 2 s (b). ……112

Figure 6.2. Conformational effect of three different bridges in BHmC-Os. a): comparison of three BHmC-Os in CE. b): zoomed window for BHmC-O_3. peak 1 and 2: J-type intra-dimer (closed clamshell form), peak 3: open forms of BHmC-Os, peak 4: J-type aggregate. Condition: 3 second pressure injection (0.5 psi), 23 kV applied voltage, 75 um x 57 cm capillary; 100 mM borate at pH 9.0. All the concentrations of BHmC-Os are 160 uM in methanol. ……...115

Figure 6.3. Possible conformations for bis(heptamethine) cyanines, and their energy level and mobility in capillary electrophoresis. Dotted and bold arrows in energy level indicate negligible and enhanced fluorescence, respectively. The mobility in capillary drew based on the conformation of BHmC-O_3. …….……...116

Figure 6.4. Concentration effect on aggregation in CE. BHmC-O_3 in methanol; a) 0.54, b) 3.27, c) 20, and d) 160 uM, respectively. peak 1 and 2: J-type intra-dimer (closed clamshell form), peak 3: open form, peak 4: J-type aggregate. Condition: 3 second pressure injection (0.5 psi), 23 kV applied voltage, 75 um x 57 cm capillary; 100 mM borate at pH 9.0. ……...117

Figure 6.5. Organic solvent composition effect in aspect of dielectric constant and dipole moment. For all sample injections, BHmC-O_3 (160 uM) was dissolved in alkyl alcohol series, methanol, ethanol, propanol and butanol. Small windows indicate zoomed data. peak 1 and 2: J-type intra-dimer (closed clamshell form), peak 3: open form, peak 4: J-type aggregate. Condition: 3 second pressure injection (0.5 psi), 23 kV applied voltage, 75 um x 57 cm capillary; 100 mM borate at pH 9.0. ……..…….118

Figure 6.6. Influence of aqueous solvents ratio in sample. 20 uM of BHmC-O_3 are maintained for all measurement. Aqueous solvent compositions with methanol are 0 (a), 20 (b), 40 (c), 60 (d), 80 (e), and 100 (f) % (v/v), respectively. peak 2: J-type intra-dimer (closed clamshell form), peak 3: open form. Condition: 3 second pressure injection (0.5 psi), 23 kV applied voltage, 75 um x 57 cm capillary; 100 mM borate at pH 9.0. ……..120

Figure 6.7. Running buffer effect on aggregation. Constant dye concentrations (160 uM) are used. Running buffer: a; 20 mM phosphate (pH 7.2), b; 20, c; 50 and d; 100 mM borate (pH 9.0). peak 1 and 2: J-type intra-dimer (closed clamshell form), peak 3: open form, peak 4: J-type aggregate. Condition: 3 second pressure injection (0.5 psi), 23 kV applied voltage, 75 um x 57 cm capillary. ……....121

Figure 6.8. Effect of applied voltages. Five different voltages were applied for the separation of BHmC-O3 (160 uM). Condition: 3 second pressure injection (0.5 psi), 75 um x 57 cm capillary; 100 mM borate at pH 9.0. …….122

Figure 6.9. Absorbance spectra. a): HSA (10 uM)-BHmC-O_3 (10 uM) complex in 20 mM phosphate, pH 7.2, b): 2 uM BHmC-O_3 in methanol, c): 10 uM BHmC-O_3 in 20 mM phosphate, pH 7.2, d) HSA (1 uM)-BHmC-O_3 (1 uM) complex in 20 mM phosphate, pH 7.2. ……123

Figure 6.10. Fluorescence spectra. Concentration of BHmC-O_3 in methanol: a); 2, c); 0.4 uM. Concentration of dye-HSA complex in 20 mM phosphate, pH 7.2: c) HSA (10 uM)-BHmC-O_3 (10 uM), d) HSA (1 uM)-BHmC-O_3 (1 uM). ……..…124

Figure 6.11. Efficient separation of dye-HSA complex. Three different running buffers are used to optimize CE separation for complex; a) 20 mM phosphate, pH 7.2, b) 20 mM borate, pH 9.0, c) 100 mM borate, pH 9.0. Individual injection was applied for on-column interaction of dye and HSA. First sample injection: 10 uM HSA is loaded for 2s (0.5 psi). Second sample injection: 20 uM BHmC-O_3 dissolved in PB is loaded for 3s (0.5 psi). 23 kV applied voltage, 75 um x 57 cm capillary. ……..…..125

Figure 6.12. Intercalation of acridine orange (AO). Various concentrations of AO were loaded for 2s (0.5 psi), followed by BHmC-O_3 for 3s (0.5 psi). All samples were dissolved in methanol. BHmC-O_3 in butanol is added for the comparison of complete open form with intercalated open form. peak 2: J-type intra-dimer (closed clamshell form), peak 3: open form. Condition: 23 kV applied voltage, 75 um x 57 cm capillary; 100 mM borate at pH 9.0. All the concentrations of BHmC-Os are 160 uM in methanol. ……..……...127

Figure 6.13. Ratio of peak areas. Percentages of peak areas are calculated by the ratio of individual peak. Symbols indicate peak 1 (●), 2 (○) and 3 (▼) in individual peak. Fat region (dotted square) shows the tolerant insertion number of AO into BHmC-O_3. ……128

Chapter 1. Introduction to Dye-Protein Labeling

: the Use of Near Infrared Carbocyanine Dyes for Protein Analysis

1.1. Background

Dyes have been used extensively in biomolecule investigations and characterizations throughout the last several decades.[1-9] When we look at the published literature, we can notice that that type of research was always dictated by the availability of dyes. It is very rare that a research group would focus on the development of a specific dye that is suitable for a given task in investigating biomolecules. The major foci of biomolecule investigations have been proteins and nucleic acids, being two important classes of biomolecules.[1, 2, 9] Many researchers who investigate biological phenomena and interested in the protein and nucleic acid research are utilizing dyes that strongly bind to these molecules. A significant part of the literature focuses on utilizing dyes that have their spectral characteristics (absorption and emission characteristics) in the visible range of the electromagnetic spectrum mostly because visible dyes have been available much earlier for these types of research than their longer wavelength counterparts. In addition, earlier detection technologies made the utilization of the longer wavelength range less attractive. Starting in the 1980s with the advent of semiconductor detector and laser technologies the tools started to become available to be used in the near-infrared (NIR) region.[10-12] This opened up avenues for the researchers that had not been available before. Since then a large number of research groups have been actively utilizing the NIR spectral region for biomolecule characterization. The area became much more specialized.

Carbocyanines are one of the most useful groups of dyes for protein characterizations due to their strong interactions with these important biomolecules.[8, 9, 13] Also, carbocyanines are relatively easy to synthesize and they exhibit significant changes in their spectral properties upon binding to biomolecules. Although nucleic acids are also important group of biomolecules, they typically require different dyes with different properties for their characterization. Thus, this chapter mainly deals with a protein and its bioanalytical

techniques

1.2. Near Infrared Carbocyanine Dyes

The carbocyanine probes can be classified by heterocyclic moiety. For example, cyanine, oxonol, merocyanine, and so forth are named by the heterocyclic moiety at the end of the polymethine chains, the polymethine chain itself can be classified by the number of methine; mono-, tri-, penta-, heptamethine, etc. The two heteroaromatic moieties linked to the polyene consist of imidazole, pyridine, pyrrole, quinoline, thiazole, etc. Of the various probes, near-Infrared (NIR) cyanine dyes have been studied in many areas. Generally, biomolecules exhibit auto-fluorescence in the ultraviolet or visible region and this is problematic in analysis.[10, 14] The use of the NIR region separates the overlapping of the spectrum between a dye and a target biomolecule. The strong advantage of the NIR dyes is that during synthesis, unreacted starting materials of NIR dyes, which commonly show spectra in UV region, can be excluded the spectra from NIR region due to the spectral separation (Figure 1.1). In chromatography or other methods using a single wavelength in NIR region, the detection signal only responses for free NIR dyes and/or labeled NIR dyes. Moreover, few biomolecules at long wavelengths undergo electronic transitions and Scattering (Ray leigh and Raman), resulting in improved signal-to-noise, and the use of compact and cheap GaAlAs laser diodes with high power output and long lifetime (≥100 000 h) make it attractive (*see* Table 1.1 and 1.2).[10]

Some research groups have investigated the use of NIR dye for protein analysis. Colyer et al. reported non-covalent labeling scheme by using capillary electrophoresis with laser-induced fluorescence detection (CE-LIF). Symmetric (NN127), asymmetric (SQ-3) dyes and indocyanine green (ICG) were used with proteins.[15-18] These dyes exhibit negligible fluorescence in aqueous solution and enhance fluorescence upon binding to proteins. They

successfully separated human serum albumin (HSA), bovine serum albumin (BSA), β-lactoglobulin A, and trypsinogen. This research shows that symmetric dye strongly interacts with HSA compared to asymmetric dye.[17-19] Patonay and Strekowski's research groups synthesized a heptamethine cyanine dyes (Figure 1.6 and 1.7). In their study, two heterocyclic moieties are linked by Vilsmeier-Haack reagent which includes a heptamethine chain and the rigid structure and conjugation of NIR dyes allows high quantum yield (Φ, 0.05-0.5) and absorptivity (ε, 150 000-250 000) and this facilitates achievement of a low detection limit.[10] A labeled NN382 shows attomole-range detection limit and noncovalently labeled RK780 provides femtomole-range detection limit.[6, 10] Therefore, the sensitive detection response of NIR probe will be beneficial for the protein-related research.

Table 1.1. Comparison of near infrared (NIR) and visible (VIS) lasers.

	Laser diode	Argon-ion laser
Wavelength	**785 nm**	**488nm**
Life span	**100,000 + hr**	**3000 hr**
Optical power output	**20 mW**	**20 mW**
Power consumption	**0.150 W**	**1800 W**
Replacement cost	**$150**	**< $5000**

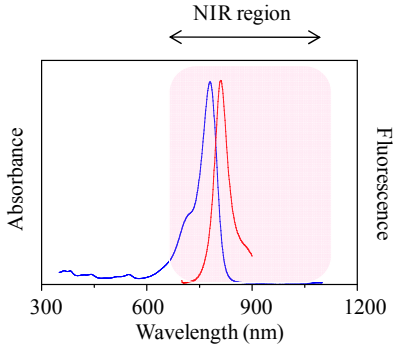

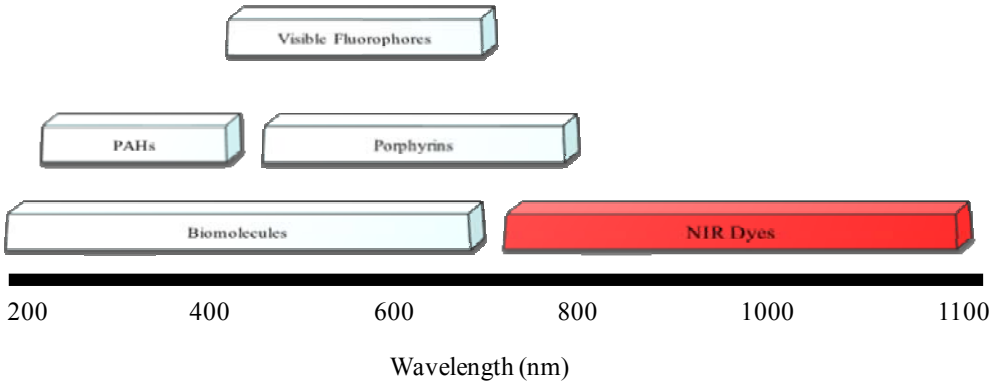

Figure 1.1. Near infrared (NIR) spectrum separated form native fluorescence in visible region. Inset spectrum shows absorbance and fluorescence of RK780 in methanol.

Table 1.2. Noise comparison of NIR and Visible region.

	NIR LIF	VIS LIF
Scatter Noise (Rayleigh and Raman)	**Reduced**	**6x greater at 520 nm vs. 820nm**
Background Fluorescence (Capillary and lenses, Background electrolyte, Sample matrix)	**Mostly Absent**	**Visible Fluorophores (Porphyrins, Biomolcules)**
Detector Noise	**Low**	**High**

1.3. Protein labeling with NIR dyes

Covalent and non-covalent labeling procedures are commonly introduced for protein analysis by NIR dyes or other dyes.[10, 14, 15, 18, 20] Covalent labeling uses a functionalized dye so that it can be linked to N-terminal or other side chains of a protein.[10, 21, 22] The method basically provides low detection limit, and quantitative and qualitative information of a protein can be also obtained since the method for labeling requires a particular amino acid for the chemical reaction with a functionalized dye. However, this method needs restricted environment for the reaction. For instant, improper pH control in solution results in unexpected labeling to other side chains of a protein. Purification of the unreacted dyes is also required.[10, 14] Thus, it takes several hours to handle the procedure. Non-covalent labeling also shows low detection limit and quantitative and qualitative information of a protein can be measured. This method is relatively simple and takes few seconds or minutes to label a dye. However, it requires a binding site in a protein and this limits the analysis of some proteins. Once a protein has a biding site, the labeling is tolerance for pH changes in solution. In addition, unlike covalent labeling, binding constant and stoichiometry are considered for non-covalent labeling since the binding pathway is dependent on a binding site of a protein.

In section 1.4, equilibria in non-covalent labeling are demonstrated in detail.

1.3.1. Covalent labeling

For covalent labeling, generic functional groups of dyes are isothiocyanate, succinimidyl ester, sulfonyl chloride etc. for α- and ε-NH_2 in amino acid and alkyl halide, maleimide etc. for thiol group in a protein.[22] The specificity of the amino acid of a protein upon reacting with a functionalized dye changes the efficiency of labeling.[7] It is also influenced by pH of solution. For instant, the amine group of lysine in the N-terminal of a protein can be protonated or deprotonated dependent on pH of the solution. Generally, above pH 8, -NH_2 exists and uses for α-amine selective labeling. However, under strong basic condition, other ε-amine groups of the lysines of a protein, instead of N-terminal group, can be substituted by a functionalized dye. Thus, labeling efficiency will be dependent on pH control in the case. In figure 1.2, their reacting pathways are shown. R^1 and R^2 represent the moiety of a dye and the N-terminal or side chain of a protein, respectively. In the case of the first example in figure 1.2, after reacting the functionalized dye with amine group at pH 8, the reaction yields a substituted thiourea. There are also many types of functional group for amine, thiol groups as well as other side chains. Recently, this labeling scheme has been reviewed by Fukushima[23] and Bardelmeijer et al.[24] They mainly react with a side chain of an amino acid and follows substitution reaction in distinct environment.

In chromatographic analysis, covalent labeling also allows sensitive detection.[10] Less than attomole range can be achieved when capillary electrophoresis (CE) with laser induced fluorescence (LIF) detection utilizes NIR dyes (see instrumental detail in Chapter 4).[2] Moreover, antibodies (Ab) labeled with NIR dyes enable capillary electrophoresis immunoassay (CEIA) to lower the detection limit and allow quantitative analysis.[25] The NIR dye labeled N-terminal of an antibody is commonly applied for the assay.[4] Since an antigen

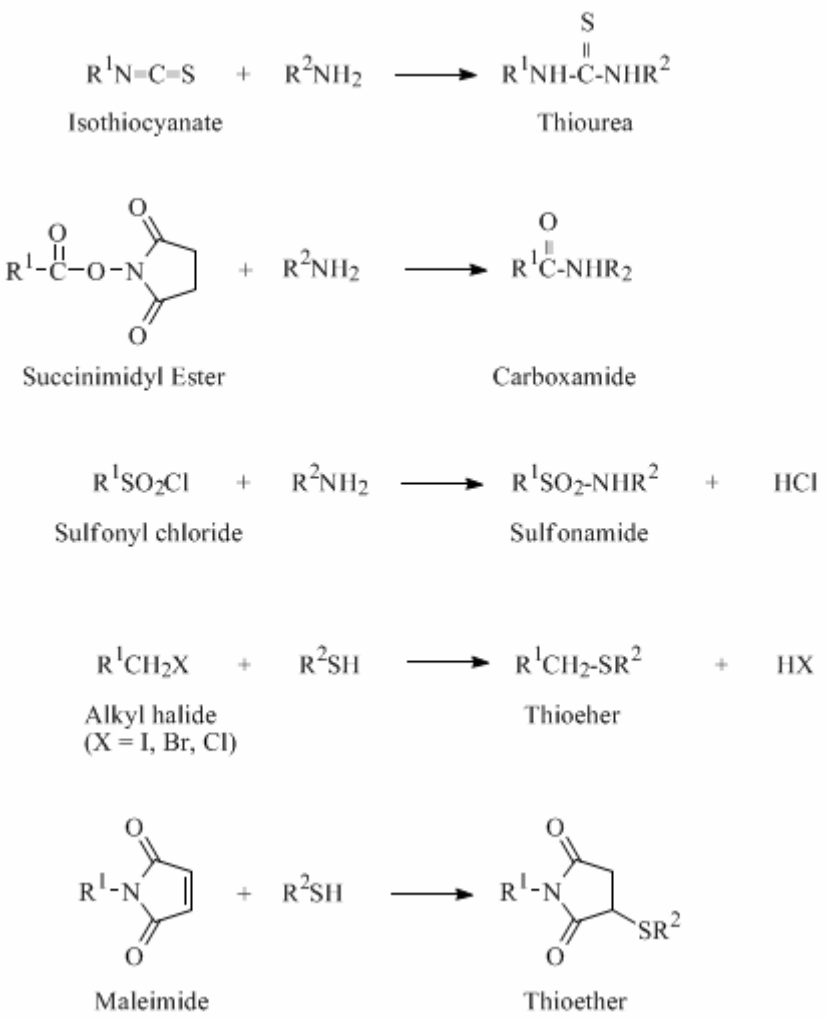

Figure 1.2. Covalent label of amine and thiol groups of proteins and peptides.

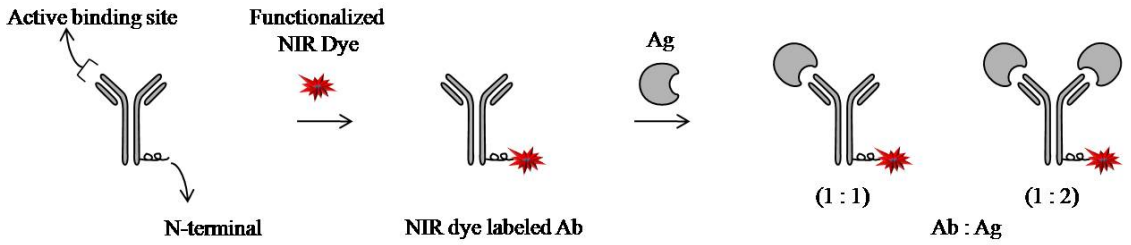

Figure 1. 3. Covalent NIR dye-Ab labeling for immunoassay.

binds to the active site of an antibody, the antibody is not influenced by the label. Likewise, for receptor-ligand interaction in affinity capillary electrophoresis (ACE), covalent labeling is also possible.[15]

Another example of qualitative and quantitative biomolecule analyses can be well demonstrated with TNBS (2,4,6-trinitrobenzene sulfonic acid).[26, 27] The molecule absorbs light in UV region (335 nm) instead of NIR region, but TNBS will be used for biomolecule analysis in this section since many publications support its uses for the qualitative and quantitative analyses and NIR dyes go same pathway.[9,10]

In TNBS method, nucleophilic aromatic substitution reaction of ε-NH_2 with TNBS produces TNB-lysine and provides how many α- and ε-NH_2 labels and the moles of the lysine in a protein can be calculated.[26, 27] The following equation provides the degree of substitution (DOS). Here, the absorbance at a wavelength, in this case 335 nm, changes dependent on how many lysine subunits are modified by TNBS and the information directly gives the moles of amine group in the protein.

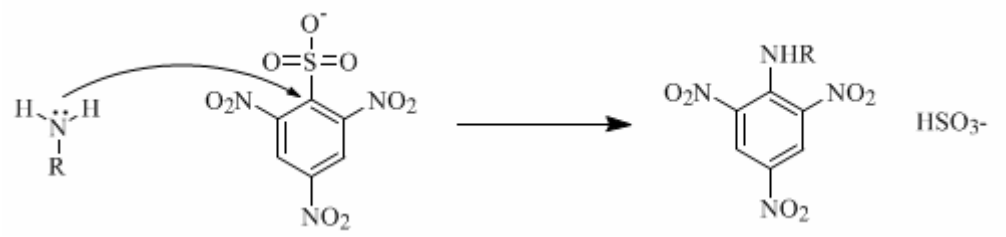

$$\frac{\text{Abs} \times \text{M.W. of protein}}{\varepsilon \times \text{concentration of protein } (\frac{\text{mg}}{\text{mL}})} = \frac{\text{moles lysine}}{\text{moles of protein}}$$

In the TNBS method, the spectral changes are simply applied. Here the net charge of the protein during labeling might be changed since the dye itself has its own charge and at a certain pH of a buffer, the pI and the net charge after modification of the protein are changed. The presence of modified net charges result in various peaks, called a charge ladder, in

capillary electrophoresis (CE) analysis.[28-30] In CE, the separation is based on the charge to size ratio, so if the lysines in a protein are modified by a differently charged chemical or a dye, the net charge of the protein would be changed, resulting in showing peaks with different mobility, and the result provides the molecular mass of a protein (see Chapter 5).

Table. 1.3. Comparison of covalent and non-covalent labeling.

Parameters	Covalent Labeling	Non-Covalent Labeling
Time	Hours	Seconds
Labeling efficiency	Often poor	Improved
Purification (for separation purpose)	Yes	Unnecessary

1.3.2. Non-covalent labeling

Unlike the covalent labeling, non-covalent labeling requires at least one binding site of a protein, and a dye can be readily mixed with a protein that provides room for the ligand, showing different spectra in spectroscopy or mobilities in chromatography. In DNA study, non-covalent labeling provides the role of minor and major grooves. The non-covalent interaction is dependent on mainly dipole-dipole forces, dispersion forces and hydrogen bond between a ligand and a biomolecule.[9] They may influence each other, or only a single factor influences the binding. In section 1.4, detailed explanations will be dealt with non-covalent labeling in aqueous solution, and data analyses for the labeling will be demonstrated.

1.4. Non-covalent labeling for protein analysis

1.4.1. Dye Aggregation in Solution

For non-covalent labeling, it is particularly important to understand dye aggregation or self-association in aqueous solution before starting experiment and data analysis. Dye aggregation in solution is important in some industrial areas such as in photographic technology and photomedicines.[31-34] Dye aggregates form due to the difference of the polarities between dyes and solvents. Generally, protein analysis needs polar solvents, such as H_2O, buffers, due to the hydrophilic surfaces of most proteins, and most dyes requires hydrophobic binding sites for the interaction, meaning that dyes should be relatively hydrophobic. Thus, hydrophobic-hydrophobic interaction exists in most dye-protein labeling. However, the hydrophobic character of the dye does not allow solvation by polar solvent. Instead, the polar environments make dyes shrink, forming dimer, trimer, tetramer, etc. It is well known that carbocyanine dyes can easily aggregate in aqueous solutions even at low concentrations or in organic solvents at higher concentration. For instant, NIR cyanine dyes (Figure 1.4 and 1.6) generally have two nitrogen heterocyclic systems conjugated through a polymethine bridge. Delocalization of positive charge generates strong intermolecular van der Waals interaction that promotes dye aggregation or self-association.

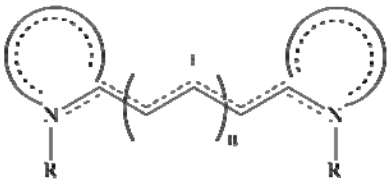

Figure 1.4. Delocalization of NIR cyanine dye. Delocalization results in resonance stabilization and is energetically favorable.

This aggregation results in formation of different structures dependent on how the carbocyanine moieties interact with each other and is usually described as H-aggregation (hypsochromic) and J-aggregation (bathochromic) depending on the angle of slippage α.[35]

The conformation of the aggregates is also dependent on several environmental factors such as concentration, solvent polarity, pH, ionic strength, and temperature.[36] Representative models of dye aggregates in solution are shown in figure 1.5. H-aggregates are referred to as "card-pack" arrangement, whereas J-aggregates are known as "brickwork" arrangement. Large molecular slippage ($\alpha < \sim 32°$) results in a bathochromic shift while small slippage ($\alpha > \sim 32°$) results in a hypsochromic shift.[37-39]

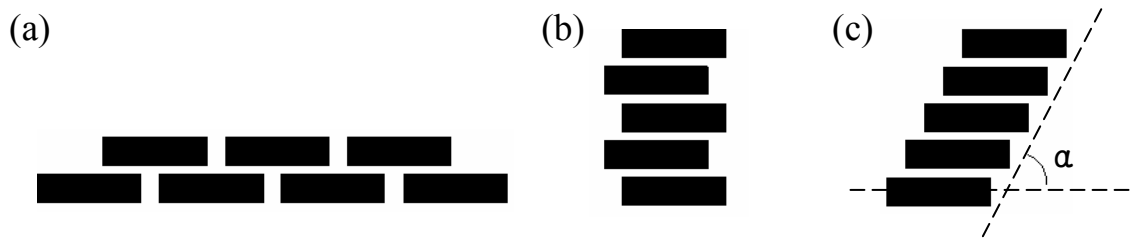

Figure 1.5. Representative models of cyanine dye aggregates in solution: Dye aggregates with brickwork (a), ladder (b), and staircase (c) molecular arrays; α is the angle of slippage. Aggregate models drawn after ref. 38.

Generally, cyanine dyes are prone to aggregate unlike merocyanine and oxonol dyes, and symmetric dyes readily form aggregates compared to asymmetrical dyes. The characteristic structure of these symmetric dyes generally produces a large slippage angle for their formation, and therefore, readily forms H-aggregates. Other factor for dye aggregation may be its structural formation; that is, dyes having planar structure favor H-aggregation. Besides, environmental influence on their aggregation has to be considered since the properties of solvent used generally make the geometrical arrangement of aggregates modified. Aggregation is an exothermic process. It has been suggested that solvent properties, dipole moment and dielectric constant, has contributed to the energetics of aggregation. Regarding that, water is the most favorable solvent since its high dielectric constant strongly influences on reducing the repulsive force between the similarly charged dyes in aggregation. Generally, the addition of inorganic salts increases the dielectric constant of a solvent and

facilitates aggregation. On the other hand, the addition of some organics reduces the dielectric constant of a solvent and increases the repulsion between two dye molecules, inhibiting aggregation. Various other factors affect aggregation as well. For instance, reducing temperature may favor aggregation in most solvents. Moreover, both H and J aggregation depend not only on temperature and dye structure, but also, pH and net dye charge.

The characteristic absorption spectra of the aggregates are different from that of the monomeric state, i.e., di-, tri-, tetramers and so forth have different electronic states. H-aggregates typically posses low molar extinction coefficients (ε) and quantum yields (Φ) compared to their monomeric absorption bands, and J-aggregates posses high ε and Φ .[2, 4, 8] H-aggregation is mainly encountered in bioorganic systems, whereas J-aggregation is generally applied in to photographic light harvesting, optical recording media, and laser technology.

Figure 1.6 shows the chemical structures of NIR bis-heptamethine cyanine (BHmC) dyes and their fluorescent spectra in phosphate buffer. The absorption spectra can be found in chapter 2 and 3. Due to the energetically favorable H-type conformation in aqueous solution, they exhibit negligible fluorescence compared to their monomer counterpart, RK780. As can be seen in chapter 1 and 2, the conformations deform and fluorescence upon reacting with a protein. Structural dependency can be also found in figure 1.7. dependent on the number of sulfonic group in same moieties, RK780, JCM783 and JCM793 form aggregates in phosphate buffer. RK780 shows non-fluorescence, but enhances fluorescence when binding to HSA in CE-LIF detection. However, JCM783 and JCM793 show low or non-fluorescence with HSA, and free dyes exhibit fluorescence. In the experiment, dye 1 is the favorable structure for non-covalent labeling.

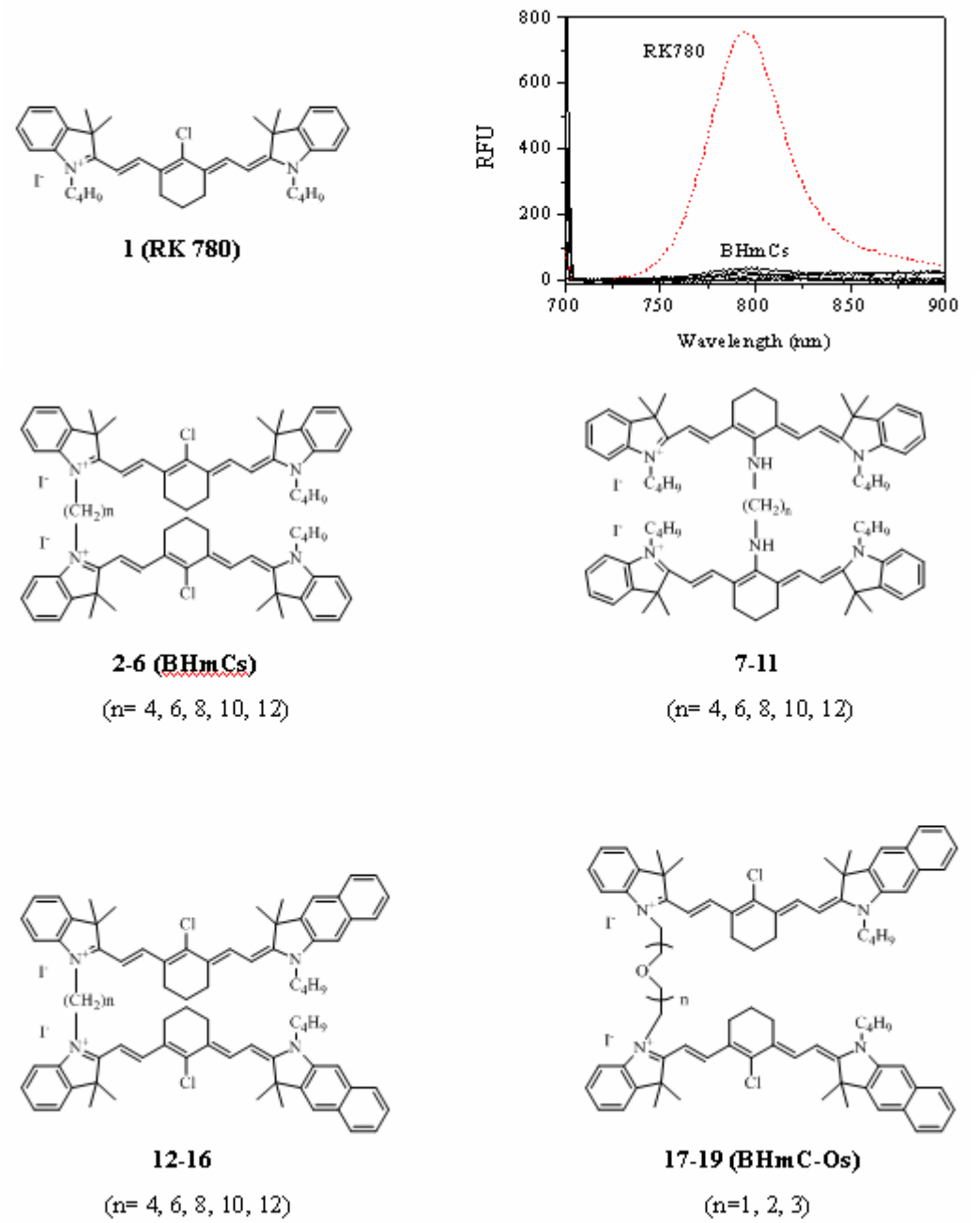

Figure 1.6. The low or non-fluorescent spectra of Bis-dyes caused by the H-characters in fluorescent spectroscopy. Fluorescence spectra of RK780 (**1**) and BHmCs (**2-19**) in 20 nM phosphate, pH 7.2. BHmCs exhibit negligible fluorescence compared to their monomer counterpart, **1**.

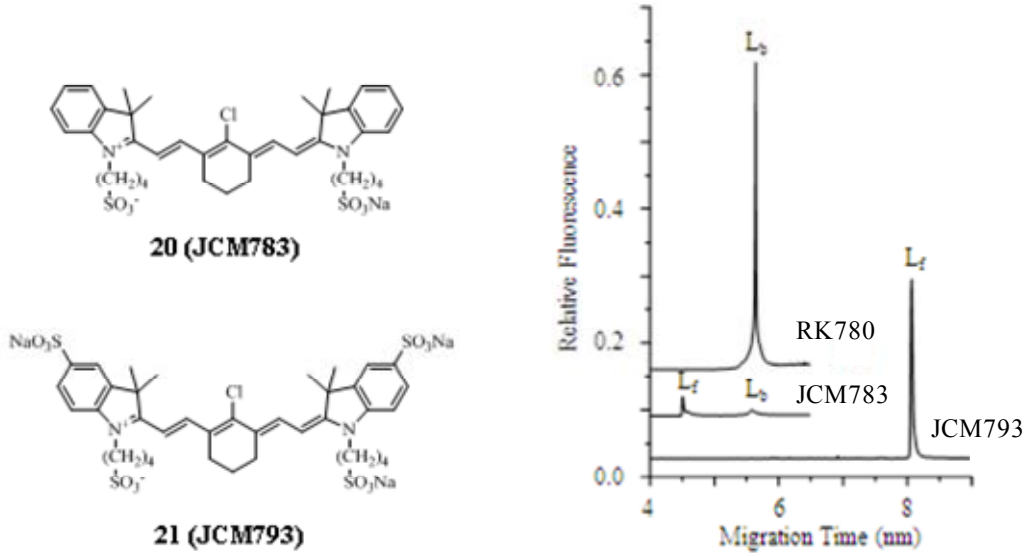

Figure 1.7. Dye **1** shows H-aggregates in spectrum and non-fluorescence in CE-LIF without a target molecule. Noncovalent labeling of human serum albumin (HSA) with CE-LIF detection. Different functional groups of heptamethine cyanine dyes influence the complexation of dye and protein. Dye **1** (RK780) shows stronger binding property to the protein relative to the other negatively charged dyes, **20** and **21**.

1.4.2. Binding stoichiometry and equilibria in non-covalent labeling

Non-covalent protein-dye labeling requires consideration of binding equilibria. The binding equilibria involve binding constant (association and dissociation constants), stoichiometry and cooperativity between a protein and a dye. Depending on binding constant and stoichiometry, the selectivity of a dye to a protein is determined, and the specificity of a dye is measured by cooperativity; cooperativity is shown is figure 1.8.[40] Spectroscopic analysis is commonly used for the measurement. Another consideration will be needed for the conformational changes of a protein upon binding to a dye since a non-covalently labeled dye may influence the secondary or the tertiary structure of a protein. Circular Dichroism (CD) and X-ray crystallography are universal for the determination. [40-42]

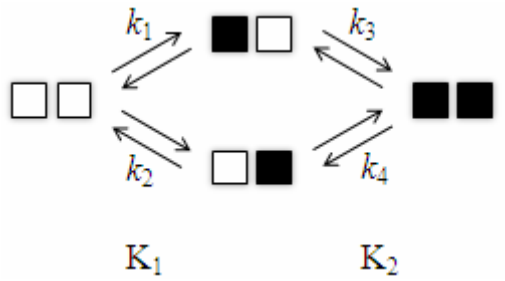

Figure 1.8. Representative cooperative pathway. Protein-dye stoichiometry is 1:2 in this figure. Two different pathways show how a binding site influences another binding site. The first bound dye weakens or strengthens the second bound dyes. Also, the second one influences the first one during complexation. Thus, marcro-binding constants, K_1 and K_2, are dependent on four micro-binding constants, k_1, k_2, k_3 and k_4. Hill's plot is used for the assay. More detailed examples and explanations are found in ref. 40.

Applications

Several methods for binding equilibria have been introduced. Hummel-Dreyer introduced for binding systems between the macro-biomolecule and small substance by gel filtration.[43, 44] Another type of measurement was achieved by ultracentrifugation. In this case, diffusion or sedimentation coefficient is used for the complex.[45] Equilibrium dialysis, gel filtration, or sedimentation requires relatively high sample concentration. The mole ratio method is utilized in the spectral change upon protein-ligand complexation.[46, 47] Wang and coworkers introduced the dicarboxylated derivative of DSTCY, 5,5'-dicarboxy-1,1'-disulfobutyl-3,3,3',3'-tetramethylindotricarbocyanine (DCDSTCY).[48] Using the molar ratio method, the binding number for DSTCY and DCDSTCY bound to BSA was 100 and 133 respectively.[48, 49] In the mid 90's, affinity capillary electrophoresis (ACE) appeared as an alternative method.[50-54] This method uses the charge-to-size ratio of CE when the mobility of complex is changed by the charged ligand and measures the binding constant of the ligand to a protein.[52] Light absorption or fluorescence is also used to study binding constants and

stoichiometry. Spectral changes of the complex at different wavelengths are used for those methods. The methods are more sensitive than others. Scatchard, modified Scatchard, Hill and Job's plot are commonly used. Hill's plot is known to measure the cooperativity of the complex, Scatchard plot requires spectral changes of unbound and bound molecules with two different absorbance maximum, and Job's plot is useful for the measurement of stoichiometry when the spectra are not separated.[40] Most experiments with NIR cyanine dyes in this dissertation used Job's plot for the stoichiometry measurement due to their H-type characters.

Spectroscopic analysis

Scatchard plot analysis has been used extensively (Equation 1 through 11) to determine association constants and stoichiometry in protein-ligand complexes.[55] When a free ligand, L_f, binds to a free protein, P_f, (1:1 stoichiometry) to form a new complex, C, the relationship can be expressed as followed:

$$P_f + L_f \Leftrightarrow C \quad (1)$$

Then equation 1 can be rearranged to give the binding constant of the protein-ligand complex in equation 2.

$$K = \frac{[C]}{[L_f][P_f]} \quad (2)$$

Once a ligand and a protein are combined in solution, there will be two homogeneous species of the protein present, one which is bound to the ligand, P_b, and the other which remains unbound and free in the solution. The total protein concentration, P_t, will be the sum of free and bound protein. Morever, bound and unbound ligand follows the same relationship.

$$P_t = P_f + P_b = P_f + C \quad (3)$$

$$L_t = L_f + L_b = L_f + C \quad (4)$$

The average number of bound ligand per protein, $\bar{\nu}$, is represented as followed:

$$\bar{\nu} = \frac{\text{moles of } L_b}{\text{Total moles of P}} = \frac{[L_b]}{[P_t]} = \frac{[C]}{[P_t]} \quad (5)$$

This can be rearranged to give,

$$\bar{\nu} = \frac{[C]}{[P_f]+[C]} = \frac{K[L_f][P_f]}{[P_f]+K[L_f][P_f]} = \frac{K[L_f]}{1+K[L_f]} \quad (6)$$

If the ligand absorbance increases with increasing protein concentration, the amount of ligand bound to protein can also be determined by the following equation:

$$f_b = \frac{A_f - A_i}{A_f - A_b} = \frac{\Delta A}{A_f - A_b} \quad (7)$$

where f_b is the fractional bound ligand, ΔA represents the change in ligand light absorption at the maximum wavelength, A_f represents the absorbance of the free ligand, and A_b is absorbance of the completely bound ligand. By using the total amount of ligand present, along with the fractional bound ligand parameter, the amount of protein-ligand complex can be determined as such:

$$L_t \cdot f_b = L_b = C \quad (8)$$

When Equation 4 is rearranged, the amount of unbound ligand is calculated:

$$L_t - C = L_f \quad (9)$$

Equation 6 is rearranged to

$$\frac{1}{\bar{\nu}} = \frac{1}{K[L_f]} + 1 \quad (10)$$

And then Equation 10 is rearranged to give the following linear relationship:

$$\frac{\bar{\nu}}{L_f} = K - K\bar{\nu} \quad (11)$$

When Equation 11 is plotted as $\bar{\nu}/[L_f]$ versus $\bar{\nu}$, the association constant, K, and the number of binding sites are calculated from the slope and x-intercept, respectively. The above relationship is called the Scatchard plot.

Cooperativity of multi-bound dyes is a need for non-covalent labeling. Suppose that two moles of a dye bind to a mole of a protein having two binding sites. This dye may or may not bind to the two different sites simultaneously. The simultaneous process of the two dye molecules to a protein can be treated as in 1:1 stoichiometry (non-cooperative pathway). In other words, the two dyes act as one molecule. However, this assumption becomes problematic when two dye molecules do not bind simultaneously. When one dye binds before the other, the binding system of the second dye molecule is affected. Furthermore, there may be a competitive interaction of the first bound dye molecule with the next dye molecule that binds. There may also be decreased binding affinity for the proceeding dye molecules if local binding sites are affected by the conformational changes (cooperative pathway). This sort of condition is well demonstrated in the Monod-Wyman-Changeau (MWC) model, the Koshland-Nemethy-Filmer (KNF) model, and elsewhere. [56-62]

Chromatographic analysis

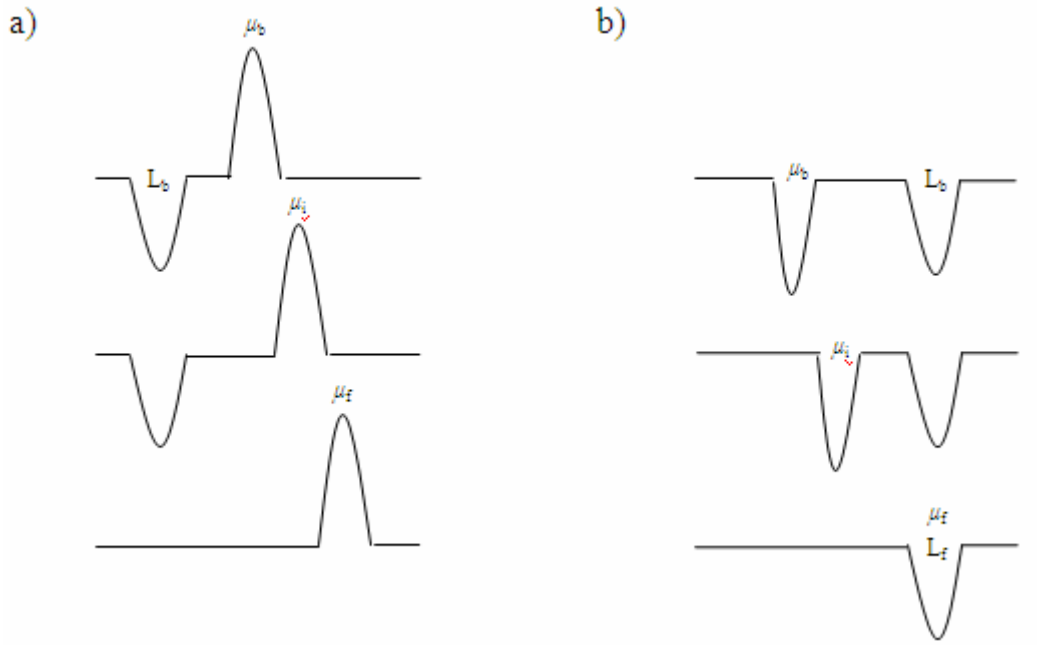

Figure 1.9. Illustration of a) affinity capillary electrophoresis (ACE) and b) vacancy affinity capillary electrophoresis (VACE). The mobility of free and bound ligand is used to find binding constant and stoichiometry.

In 1962, Hummel and Dreyer introduced a valuable theory for the separation of macromolecules and small ligands using gel-filtration.[43] In this method, the separation was dependent on not only the size of the free ligand and complex, but also the sieving material. Nowadays, with the increasing use of a capillary electrophoresis (CE) in the areas of chemistry and biology, the Hummel-Dreyer method has been reapplied. In CE, a minute sample is generally separated in a few minutes with high detection response. The separation

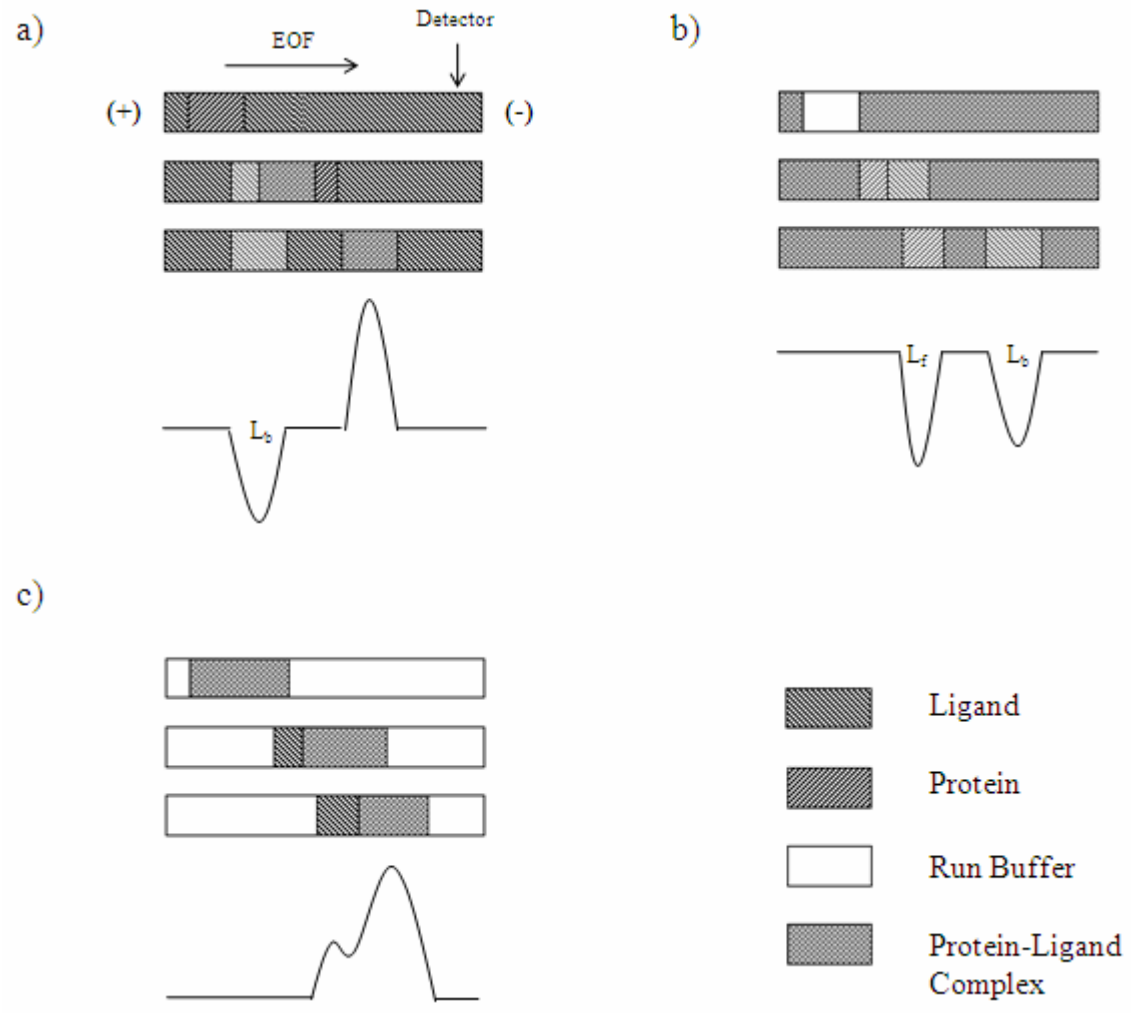

Figure 1.10. Illustration of a) Hummel-dreyer (HD), b) vacancy peak (VP) and c) frontal analysis methods. Peak areas or heights of free and bound ligand are used to find binding constant and stoichiometry. Redrawn after Hummel-Dreyer method.[43]

is based on the charge to size ratio of a molecule, so that the bound ligand and free ligand possessing different charges and size inside the capillary can be readily separated.

In CE, there are generally five methods of binding analysis: Hummel-Dreyer (HD), vacancy peak (VP), frontal analysis (FA), affinity capillary electrophoresis (ACE), vacancy affinity capillary electrophoresis (VACE).[7, 62, 63] In the Hummel-Dreyer method, the capillary is filled with a ligand dissolved in running buffer and a protein prepared in the same buffer is injected. This method is useful when the mobilities of unbound protein and the protein-ligand complex are identical. The negative, or vacant peak, corresponds to the absence of unbound ligand when the ligand binds to a protein; the positive peak represents the protein-ligand complex. In order to quantify the bound ligand, a simple relationship between the negative and positive peaks using either peak area or peak height can be used. Either an internal or external standard are used for these measurements.[53] In the vacancy peak method, the complex is prepared in running buffer and the concentration of the ligand is changed. Two negative peaks are observed; the first peak corresponding to the complex and the second representing the free ligand. Using internal calibration, the concentration of bound ligand can be calculated. It is important to note that in this method the mobility of the protein and the complex is nearly identical.[63] In frontal analysis, the capillary is filled with only buffer and the sample plug contains unbound ligand, unbound protein, and the protein-ligand complex. During analysis, the components are separated based on their mobilities. The mobility of bound and unbound protein is nearly identical, but the mobility the unbound ligand is sufficiently different. Therefore, by using a calibration curve, the concentration of bound ligand can be calculated. The experimental set-up for the affinity capillary electrophoresis method is the same as the Hummel-Dreyer method, but the mobility of the free protein and bound protein is different and their relationship is applied as follows:

$$f_b = \frac{\mu_i - \mu_f}{\mu_b - \mu_f} = \frac{\Delta\mu}{\mu_b - \mu_f} = \frac{[P_b]}{[P_t]} \quad (12)$$

where μ_i is the mobility of bound ligand, μ_f is the mobility of unbound protein, and μ_b is the mobility of completely bound ligand. Thus, the amount of unbound ligand, L_f can be calculated. Kawaoka introduced a modified Scatchard plot to estimate the binding constant of ligands to proteins.[65]

$$\frac{\Delta M_{P,L}}{[L]} = K_b \Delta M_{P,L}^{max} - K_b \Delta M_{P,L} \quad (13)$$

In this equation, $\Delta M_{P,L}$ is the difference in the migration ratio as a function of the concentration of the ligand, and $\Delta M_{P,L}^{max}$ is the maximum mobility of highly concentrated ligand, where $M=t_{eo}/t_p +1$, t represents the measured migration time of a neutral mobility marker, t_{eo} , and a protein, t_p .[53, 65-67] The Scatchard plot is given by $\Delta M_{P,L}/[L]$ versus $\Delta M_{P,L}$. Similarly, the experimental set-up of vacancy affinity capillary electrophoresis method is the same as the VP method,[64, 68] And binding analysis is expressed as followed:

$$f_b = \frac{\mu_i - \mu_f}{\mu b - \mu_f} = \frac{\Delta\mu}{\mu_b - \mu_f} = \frac{[L_b]}{[L_t]} \quad (14)$$

Table 1.4 compares the experimental set-up and analysis of the five methods.

Table 1.4. Comparison of five binding analysis methods with capillary electrophoresis. The similarity of their experimental set-ups and analytical methods is demonstrated.

Experimental set-up		Binding Analysis	
Injection plug	Run buffer	Peak area or height	Mobility
protein	ligand	HD	ACE
run buffer	complex	VP	VACE
complex	run buffer	FA	

Other techniques for binding analysis

As previously mentioned, diffusion or sedimentation coefficient analysis can be used to determine binding parameters as well. First, the diffusion (D) and sedimentation (s) coefficients are used to calculate the molecular mass of the complex. Subsequently, the stoichiometry is determined by comparing the molecular mass of the macromolecule-ligand complex with free macromolecule. D can be determined either through laser-light scattering measurements or using by using the following equation:

$$\mathrm{D} = \frac{k\mathrm{T}}{f} = \frac{\mathrm{RT}}{\mathcal{N} f} \tag{15}$$

where k is the Boltzmann constant, T is the absolute temperature, R is the gas constant, N is Avogadro's number, and f is the frictional coeffiecient.[69, 70] The frictional coefficient is the measurement of the resistance of a molecule in solvent. This value is dependent on the size and shape of the molecule. Fortunately, this complicated value can be eliminated by substituting it with the sedimentation coefficient. The sedimentation coefficient is determined by the following relationship:

$$\frac{\mathrm{M}(1-\bar{v}\rho)}{\mathcal{N} f} = \mathrm{s} \tag{16}$$

where M is the molecular weight, $\bar{v}$ is the partial specific volume of the particle, and ρ is the solution density. Therefore, the molecular weight can be calculated from Equation 15 and 16. Note that the $\bar{v}$ in Equation 18 is different from the $\bar{\mathrm{v}}$ in Equation 5. Alternately, the Svedberg equation (Equation 17) can be used to determine M as followed:

$$\mathrm{M} = \frac{\mathrm{sRT}}{\mathrm{D}(1-\bar{v}\rho)} \tag{17}$$

The drawback of methods utilizing sedimentation or diffusion methods is that a ligand must have a relatively large mass, because a protein or macromolecule bound to a small ligand will be not be distinguishable.

1.5. Summary

The high ε and Φ of NIR cyanine dyes allow low LOD, and the simple synthesis procedure and the notable spectral difference enable NIR dyes to apply bio-analysis. Moreover, compared to radio-labeling, MIR cyanine dye labeling provides simple labeling scheme and safe experimental environment to handle whole procedures. Covalent and non-covalent labeling s are a representative example of the protein analysis. The covalent labeling needs a functionalized dye and a particular amino acid and requires complicated labeling procedure. In contrast, the non-covalent labeling needs a binding site of a protein and requires a consideration of binding equilibria. However, both give low LOD with NIR cyanine dyes. In the following chapters, non-covalent labeling of bis-heptamethine cyanine (BHmC) dyes and their bioanalytical applications will be presented.

References

1. Kashida, H.; Asanuma, H.; Komiyama, M., Alternating hetero H aggregation of different dyes by interstrand stacking from two DNA-dye conjugates. *Angew Chem Int Ed Engl* **2004,** 43, (47), 6522-5.

2. Yarmoluk, S. M.; Lukashov, S. S.; Ogul'Chansky, T. Y.; Losytskyy, M. Y.; Kornyushyna, O. S., Interaction of cyanine dyes with nucleic acids. XXI. Arguments for half-intercalation model of interaction. *Biopolymers* **2001,** 62, (4), 219-27.

3. Ogulchansky, T. Y.; Losytskyy, M. Y.; Kovalska, V. B.; Lukashov, S. S.; Yashchuk, V. M.; Yarmoluk, S. M., Interaction of cyanine dyes with nucleic acids. XVIII. Formation of the carbocyanine dye J-aggregates in nucleic acid grooves. *Spectrochim Acta A Mol Biomol Spectrosc* **2001,** 57, (13), 2705-15.

4. Ogul'chansky, T.; Losytskyy, M.; Kovalska, V. B.; Yashchuk, V. M.; Yarmoluk, S. M., Interactions of cyanine dyes with nucleic acids. XXIV. Aggregation of monomethine cyanine dyes in presence of DNA and its manifestation in absorption and fluorescence spectra. *Spectrochim Acta A Mol Biomol Spectrosc* **2001,** 57, (7), 1525-32.

5. Ogul'chansky, T.; Yashchuk, V. M.; Losytskyy, M.; Kocheshev, I. O.; Yarmoluk, S. M., Interaction of cyanine dyes with nucleic acids. XVII. Towards an aggregation of cyanine dyes in solutions as a factor facilitating nucleic acid detection. *Spectrochim Acta A Mol Biomol Spectrosc* **2000,** 56, (4), 805-14.

6. Patonay, G.; Strekowski, L.; Kim, J. S.; Henary, M., The increasing role of NIR fluorescence spectroscopy in bioanalytical chemistry *NIR news* **2007,** 18, (3), 7-9.

7. Yan, W.; Colyer, C. L., Investigating noncovalent squarylium dye-protein interactions by capillary electrophoresis-frontal analysis. *Journal of Chromatography, A* **2006,** 1135, (1), 115-121.

8. Kim, J. S.; Kodagahally, R.; Strekowski, L.; Patonay, G., A study of intramolecular

H-complexes of novel bis(heptamethine cyanine) dyes. *Talanta* **2005,** 67, (5), 947-954.

9. Patonay, G.; Kim, J. S.; Kodagahally, R.; Strekowski, L., Spectroscopic study of a novel bis(heptamethine cyanine) dye and its interaction with human serum albumin. *Appl Spectrosc* **2005,** 59, (5), 682-90.

10. Baars, M.; Patonay, G., Ultrasensitive detection of closely related angiotensin I peptides using capillary electrophoresis with near-infrared laser-induced fluorescence detection. *Anal Chem* **1999,** 71, (3), 667-71.

11. Tarazi, L. G., A.; Patonay, G.; Strekowski, L., Spectral characterization of a novel near-infrared cyanine dye: a study of its complexation with metal ions. *Talanta* **1998,** 46, (6).

12. Legendre, B. L.; Moberg, D. L.; Williams, D. C.; Soper, S. A., Ultrasensitive near-infrared laser-induced fluorescence detection in capillary electrophoresis using a diode laser and avalanche photodiode. *Journal of Chromatography A* **1997,** 779, (1-2), 185-194.

13. Tatikolov, A. S.; Costa, S. M., Complexation of polymethine dyes with human serum albumin: a spectroscopic study. *Biophys Chem* **2004,** 107, (1), 33-49.

14. Sowell, J.; Agnew-Heard, K. A.; Christian Mason, J.; Mama, C.; Strekowski, L.; Patonay, G., Use of non-covalent labeling in illustrating ligand binding to human serum albumin via affinity capillary electrophoresis with near-infrared laser induced fluorescence detection. *Journal of Chromatography, B: Biomedical Sciences and Applications* **2001,** 755, (1-2), 91-99.

15. Moody, E. D.; Viskari, P. J.; Colyer, C. L., Non-covalent labeling of human serum albumin with indocyanine green: a study by capillary electrophoresis with diode laser-induced fluorescence detection

Journal of Chromatography, B: Biomedical Sciences and Applications

1999, 729, (1 + 2), 55-64.

16. Colyer, C. L., Noncovalent labeling of proteins in capillary electrophoresis with

laser-induced fluorescence detection. *Cell Biochemistry and Biophysics* **2000,** 33, 323-337.

17. McCorquodale, E. M.; Colyer, C. L., Indocyanine green as a noncovalent, pseudofluorogenic label for protein determination by capillary electrophoresis. *Electrophoresis* **2001,** 22, (12), 2403-2408.

18. Welder, F.; Paul, B.; Nakazumi, H.; Yagi, S.; Colyer, C. L., Symmetric and asymmetric squarylium dyes as noncovalent protein labels: a study by fluorimetry and capillary electrophoresis. *J Chromatogr B Analyt Technol Biomed Life Sci* **2003,** 793, (1), 93-105.

19. Moody, E. D.; Viskari, P. J.; Colyer, C. L., Non-covalent labeling of human serum albumin with indocyanine green: a study by capillary electrophoresis with diode laser-induced fluorescence detection. *Journal of Chromatography, B: Biomedical Sciences and Applications* **1999,** 729, (1 + 2), 55-64.

20. Patonay, G.; Salon, J.; Sowell, J.; Strekowski, L., Noncovalent labeling of biomolecules with red and near-infrared dyes. *Molecules* **2004,** 9, (3), 40-49.

21. Narayanan, N. Cyanine dye compounds and labeling methods. 6593148, 2003.

22. Mishra, A.; Behera, R. K.; Behera, P. K.; Mishra, B. K.; Behera, G. B., Cyanines during the 1990s: A Review. In 2000; Vol. 100, pp 1973-2012.

23. Fukushima, T.; Usui, N.; Santa, T.; Imai, K., Recent progress in derivatization methods for LC and CE analysis. *J Pharm Biomed Anal* **2003,** 30, (6), 1655-87.

24. Bardelmeijer, H. A.; Lingeman, H.; De Ruiter, C.; Underberg, W. J. M., Derivatization in capillary electrophoresis. *Journal of Chromatography, A* **1998,** 807, (1), 3-26.

25. Sowell, J.; Parihar, R.; Patonay, G., Capillary electrophoresis-based immunoassay for insulin antibodies with near-infrared laser induced fluorescence detection. *J Chromatogr B Biomed Sci Appl* **2001,** 752, (1), 1-8.

26. Okuyama, T.; Kasai, H., [Protein determination by TNBS method (author's transl)]. *Tanpakushitsu Kakusan Koso* **1973,** 18, (13), 1153-9.

27. Jacobsen, C., Trinitrophenylation of the bilirubin binding site of human serum albumin. *Int J Pept Protein Res* **1975,** 7, (2), 161-5.

28. Anderson, J. R.; Chemiavskaya, O.; Gitlin, I.; Engel, G. S.; Yuditsky, L.; Whitesides, G. M., Analysis by capillary electrophoresis of the kinetics of charge ladder formation for bovine carbonic anhydrase. *Anal Chem* **2002,** 74, (8), 1870-8.

29. Menon, M. K.; Zydney, A. L., Determination of effective protein charge by capillary electrophoresis: effects of charge regulation in the analysis of charge ladders. *Anal Chem* **2000,** 72, (22), 5714-7.

30. Gao, J.; Mammen, M.; Whitesides, G. M., Evaluating electrostatic contributions to binding with the use of protein charge ladders. *Science (Washington, D. C.) FIELD Full Journal Title:Science (Washington, D. C.)* **1996,** 272, (5261), 535-7.

31. S. Sinha , S. S., A.K. Ray and K. Dasgupta, The effect of dye photodegradation on the performance of dye lasers *Applied Physics B* **2004,** 78, 401-408.

32. Dougherty, T. J.; Kaufman, J. E.; Goldfarb, A.; Weishaupt, K. R.; Boyle, D.; Mittleman, A., Photoradiation therapy for the treatment of malignant tumors. *Cancer Res* **1978,** 38, (8), 2628-35.

33. West, W.; Gilman, P. B., *Theory of the Photographic Process*. Macmillan: New York, 1977.

34. Sturmer, D. M. a. H., D. W., *The Theory of the Photographic Process*. 4th ed ed.

35. Jelley, E. E., Molecular, nematic and crystal states of 1,1'-diethyl-y-cyanine chloride. *Nature (London, United Kingdom)* **1937,** 139, 631-2.

37. Herz, A., Aggregation of sensitizing dyes in solution and their adsorption onto silver halides. *Advances in Colloid and Interface Science* **1977,** 8, (4), 237-298.

38. Czikkely V; Försterling H D; H, K., Extended dipole model for aggregates of dye molecules. *Chemical Physics Letters* **1970,** 6, (3), 207-210.

39. Czikkely V; Försterling H D; H, K., Light absorption and structure of aggregates of dye molecules. *Chem. Phys. Lett* **1970,** 6.

40. Holde, K. E. v.; Johnson, W. C.; Ho, P. S., *Principles of Physical Biochemistry*. 2nd ed. ed.; Pearson Education, Inc.: New Jersey, 2006; p 605 pp.

41. Bulheller, B. M.; Rodger, A.; Hirst, J. D., Circular and linear dichroism of proteins. *Phys Chem Chem Phys* **2007,** 9, (17), 2020-35.

42. Drenth, J., *Principles of Protein X-Ray Crystallography*. 3rd ed. ed.; Springer Science New York, 2007.

43. Soltes, L., The Hummel-Dreyer method: Impact in pharmacology. *Biomedical Chromatography* **2004,** 18, (4), 259-271.

44. Hummel, J. P.; Dreyer, W. J., Measurement of protein-binding phenomena by gel filtration. *Biochim Biophys Acta* **1962,** 63, 530-2.

45. Boudier, C.; Bieth, J. G., The proteinase:mucus proteinase inhibitor binding stoichiometry. *Journal of Biological Chemistry* **1992,** 267, (7), 4370-5.

46. Meyer, A. S., Jr.; Ayres, G. H., The mole ratio method for spectrophotometric determination of complexes in solution. *Journal of the American Chemical Society* **1957,** 79, 49-53.

47. Chriswell, C. D.; Schilt, A. A., New and improved techniques for applying the mole ratio method to the identification of weak complexes in solution. *Analytical Chemistry* **1975,** 47, (9), 1623-9.

48. Wang, H.; Li, W. R.; Guo, X. F.; Zhang, H. S., Spectrophotometric determination of total protein in serum using a novel near-infrared cyanine dye, 5,5 '-dicarboxy-1,1 '-disulfobutyl-3,3,3 ',3 '-tetramethylindotricarbocyanine. *Analytical and Bioanalytical*

Chemistry **2007,** 387, (8), 2857-2862.

49. Van Dyck, S.; Kaale, E.; Novakova, S.; Glatz, Z.; Hoogmartens, J.; Van Schepdael, A., Advances in capillary electrophoretically mediated microanalysis. *Electrophoresis* **2003,** 24, (22-23), 3868-3878.

50. Avila, L. Z.; Chu, Y. H.; Blossey, E. C.; Whitesides, G. M., Use of affinity capillary electrophoresis to determine kinetic and equilibrium constants for binding of arylsulfonamides to bovine carbonic anhydrase. *Journal of Medicinal Chemistry* **1993,** 36, (1), 126-33.

51. Chu, Y. H.; Whitesides, G. M., Affinity capillary electrophoresis can simultaneously measure binding constants of multiple peptides to vancomycin. *Journal of Organic Chemistry* **1992,** 57, (13), 3524-5.

52. Chu, Y. H.; Avila, L. Z.; Biebuyck, H. A.; Whitesides, G. M., Use of affinity capillary electrophoresis to measure binding constants of ligands to proteins. *J Med Chem FIELD Full Journal Title:Journal of medicinal chemistry* **1992,** 35, (15), 2915-7.

53. Gomez, F. A.; Avila, L. Z.; Chu, Y. H.; Whitesides, G. M., Determination of binding constants of ligands to proteins by affinity capillary electrophoresis: compensation for electroosmotic flow. *Anal Chem FIELD Full Journal Title:Analytical chemistry* **1994,** 66, (11), 1785-91.

54. Kraak, J. C.; Busch, S.; Poppe, H., Study of protein-drug binding using capillary zone electrophoresis. *J Chromatogr FIELD Full Journal Title:Journal of chromatography* **1992,** 608, (1-2), 257-64.

55. Scatchard, G., The attractions of proteins for small molecules and ions. *Ann. N. Y. Acad. Sci.* **1949,** 51, 660-672.

56. Monod, J.; Wyman, J.; Changeux, J. P., On the Nature of Allosteric Transitions: a Plausible Model. *J Mol Biol* **1965,** 12, 88-118.

57. Koshland, D. E., Jr.; Nemethy, G.; Filmer, D., Comparison of experimental binding data and theoretical models in proteins containing subunits. *Biochemistry* **1966,** 5, (1), 365-85.

58. Perutz, M. F., Mechanisms of cooperativity and allosteric regulation in proteins. *Q. Rev. Biophys. FIELD Full Journal Title:Quarterly Reviews of Biophysics* **1989,** 22, (2), 139-237, 8 plates.

59. Ackers, G. K.; Doyle, M. L.; Myers, D.; Daugherty, M. A., Molecular code for cooperativity in hemoglobin. *Science (Washington, D. C., 1883-) FIELD Full Journal Title:Science (Washington, DC, United States)* **1992,** 255, (5040), 54-63.

60. Ben-Naim, A., *Cooperativity and Regulation in Biochemical Processes*. Kluwer Academic/ Plenum Publishers: New York, 2001.

61. Sackett, D. L.; Saroff, H. A., The multiple origins of cooperativity in binding to multi-site lattices. *FEBS Lett* **1996,** 397, (1), 1-6.

62. Spassov, V.; Bashford, D., Electrostatic coupling to pH-titrating sites as a source of cooperativity in protein-ligand binding. In 1998; Vol. 7, pp 2012-2025.

63. Busch, M. H. A.; Kraak, J. C.; Poppe, H., Principles and limitations of methods available for the determination of binding constants with affinity capillary electrophoresis. *Journal of Chromatography, A* **1997,** 777, (2), 329-353.

64. Busch, M. H. A.; Carels, L. B.; Boelens, H. F. M.; Kraak, J. C.; Poppe, H., Comparison of five methods for the study of drug-protein binding in affinity capillary electrophoresis. *Journal of Chromatography, A* **1997,** 777, (2), 311-328.

65. Kawaoka, J.; Gomez, F. A., Use of mobility ratios to estimate binding constants of ligands to proteins in affinity capillary electrophoresis. *Journal of Chromatography, B: Biomedical Sciences and Applications* **1998,** 715, (1), 203-210.

66. Yang, J.; Bose, S.; Hage, D. S., Improved reproducibility in capillary electrophoresis through the use of mobility and migration time ratios. *Journal of Chromatography A* **1996,**

735, (1-2), 209-220.

67. Bose, S.; Yang, J.; Hage, D. S., Guidelines in selecting ligand concentrations for the determination of binding constants by affinity capillary electrophoresis. *Journal of Chromatography B: Biomedical Sciences and Applications* **1997,** 697, (1-2), 77-88.

68. Erim, F. B.; Kraak, J. C., Vacancy affinity capillary electrophoresis to study competitive protein-drug binding. *Journal of Chromatography, B: Biomedical Sciences and Applications* **1998,** 710, (1 + 2), 205-210.

69. James L. Cole; Hansen, J. C., Analytical Ultracentrifugation as a Contemporary Biomolecular Research Tool *Journal of Biomolecular Techniques* **1999,** 10, (4), 163-176.

70. Laue, T. M.; Stafford, W. F., 3rd, Modern applications of analytical ultracentrifugation. *Annu Rev Biophys Biomol Struct* **1999,** 28, 75-100.

Chapter 2. Spectroscopic Study of a Novel Bis(heptamethine cyanine) Dye and Its Interaction with Human Serum Albumin

2.1. Introduction

Carbocyanines have recently received significant attention as non-covalent labels for the detection of protein and other biomolecules.[1-5] In most case, the labeling requires hydrophobic dyes that commonly aggregate in aqueous solutions.[4, 6-10] In the presence of protein or other large biomolecules, the aggregates are broken up as the fluorescence intensity of the monomer band of dyes is enhanced. Examples of such applications have been demonstrated by using human serum albumin (HSA), transport blood plasma protein, and DNA, among others.[11-14] The main spectroscopic feature of this non-covalent interaction is the increase in the fluorescence quantum yield (Φ), facilitating the detection of biomolecules.[5, 13, 15, 16] Several non-covalent interactions have been studied in the past.[14, 16, 17] The main driving factor in studying non-covalent interactions is to replace the labor-intensive conventional covalent label methods.[13, 16] In addition to the relatively complicated chemistry of covalent labeling, often there is either no proper functionality available for covalent labeling on the biomolecule or covalent labeling may influence the proper function of the biomolecule.[18, 19] By contrast, non-covalent labels can be simply mixed with the biomolecule with no additional preparation steps.[20, 21] However, there is a difficulty in determining a non-covalent label's physical mechanisms; hydrophobic interactions, electrostatic interactions and hydrogen bonding. All these factors are important during the complex formation with the biomolecule. One of the most important variables that needs to be measured during this binding process is the determination of the binding constant and the binding stoichiometry. The dye-protein complex can be characterized by simply measuring the emission of the complex relative to that of free dye.[13]

The major problem with non-covalent interactions is that the dye that is not bound to the biomolecule exhibits significant fluorescence.[2, 11, 22] Although NIR dyes tend to form non-fluorescent aggregates when in aqueous solutions, aggregate formation is not significant at

low concentrations. The use of higher concentrations is impractical in most non-covalent labeling situations. In the ideal case, the free dye would be in a non-fluorescent aggregate state at any concentration. As part of these studies, a conformationally flexible bis-heptamethine cyanine dye linked with decamethylene chain (BHmC-10) has been synthesized (Figure 2.1). The monomer counterpart of BHmC-10 is RK780. H-type intra-dimerization of BHmC-10 was expected so that it exhibits low or non-fluorescence compared to its monomer counterpart in aqueous solutions (closed clam-shell form). Also, it was expected that the complexation of BHmC-10 with a protein breaks up the intra-dimer form (open clam-shell form) and increases fluorescence. The choice of this dimmer for synthesis was made after inspecting molecular models[23] of several dye candidates with internal bridges ranging from four to ten carbon atoms (see supplementary research in ref. 13). The analysis strongly suggested that unfavorable steric interactions within the polymethylene bridge were the lowest for the molecule of BHmC-10 in a number of conformations mimicking intramolecular aggregation.

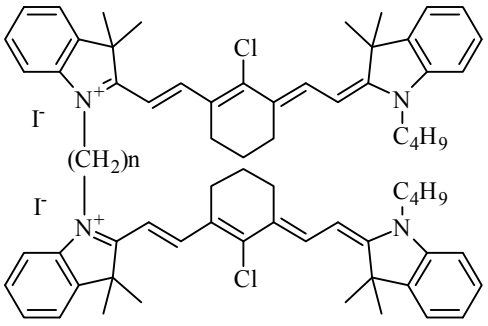

BHmC-10 (n=10)

Figure 2.1. Chemical structure of bis-heptamethin cyanine dye linked with decamethylene chain.

2.2. Experimental

2.2.1. Materials and solvents

Fatty acid free HSA (≥ 96% purity) was obtained from Sigma (St. Louis, MO). Sodium phosphate monobasic (monohydrate) and sodium phosphate dibasic (monohydrate) were purchased from Fisher Scientific (Fair Lawn, NJ). Water was Nanopure grade (Barnstead model D4751 ultrapure water system). Methanol was obtained from the Aldrich Chemical Company (Milwaukee, WI) in HPLC grade.

2.2.2. Instrumentation

Absorption measurements were acquired on a Perkin-Elmer Lambda UV/VIS/NIR (Lambda 50) spectrophotometer (Norwalk, CT). Fluorescence emission spectra were taken with a K2 spectrofluorometer (ISS, Champaign, IL) equipped with a R928 Hamamatsu photomultiplier tube (Bridgewater, NJ). Commercial GaAlAs laser diodes (Laser Max, Rochester, NY) were used as the excitation source at 690 nm. The slit widths were 2 mm and the integration time was 3 sec. All absorption and fluorescence measurements were taken in a 1 cm cuvette.

2.2.3. Methods

Stock solutions of RK780 (2 mM) and BHmC-10 (1 mM) in methanol were stored in the dark at 4 °C when not in use. The 0.1 mM stock solution of HSA was prepared in 20 mM dibasic phosphate buffer solution and adjusted to pH 7.2 with phosphoric acid. Stock solution of HSA was prepared fresh daily.

The dye-HSA mixture was vortexed for 30 s to allow for equilibration. Various dye-HSA ratios were investigated to determine the utility of BHmC-10 as a noncovalent label for serum albumin. For all non-covalent labeling, the stock solution of the dimeric cyanine in

methanol was diluted with phosphate buffer because the dye has relatively poor solubility in aqueous solutions. All working solutions contained only 1 % (v/v) methanol to facilitate dye dissolution but to avoid denaturation of HSA. All measurements were performed at room temperature.

2.3. Results and discussion

The photophysical properties of conformationally flexible BHmC-10 were investigated with various conditions. It was expected that the spectral shift of BHmC-10 in absorption measurement can be seen when inter and/or intra-aggregates are presented as fluorescent intensity changes. In addition, the flexibility of BHmc-10 is studied in presence of various HSA concentrations. The binding equilibria of the complex were also studied.

2.3.1. Photophysical properties of BHmC-10

In this study, photophysical properties of a novel dimeric dye, BHmC-10 in organic solvent and aqueous buffer were characterized. All spectra were normalized for easy comparison. In general, monomeric carbocyanines form aggregates with increasing dye concentration even in organic solvent.[11, 24-27] Figure 2.2. shows the normalized spectra of various concentrations of BHmC-10 in methanol. No significant spectral changes can be observed. It is clear that the spectra of bis-dye are less dependent on dye concentration in methanol compared to those of monomeric carbocyanine dyes, RK780.

The spectra of RK780 were also obtained in phosphate buffer. When comparing normalized spectra of RK780 and BHmC-10 in aqueous buffer solution (Figure. 2.3.), two significant differences can be observed at 435 nm and 710 nm. According to the literature, these features are characteristic of H aggregation. As can be seen, the H bands for RK780 are much weaker than those for BHmC-10. It is likely, that both intra and intermolecular

aggregation take place in the case of dimeric dye.

2.3.2. Dye-HSA interaction

Absorption spectra

The absorption spectrum of BHmC-10 in methanol has a characteristic band at 781 nm. This band intensity is diminished in phosphate buffer (Figure. 2.4.). The absorption maximum of the dye in phosphate buffer is slightly red shifted (λ_{max}= 792 nm) compared to its maximum in methanol. It is likely that this dye forms mostly intramolecular aggregation in aqueous solution, but some intermolecular aggregation is also likely. In the presence of HSA the spectra become similar to that in methanol (λ_{max}= 787 nm). This shift is most likely caused by the decrease in intramolecular van der Waals interactions as the clam-shell opens up. Similar shifts have been observed for monomeric carbocyanine dye aggregates upon the formation of the dye–HSA complex.

Representative absorption spectra of BHmC-10 in the presence and absence of HSA are given in Figure. 2.5. Two characteristic bands (λ_{max} at 792 nm and 435 nm) can be distinguished in the absorption spectra in buffer solution compared to dye solution in methanol at the same concentration. The long wavelength absorption band (λ_{max}= 792 nm) is S0-S1 transition of the strong clam-shell intramolecular dimer dye and weak intermolecular aggregates in aqueous buffer solution that is red-shifted about 11 nm in comparison to the similar transition in methanol due to intramolecular interactions between the two carbocyanine moieties and intermolecular interaction between the two or more dimeric molecules. Upon addition of HSA the inter- and intramolecular aggregates break up and concomitant changes in the H, D, and M bands are observed. The absorption spectra of the dimeric dye at constant concentration of 10^{-5} M with different amounts of HSA added are

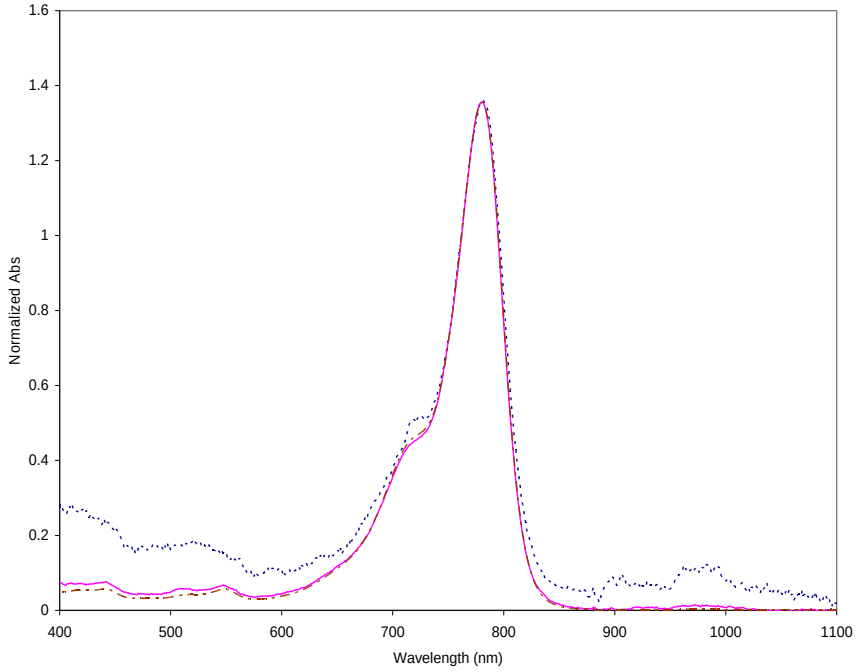

Figure 2.2. Concentration effect on aggregation of BHmC-10 in methanol. Normalized absorption spectra were taken at three different concentrations: 0.1 μM (dotted line), 1 μM (dashed line), and 10 μM (solid line).

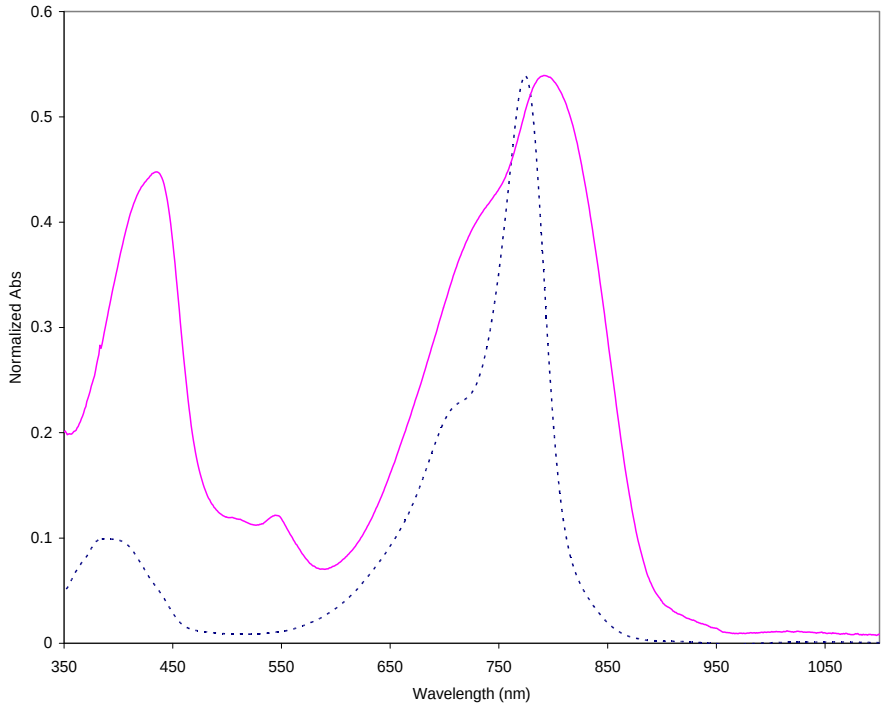

Figure 2.3. Normalized absorption spectra of RK780 (dotted line) and BHmC-10 (solid line) in phosphate buffer at 10 μM dye concentration.

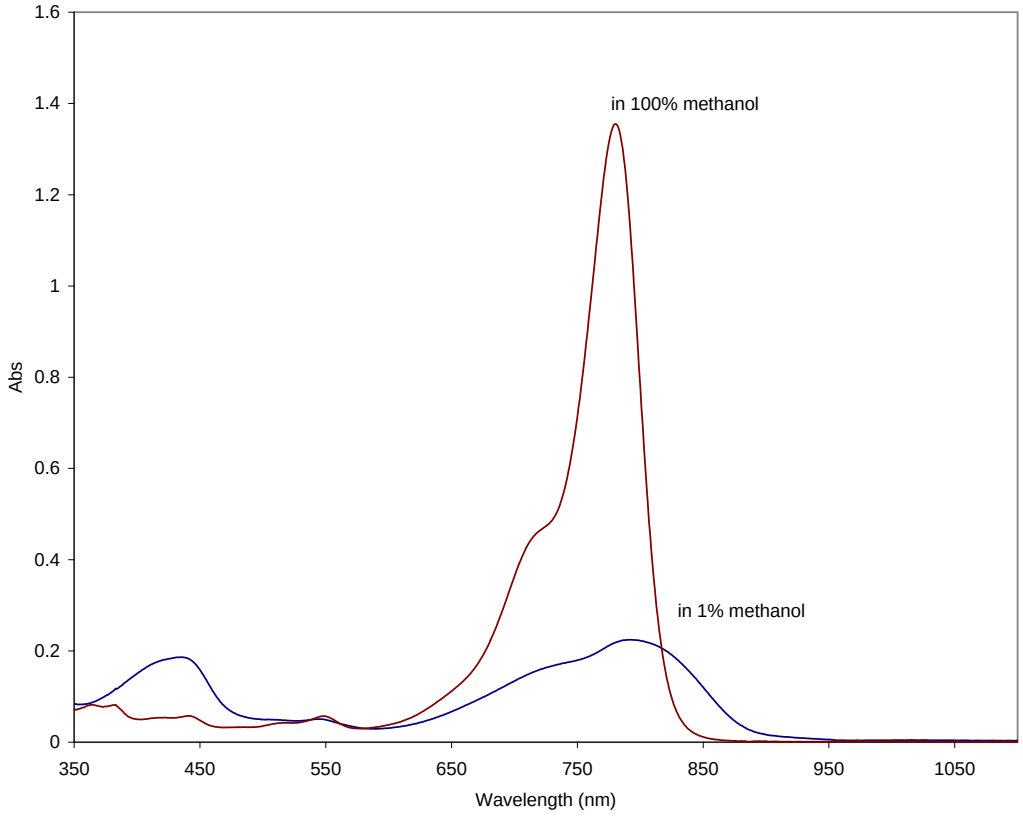

Figure 2.4. Absorption spectra of BHmC-10 in methanol (top) and methanol-phosphate buffer mixture (bottom) at room temperature.

also depicted in Figure 2.6.. Upon increase in the HSA concentration, up to C_{HSA}=50 µM, the characteristic features of the dimeric dye absorption spectra change sharply. The M-band relative intensity increases strongly while the D-band and H-band dramatically decrease in intensity. Up to C_{HSA}=50 µM, a continuous decrease can be observed in the H-band intensity. However, at C_{HSA}=70 µM, there is negligible change in the intensities of H-, D-, and M-bands and absorption of HSA becomes more pronounced. Unfortunately, the overlap of the HSA absorption in this range prevents the observation of additional changes. Clearly, as the HSA concentration increases, the concentration of the inter- and intramolecular H-aggregates decreases and a fraction of the dimeric dye molecules bound to HSA in an open form

increases. This indicates that the interaction between the HSA and the open form dimeric cyanine dye is stronger than the intramolecular interaction between the two carbocyanine moieties in a dye free in solution. This is in good agreement with similar studies utilizing monomeric cyanines and HSA. Clearly, binding of BHmC-10 to HSA is more favorable than forming an intramolecular H-aggregate. It can be expected that intermolecular interactions between bis-carbocyanine molecules are even weaker, especially at low concentrations.

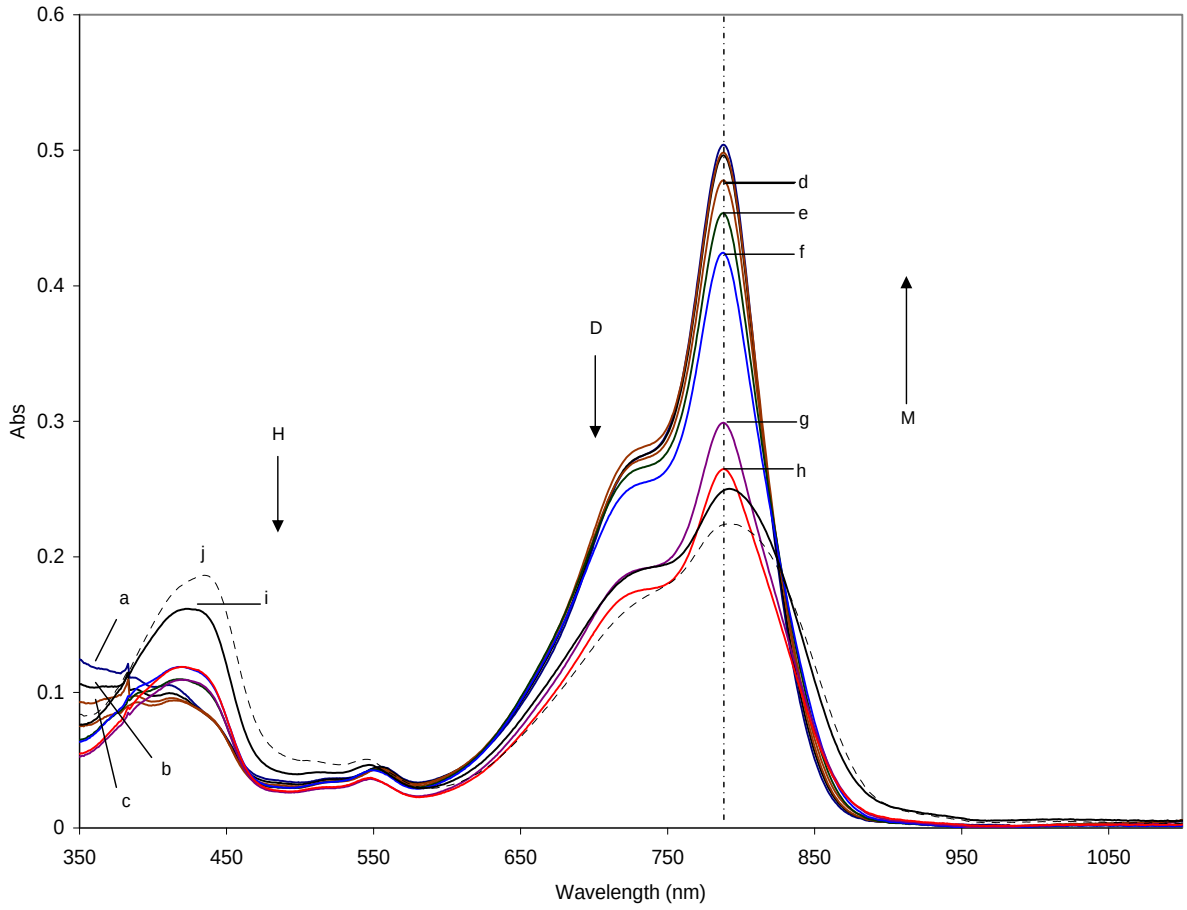

Figure 2.5. Absorption of BHmC-10 (10 μM) in the presence of HSA: (a) 100, (b) 70, (c) 50, (d) 30, (e) 10, (f) 5, (g) 1, (h) 0.5, (i) 0.1, and (j) 0 μM. The arrows indicate the spectral changes of H-, D-, and M-band.

Fluorescence spectra

The novel bis-cyanine, BHmC-10 was found to interact with HSA, resulting in significantly enhanced fluorescence. The fluorescence emission of the dye is very weak in aqueous solutions relative to pure methanol. This is very advantageous for the use of bis-cyanine as a non-covalent label because the unbound form of the dye has much lower quantum yield (Figure. 2.6.). It should be noted that one of the major drawbacks of using monomeric carbocyanines as non-covalent labels is the existence of a relatively strong fluorescence of the unbound free form of the non-covalent label.

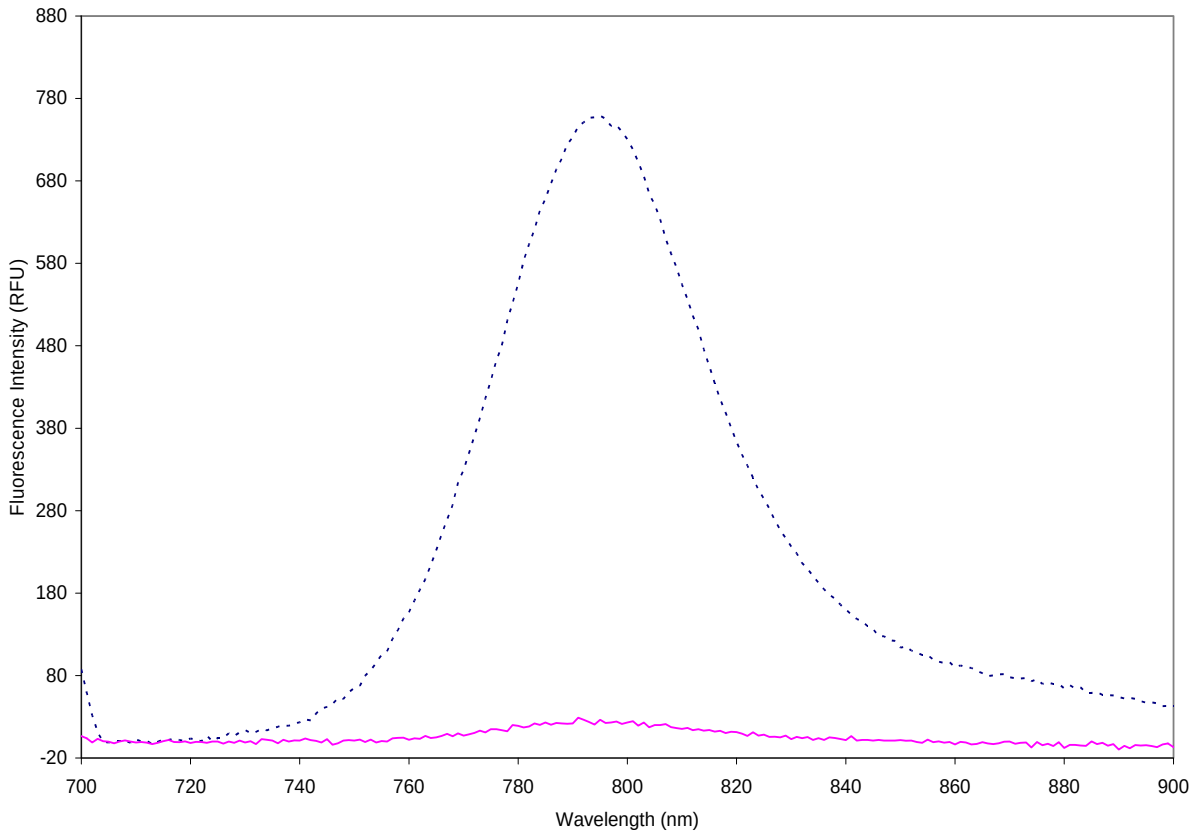

Figure 2.6. Fluorescence emission spectra of RK780 (dotted line) and BHmC-10 (solid line) in phosphate buffer at 10 µM dye concentration.

In free dye solutions, a fluorescence band at λ_{max} = 810 nm becomes clearly apparent at the dye concentration of 10 µM in methanol. The emission band at λ_{max} = ~794 nm can be

interpreted as a band of inherent dimeric dye fluorescence in buffer solution that is blue-shifted over 16 nm in comparison to the emission in methanol.

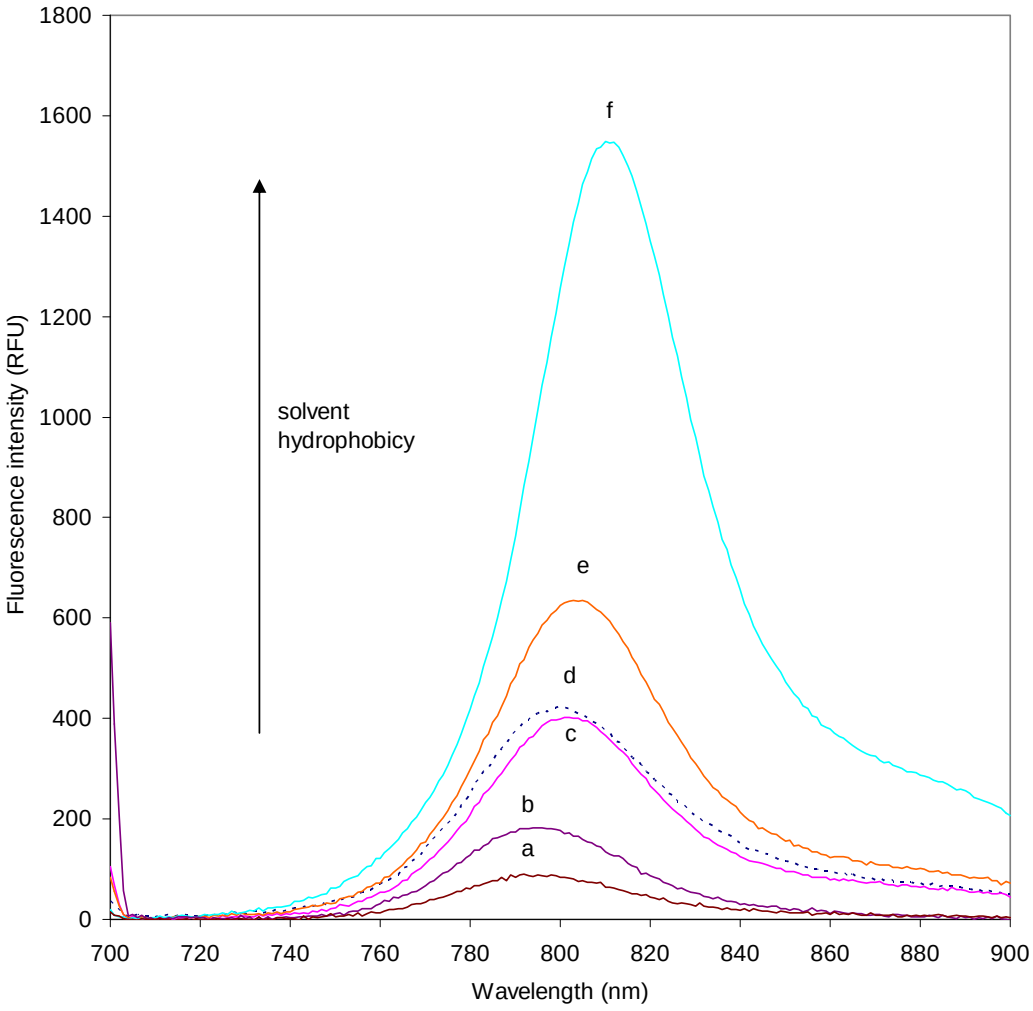

Figure 2.7. Fluorescence emission spectra of BHmC-10 (10 µM) in various solvent systems, at room temperature. a, 25% (v/v) methanol in water; b, 25% (v/v) methanol in PB; c, 50% (v/v) methanol in water; d, 1 : 1 ratio, 20 µM total cons., of dye 7-HSA complex in 1% (v/v) methanol in PB; e, 50% (v/v) methanol in PB; f, 100% methanol.

This indicates that the bis-cyanine dye when bound to HSA is in an environment that is more hydrophobic than aqueous buffer but less hydrophobic than methanol (Figure. 2.7.). The data of Figure 2.7. also indicate that the microhydrophobicity of the binding site is about equivalent to that of the hydrophobicity of 50% methanol in water.

The emission spectra of the bis-cyanine dye at constant concentration of 10 µM with

different amounts of HSA added are given in Figure. 2.8. Upon an increase in the HSA concentration, up to 70 µM, a strong fluorescence enhancement can be observed.

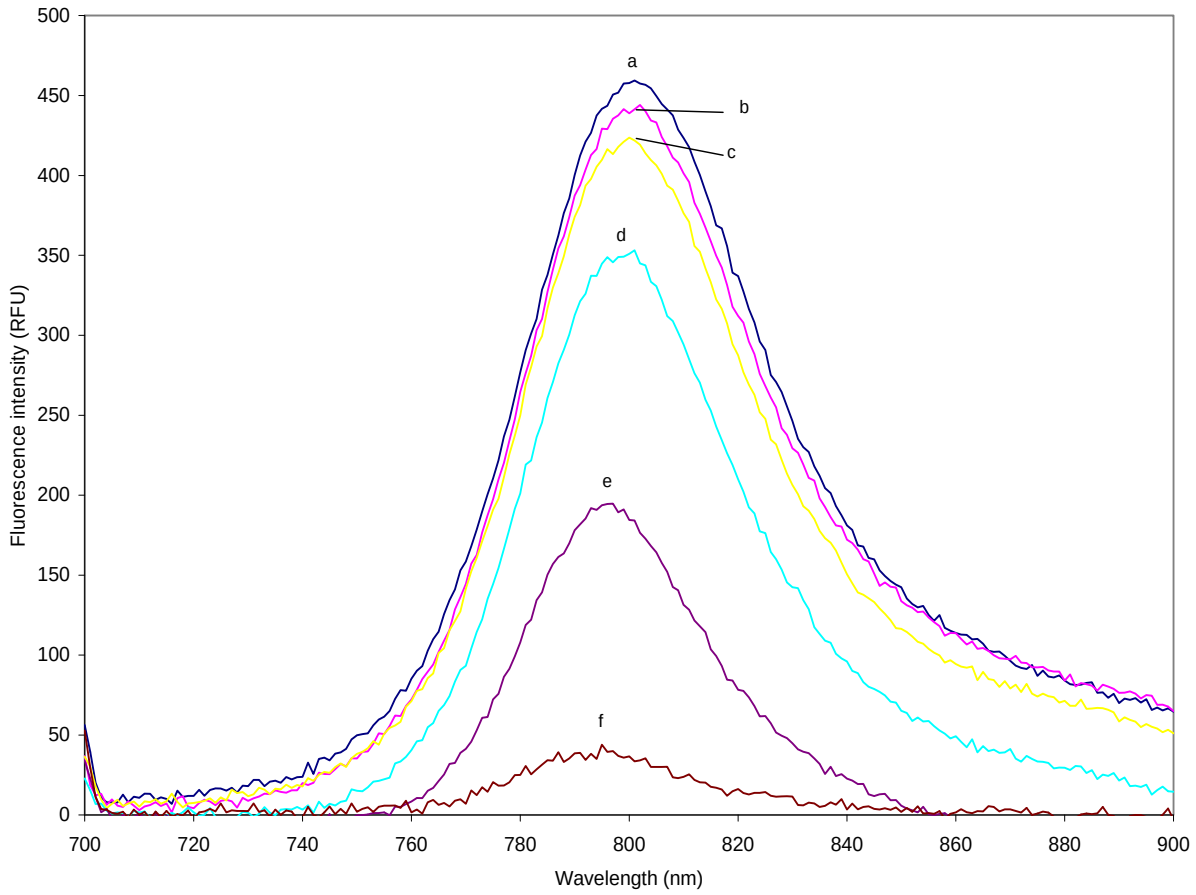

Figure 2.8. Fluorescence emission spectra of BHmC-10 (10 µM) in the presence of HSA: (a) 70, (b) 50, (c) 30, (d) 10, (e) 1, and (f) 0.1 µM.

These results can be explained in terms of a decrease in concentration of weakly fluorescent intra- and intermolecular dye aggregates free in solution as the concentration of a highly fluorescent complex of the open linear form of the dye with HSA increases. The fluorescence emission spectra clearly show a difference between the fluorescent intensity of the dye in the absence (Figure. 2.7.) and presence (Figure. 2.8.) of HSA.

2.3.3. Dye-HSA saturation and stoichiometry

The saturable binding curve for the complex of BHmC-10 with HSA is shown in

Figure. 2.9.. The fluorescence intensity change at 800 nm is plotted at a fixed concentration of the dye. The HSA concentrations of over 100 μM cause no further increase in fluorescence, indicating that the dye is fully complexed with HSA and, as a result, the addition of HSA has no effect on the fluorescent intensity measured. This plot indicates that a strong binding exists between the dimeric dye and HSA.

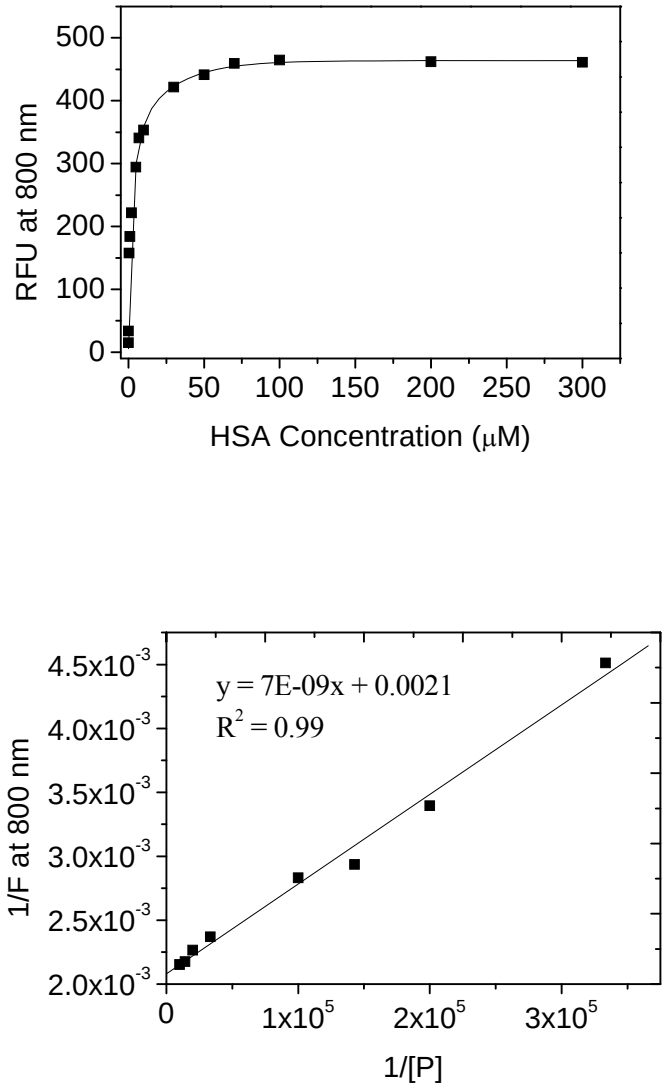

Figure 2.9. Saturable binding curve as a function of increasing HSA concentration. The concentration of BHmC-10 was constant at 10 μM, and the fluorescence was measured at 800 nm.

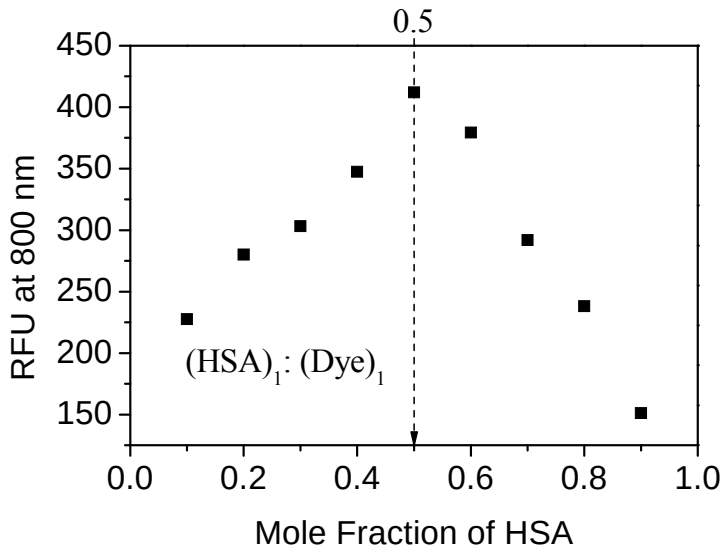

Figure 2.10. Job's plot to determine the stoichiometry of dye-HSA complex at 800 nm. The total concentration of the complex was $2x10^{-5}$ M.

The predominant stoichiometry of the dye-HSA complex was determined using Job's method (Figure. 2.10.). Fluorescence versus mol fraction of HSA was determined with a constant total concentration of 2.0 x 10^{-5} M. The Job's plot indicates a predominant stoichiometry of 1:1. Absorbance spectra are less suitable to obtain this stoichiometry due to a severe overlap of the spectra of the free and bound species present in the mixture. However, the practically non-existent fluorescence of the clam-shell form allows this calculation from the fluorescence data.

2.3.4. Association constant

The maximum absorption wavelength of the free BHmC-10 is not different enough from that of the bound dye to reliably calculate the association constant (Figure. 2.9.). In addition, there are no isosbestic points between free and bound dye. Nevertheless, it was possible to determine the association constant utilizing the quantum yield change of the

complex because, as shown in Figure. 2.8., the fluorescence upon the addition of HSA increases and free dye has low fluorescence. The association constant K_a was determined by using the method similar to that reported previously by Tarazi, et. al.[28] According to this method, the interaction between dye D and protein P can be represented by Eq. (1), which is a good assumption due to job's plot,

$$D + P \Leftrightarrow DP \tag{1}$$

The association constant for the dye-protein complex formation can be expressed by Eq. 2,

$$K_a = \frac{[DP]}{[D][P]} \tag{2}$$

where [DP], [D] and [P] are molar concentrations at equilibrium. Subsequently, the association constant K_a of the dye-protein complex was calculated from the data for the fluorimetric titration of the dye with HSA by using Eq. 3,[29] where k is a constant dependent upon the instrumentation and quantum efficiency of the process and is the measured fluorescence emission intensity of the dye-protein mixture.

$$\frac{1}{F} = \frac{1}{k[D]} + \left(\frac{1}{k[D]K_a}\right)\frac{1}{[P]} \tag{3}$$

Therefore, a plot of 1/F versus 1/[P] produces a straight line, with K_a equal to the intercept divided by the slope of the line. The association constant K_a of 3×10^5 M^{-1} was obtained. However, it should be noted that Eq. 3 is valuable only for dye-protein complex formed with a 1:1 stoichiometry, which appears to be the prevelant stochiometry in this case.

2.4. Conclusions

In polar solvents, the novel bis-cyanine dye is self-associated to form an intramolecular H-aggregate due to strong intramolecular van der Waals interaction between the carbocyanine moieties. H-aggregates are generally weakly fluorescent and often have

lower extinction coefficients compared to their monomeric counterparts. Deaggregation of dye aggregates in the presence of HSA or in hydrophobic solvents results in a greatly increased quantum yield and the appearance of the monomeric absorption band. In the case of bis-dye, the intramolecular clam-shell like dimer opens up and the concentration of the clam-shell aggregate formed by the intramolecular interaction decreases with concomitant changes in the spectral features. The main advantage of this bis-cyanine dye is that the intramolecular aggregation is independent on concentration, which is not the case with monomeric carbocyanines. This enhances the analytical utility of BHmC-10 as a non-covalent label. According to the data shown in Figure. 2.5., addition of HSA leads to opening of the intramolecular H-aggregate. It can be suggested that this novel bis-heptamethine cyanine dye associates with hydrophobic cavities of HSA. Alternatively, it may interact with charged region on HSA surface since the charge of HSA (pI 4.8) under pH 7.2 is negative.

The newly synthesized NIR bis-dye has considerable advantages over the commonly used visible dyes. First, spectral interferences generated by biomolecules, which generally have autofluorescence in UV and visible region, are virtually eliminated with BHmC-10. Second, its strong intramolecular H-aggregation results in low fluorescent signal in aqueous solution. Importantly, this feature is concentration independent. In summary, the novel NIR dimeric heptamethine cyanine dye should be of interest for the bioanalytical community.

References

1. Zhang, Y. Z. X., J. F.; Tang, Y. L.; Xu, G. Z.; Yan, W. P., Chiral transformation of achiral J-aggregates of a cyanine dye templated by human serum albumin. *Chemphyschem* **2007,** 8, (2).

2. Patonay, G.; Strekowski, L.; Kim, J. S.; Henary, M., The increasing role of NIR fluorescence spectroscopy in bioanalytical chemistry *NIR news* **2007,** 18, (3), 7-9.

3. Tatikolov, A. S.; Costa, S. M., Complexation of polymethine dyes with human serum albumin: a spectroscopic study. *Biophys Chem* **2004,** 107, (1), 33-49.

4. Yarmoluk, S. M.; Lukashov, S. S.; Ogul'Chansky, T. Y.; Losytskyy, M. Y.; Kornyushyna, O. S., Interaction of cyanine dyes with nucleic acids. XXI. Arguments for half-intercalation model of interaction. *Biopolymers* **2001,** 62, (4), 219-27.

5. Yan, W.; Colyer, C. L., Investigating noncovalent squarylium dye-protein interactions by capillary electrophoresis-frontal analysis. *Journal of Chromatography, A* **2006,** 1135, (1), 115-121.

6. Ogulchansky, T. Y.; Losytskyy, M. Y.; Kovalska, V. B.; Lukashov, S. S.; Yashchuk, V. M.; Yarmoluk, S. M., Interaction of cyanine dyes with nucleic acids. XVIII. Formation of the carbocyanine dye J-aggregates in nucleic acid grooves. *Spectrochim Acta A Mol Biomol Spectrosc* **2001,** 57, (13), 2705-15.

7. von Berlepsch, H.; Kirstein, S.; Bottcher, C., Effect of Alcohols on J-Aggregation of a Carbocyanine Dye. In 2002; Vol. 18, pp 7699-7705.

8. Kashida, H.; Asanuma, H.; Komiyama, M., Alternating hetero H aggregation of different dyes by interstrand stacking from two DNA-dye conjugates. *Angew Chem Int Ed Engl* **2004,** 43, (47), 6522-5.

9. Herz, A., Aggregation of sensitizing dyes in solution and their adsorption onto silver halides. *Advances in Colloid and Interface Science* **1977,** 8, (4), 237-298.

10. Zhang, Y. Z. X., J. F.; Tang, Y. L.; Xu, G. Z.; Yan, W. P., Aggregation behaviour of two thiacarbocyanine dyes in aqueous solution. Dyes and Pigments. *Dyes and Pigments* **2008,** 76, (1).

11. Kim, J. S.; Kodagahally, R.; Strekowski, L.; Patonay, G., A study of intramolecular H-complexes of novel bis(heptamethine cyanine) dyes. *Talanta* **2005,** 67, (5), 947-954.

12. Ogul'chansky, T.; Yashchuk, V. M.; Losytskyy, M.; Kocheshev, I. O.; Yarmoluk, S. M., Interaction of cyanine dyes with nucleic acids. XVII. Towards an aggregation of cyanine dyes in solutions as a factor facilitating nucleic acid detection. *Spectrochim Acta A Mol Biomol Spectrosc* **2000,** 56, (4), 805-14.

13. Welder, F.; Paul, B.; Nakazumi, H.; Yagi, S.; Colyer, C. L., Symmetric and asymmetric squarylium dyes as noncovalent protein labels: a study by fluorimetry and capillary electrophoresis. *J Chromatogr B Analyt Technol Biomed Life Sci* **2003,** 793, (1), 93-105.

14. McCorquodale, E. M.; Colyer, C. L., Indocyanine green as a noncovalent, pseudofluorogenic label for protein determination by capillary electrophoresis. *Electrophoresis* **2001,** 22, (12), 2403-2408.

15. Lacroix, M.; Poinsot, V.; Fournier, C.; Couderc, F., Laser-induced fluorescence detection schemes for the analysis of proteins and peptides using capillary electrophoresis. *Electrophoresis* **2005,** 26, (13), 2608-21.

16. Sowell, J.; Mason, J. C.; Strekowski, L.; Patonay, G., Binding constant determination of drugs toward subdomain IIIA of human serum albumin by near-infrared dye-displacement capillary electrophoresis. *Electrophoresis* **2001,** 22, (12), 2512-2517.

17. Patonay, G.; Salon, J.; Sowell, J.; Strekowski, L., Noncovalent labeling of biomolecules with red and near-infrared dyes. *Molecules* **2004,** 9, (3), 40-49.

18. Mishra, A.; Behera, R. K.; Behera, P. K.; Mishra, B. K.; Behera, G. B., Cyanines

during the 1990s: A Review. In 2000; Vol. 100, pp 1973-2012.

19. Baars, M.; Patonay, G., Ultrasensitive detection of closely related angiotensin I peptides using capillary electrophoresis with near-infrared laser-induced fluorescence detection. *Anal Chem* **1999,** 71, (3), 667-71.

20. Sowell, J.; Agnew-Heard, K. A.; Christian Mason, J.; Mama, C.; Strekowski, L.; Patonay, G., Use of non-covalent labeling in illustrating ligand binding to human serum albumin via affinity capillary electrophoresis with near-infrared laser induced fluorescence detection. *Journal of Chromatography, B: Biomedical Sciences and Applications* **2001,** 755, (1-2), 91-99.

21. Colyer, C. L., Noncovalent labeling of proteins in capillary electrophoresis with laser-induced fluorescence detection. *Cell Biochemistry and Biophysics* **2000,** 33, 323-337.

22. Patonay, G.; Kim, J. S.; Kodagahally, R.; Strekowski, L., Spectroscopic study of a novel bis(heptamethine cyanine) dye and its interaction with human serum albumin. *Appl Spectrosc* **2005,** 59, (5), 682-90.

23. Amy, D. W. BINDING STUDIES OF NEAR INFRARED CYANINE DYES WITH HUMAN SERUM ALBUMIN AND POLY-L-LYSINE USING OPTICAL SPECTROSCOPY METHODS. Dissertation, Goergia State University, Atlanta, 2007.

24. Dougherty, T. J.; Kaufman, J. E.; Goldfarb, A.; Weishaupt, K. R.; Boyle, D.; Mittleman, A., Photoradiation therapy for the treatment of malignant tumors. *Cancer Res* **1978,** 38, (8), 2628-35.

25. Dougherty, T. J. a. T., R. E. , *"Lasers", in Photomedicine and Photobiology*. Springer-Verlag: Berlin, 1980.

26. Ogul'chansky, T.; Losytskyy, M.; Kovalska, V. B.; Yashchuk, V. M.; Yarmoluk, S. M., Interactions of cyanine dyes with nucleic acids. XXIV. Aggregation of monomethine cyanine dyes in presence of DNA and its manifestation in absorption and fluorescence spectra.

Spectrochim Acta A Mol Biomol Spectrosc **2001,** 57, (7), 1525-32.

27. Czikkely V; Försterling H D; H, K., Light absorption and structure of aggregates of dye molecules. *Chem. Phys. Lett* **1970,** 6.

28. Tarazi, L. N., N.; Patonay, G., Investigation of the spectral properties of a squarylium near-infrared dye and its complexation with Fe(III) and Co(II) ions. *Microchemical Journal* **2000,** 64, (3).

29. Casay, G. A. S., D. B.; Patonay, G., *Fluorescence Spectroscopy*. Plenum: New York, 1994.

Chapter 3. A Study of Intramolecular H-complexes of Novel Bis(heptamethine cyanine) Dyes

3.1. Introduction

Near-infrared (NIR) bis(heptamethine cyanine) (BHmC) dyes containing a flexible polymethylene linker between the two cyanine subunits are a novel class of compounds with versatile spectroscopic properties. The first bis-cyanine of this type is BHmC-10 (with a decamethylene bridge) (*see* chapter 2.). The designation BHmC-10 refers to a bis(heptamethine cyanine) with a 10-methylene (decamethylene) linker between the two cyanine subunits. BHmC-10 exhibits intramolecular and intermolecular van der Waals interaction that promotes H-aggregation, resulting in negligible fluorescence emission. Upon the addition of HSA, the inter- and intramolecular complexes of BHmC-10 dissociate with concomitant increase in fluorescence, indicating a strong noncovalent interaction in the dye-HSA complex. The BHmC-10 dye-HSA interaction seems to readily promote opening up of the clam-shell form of the dimeric dye. As part of this work, additional bis-cyanines BHmC-4, BHmC-6, BHmC-8 and BHmC-12 were synthesized and their spectral properties were evaluated for the dyes free in solution and in the presence of human serum albumin (HSA). These bis-cyanines undergo H-type aggregation, mainly H-type intramolecular complexation between the two cyanine subunits, when free in aqueous solution. This H-type interaction in phosphate buffer (pH 7.2) is characterized by hypsochromic (H) absorption at 700 nm, low extinction coefficient, and low fluorescence quantum yield. By contrast, an analogous monomeric cyanine exhibits strong fluorescence under similar conditions. The results were compared to those of our previous studies with BHmC-10 and their monomeric counterpart (RK780).

The aim was to better understand the spectral properties of a series of BHmCs containing polymethylene linkers of various lengths (Figure 1.4.). It was found that the different linkers strongly affect the strength and mode of intermolecular interaction in BHmCs which, in turn, has important ramifications for the interaction of these bis-cyanines

with HSA.

3.2. Experimental

3.2.1. Materials and solvents

Fatty acid free HSA (≥ 96% purity) was obtained from Sigma (St. Louis, MO). Sodium phosphate monobasic (monohydrate) and sodium phosphate dibasic (monohydrate) were purchased from Fisher Scientific (Fair Lawn, NJ). Water was Nanopure grade (Barnstead model D4751 ultrapure water system). Methanol was obtained from the Aldrich Chemical Company (Milwaukee, WI) in HPLC grade.

3.2.2. Instrumentation

Absorption measurements were acquired on a Perkin-Elmer Lambda UV/VIS/NIR (Lambda 50) spectrophotometer (Norwalk, CT). Fluorescence emission spectra were taken using a K2 spectrofluorometer (ISS, Champaign, IL) equipped with a R928 Hamamatsu photomultiplier tube (Bridgewater, NJ). Commercial GaAlAs laser diodes (Laser Max, Rochester, NY) were used as the excitation source at 690 nm. The slit widths were 2 mm and the integration time was 3 sec. All absorption and fluorescence measurements were taken in a 1 cm cuvette.

3.2.3. Methods

Stock solutions of the monomeric dye, RK780 (2 mM) and BHMCs (1 mM) in methanol were stored in the dark at 4 °C. The 0.1 mM stock solution of HSA was prepared in 20 mM dibasic phosphate buffer solution and adjusted to pH 7.2 with phosphoric acid. Stock solution of HSA was prepared fresh daily.

The dye-HSA mixture was vortexed for 30 s to allow for equilibration. Various dye-

HSA ratios were investigated to determine the utility of BHmCs as noncovalent labels for serum albumins. For all experiments, the stock solution of BHmCs in methanol was diluted with phosphate buffer due to the relatively poor solubility of the dyes in aqueous solution. All working solutions contained only 1 % (v/v) methanol to facilitate dye dissolution but to avoid denaturation of HSA. All measurements were performed at room temperature.

3.3. Results and Discussion

3.3.1. Photophysical properties of BHmCs[1-4]

The quantum yields of H- and J-aggregates typically increase and decrease, respectively, upon binding with proteins or other biomolecules.[5-11] Fluorescence enhancement can be utilized for non-covalent labeling of the biomolecules.[8, 12, 13] Unfortunately, the monomeric cyanine dyes currently in use for non-covalent labeling purposes exhibit spectral properties that are strongly concentration-dependent. Concentration dependence is a major drawback in any bioanalytical application. This concentration dependence is significantly reduced with a bis(heptamethine cyanine) dye BHmC-10, which has been evaluated in chapter 2. Likewise, this chapter presented the concentration dependency of four different BHmCs in methanol and performed spectroscopic study of BHmCs with various HSA concentration.

BHmCs in methanol

Photophysical properties of these novel dimeric dyes in methanol were characterized. Spectral data obtained at the same concentrations (10 μM) of RK780, BHmC-4, -6, and -8, were normalized for direct comparison. The molar absorptivities (ε) of these dyes were determined using multiple concentrations, and no significant spectral changes could be observed as a function of concentration. It is clear that the spectra of BHmCs in methanol are

less concentration-dependent compared to that of the monomeric dye (RK780). It is expected that BHmCs in methanol would open up its H-dimeric form (or intermolecular H-aggregates) and give spectral data that are similar to that of RK780. Several factors can influence the spectra of bis-cyanines. The major factors are the magnitude of the interaction between the carbocyanine moieties and the conformational energy of the polymethylene linker. Since the carbocyanine moieties are positively charged, in the intramolecular dimeric complex these dyes most likely have an increased dipole due to charge separation. The two moieties most likely are not in complete overlap, and they are somewhat rotated with respect to one another.

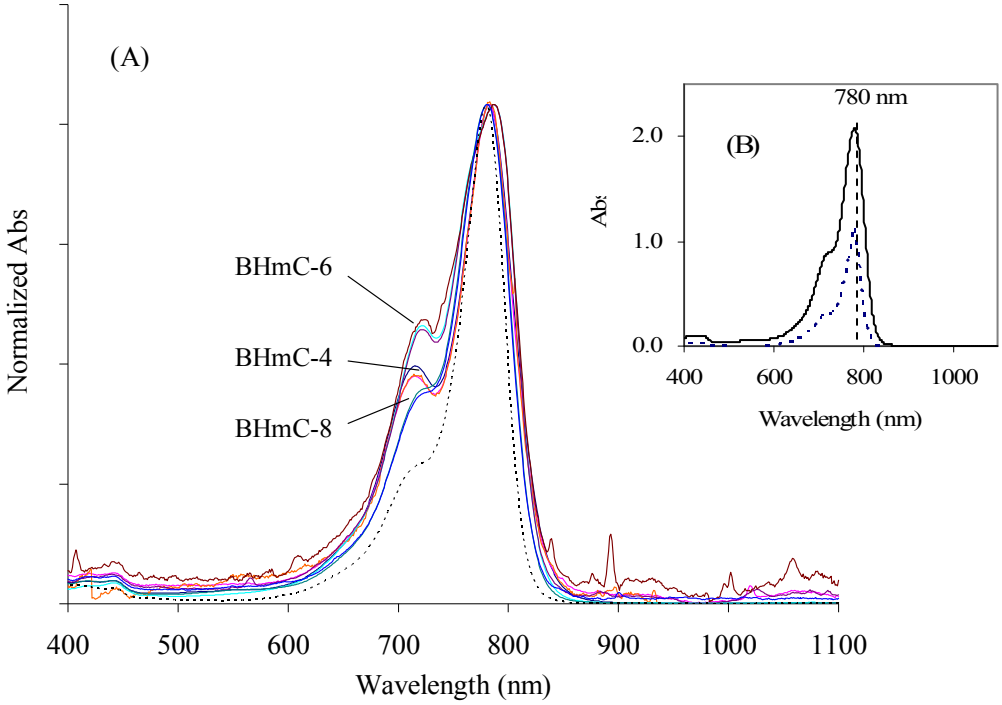

Figure 3.1. Absorption spectra of RK780 (dotted line) and BHmCs (solid lines) in methanol: (A), concentration effect on the aggregation of BHmCs at three different concentration, at 0.1 μM, 1 μM, and 10 μM. Normalized absorption spectra were taken.; (B), spectral response comparison (λ_{max} at 780 nm) of RK780 and BHmCs at 10 μM.

Significant spectral features of BHmC-4 and -6 are observed at around 780 and 720 nm. As judged from absorption at 720 nm, BHmC-6 prefers forming an H-dimer (or H-aggregates). On the other hand, the spectral data for BHmC-4 is consistent with an intermediate state between BHmC-6 and -8. Dye BHmC-8 appears to have a more favorable structure than the others for opening up its clam-shell H-dimer (or to dissociate H-aggregates). To support this hypothesis, the spectral difference between M- and H-bands can be compared. These spectral features indicate an approximately 65 nm difference for both BHmC-4 and -6. Thus, it can be inferred that these dyes exhibit similar properties regarding their H-aggregation. Even at low concentration in methanol, they have similar spectral changes. However it should be noted that the spectral changes at around 720 nm cannot be solely assigned to H-dimerization, since this characteristic band can also be a result hypsochromic di-, tri-, tetramerization or higher aggregation. Nevertheless, at the low concentrations in methanol this is an unlikely event, owing to the relatively small formation constants of these aggregates.[14, 15]

Interestingly, BHmC-8 exhibits another particular spectral behavior that is different from those of BHmC-4 and -6. Thus, when BHmC-8 M-band is compared to those of the other two BHmCs, a slight red-shift can be observed as a function of increasing polymethylene chain length. However, BHmC-8 and RK780 exhibit a virtually identical lambda maximum at 780 nm, and the molar absorptivity of BHmC-8 is approximately twice as large as that for RK780. This is expected if the two moieties do not interact in methanol (see Fig. 3.1. (B)). It is reasonable to assume that BHmC-8 in methanol completely opens up from its dimeric form resulting in the aforementioned spectral behavior.

BHmCs in phosphate buffer

Photophysical properties of novel dimeric dyes in 20 mM phosphate buffer at pH 7.2

were characterized. The absorbance spectra of RK780 and BHmCs in Figure 3.2.(A). were normalized for direct comparison. Significant spectral changes can be observed at around 780 and 700 nm. According to Figure 3.2., the BHmCs form inter- and intramolecular H-aggregates in phosphate buffer indicated by the spectral features. Spectral data of RK780 clearly show that it forms intermolecular H-aggregates. It is also clear that BHmCs in Figure 3.2.(B). give much lower fluorescence intensity than RK780, indicating strong intramolecular H-dimerization. Intermolecular aggregation would not result in as much change in fluorescence as the monomeric dye data indicate.

It can be seen from Figure 3.2(A). that BHmC-6 forms stronger H-dimer (or intermolecular H-aggregates) than the other BHmCs, and the fluorescence spectra in Figure 3.2.(C). show that BHmC-6 has the lowest fluorescence intensity relative to the others. This observation is consistent with the well-known dye theories on aggregates, indicating that dyes forming strong H-aggregates have low fluorescence quantum yield.[5, 14]

It can be suggested that the hexamethylene bridge in BHmC-6 can attain a low-energy conformation that is favorable for strong intramolecular H-dimerization. According to the spectra shown in Figures 3.1. and 3.2., BHmC-4 exhibits relatively higher monomer and lower H-aggregate bands in the absorption spectra and slightly higher fluorescence intensity than the other BHmCs. On the other hand, BHmC-8 forms a strong intramolecular complex in phosphate buffer. It seems that the length of the linker arms of BHmCs affects the energetically favorable formation in phosphate buffer. In following section, BHmC-12 is introduced for more detailed comparison regarding the length of linkers.

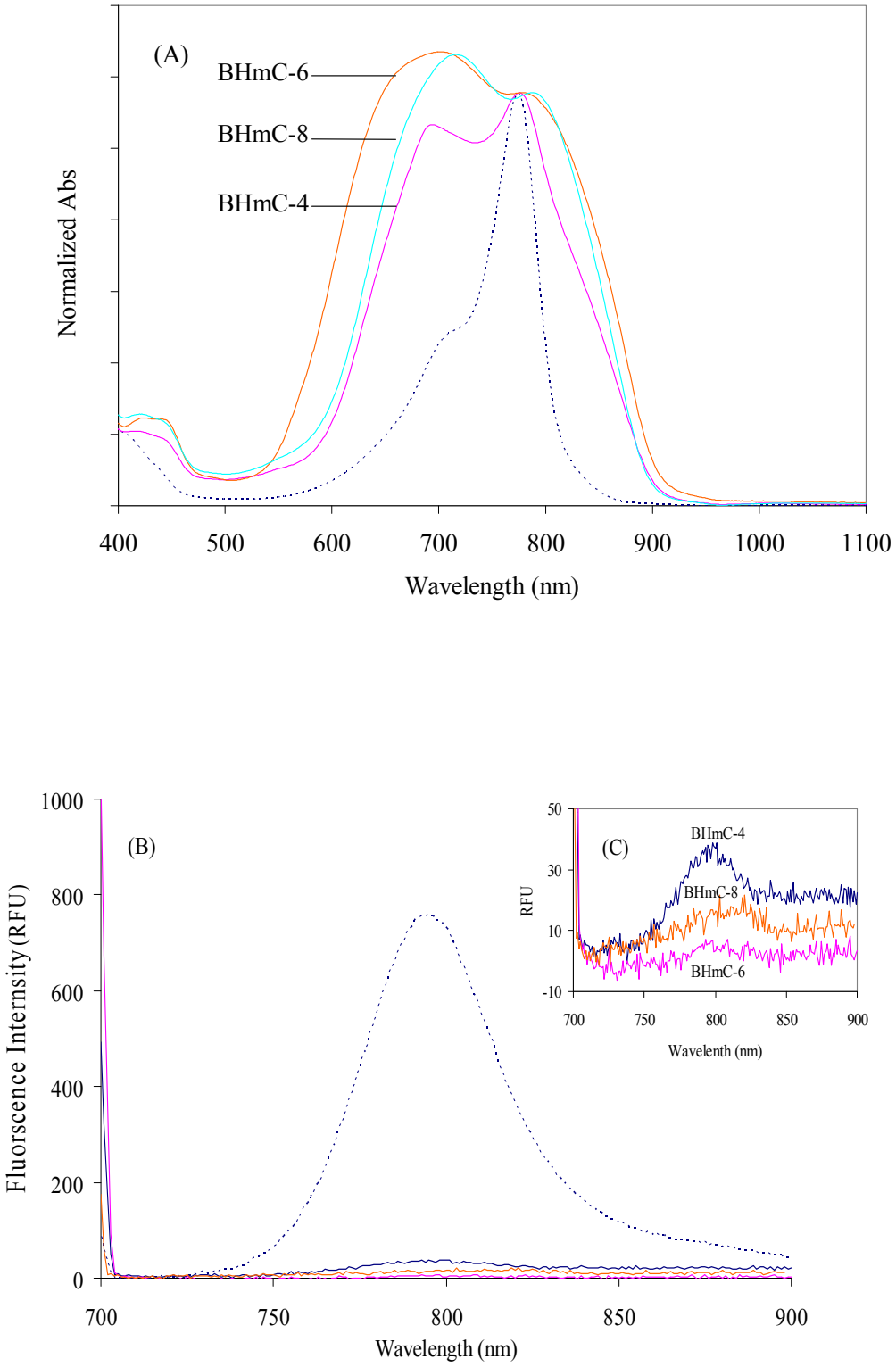

Figure 3.2. Spectral comparison of RK780 (dotted line) and BHmCs (solid lines) in phosphate buffer, pH 7.2, at 10 μM dye concentration. (A): Normalized absorption spectra. (B) and (C): Fluorescence emission spectra.

3.3.2. BHmC-HSA interaction

Absorption spectra

The absorption spectra of the dimeric dyes in methanol have characteristic bands at 783, 787, and 780 nm for BHmC-4, 6, and 8, respectively. The band intensities are diminished in phosphate buffer. It is likely that these dyes form a strong intramolecular dimer in aqueous solution, but some intermolecular aggregates cannot be ruled out. This spectral shift is most likely caused by the decrease in intramolecular pi-pi* interactions as the clam-shell opens up. Similar shifts have been observed for the aggregates of RK780 upon the formation of the dye–HSA complex.

Representative absorption spectra of BHmCs in the presence and absence of HSA are given in Fig 3. Two characteristic bands for individual BHmCs ($\lambda_{\max}^{BHC-4}$ at 776 and 694 nm, $\lambda_{\max}^{BHC-6}$ at 778 and 701 nm, and $\lambda_{\max}^{BHC-8}$ at 788 and 717 nm) can be distinguished in the absorption spectra in buffer solution compared to dye solution in methanol at the same concentration. Upon addition of HSA the inter- and intramolecular aggregates break up with concomitant changes in the H- and M- bands. The absorption spectra of the dimeric dyes at constant concentration of 10 μM with different amounts of HSA added are also depicted in Fig. 3.3. Upon increase in the HSA concentration, up to 50 μM, and up to 100 μM for BHmC-4, -6, -8, and -12 the characteristic features of the dimeric dye absorption spectra change.

The M-band relative intensity increases significantly in the case of BHmC-4 and -12 while the H-aggregate band intensity dramatically decreases. Up to C_{HSA} = 50 μM, a continuous decrease can be observed in the H-band intensity. However, at C_{HSA} = 70 μM, there is negligible change in the intensities of H- and M-bands and absorption of HSA becomes more pronounced. On the other hand, the M-band intensities in BHmC-6 and -8

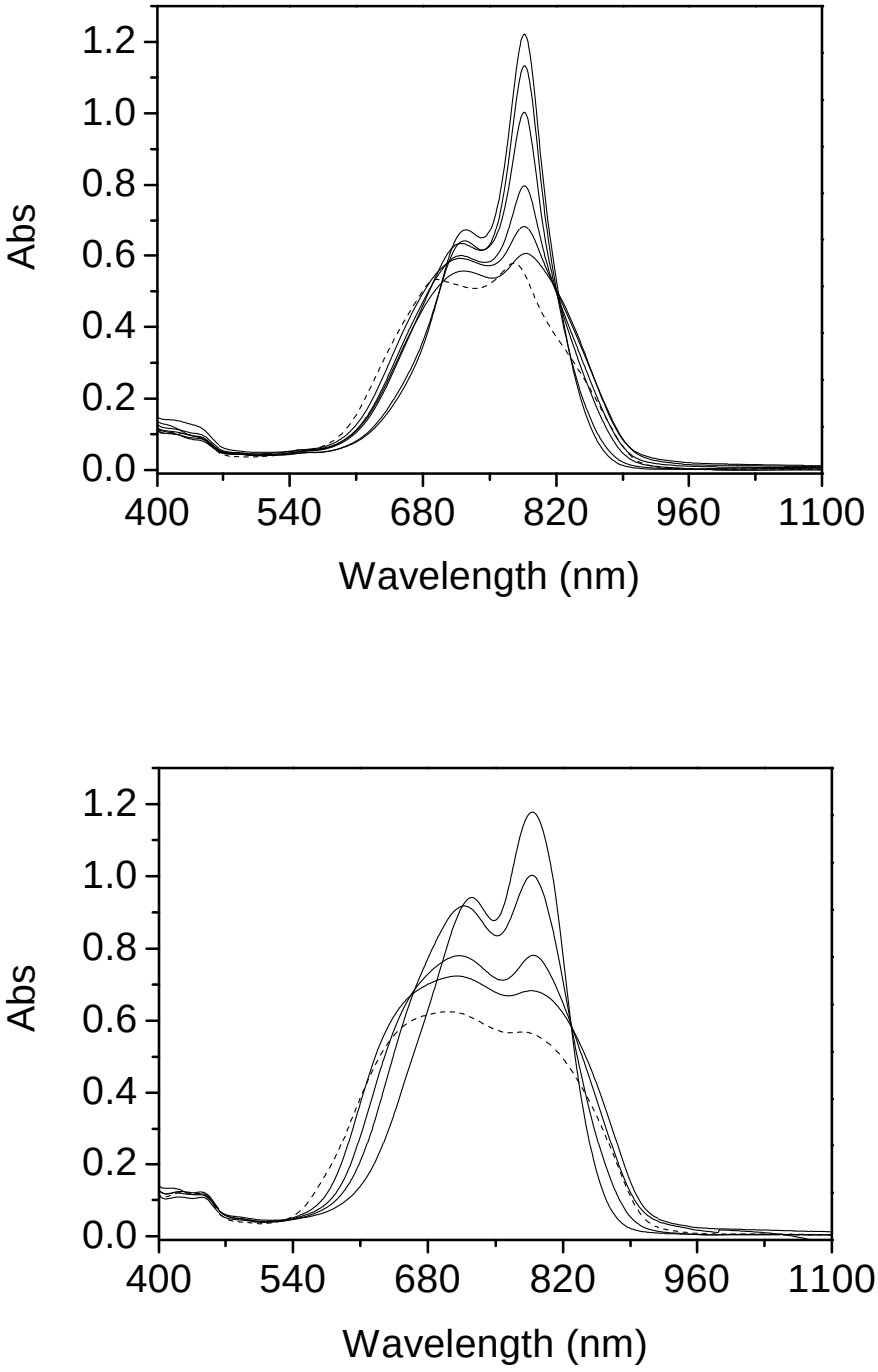

Figure 3.3. A. Absorption of BHmCs (10 μM) in the absence (dotted line) and the presence (solid line) of HSA (0.1 to 100 uM). Upper; BHmC-4, bottom; BHmC-6.

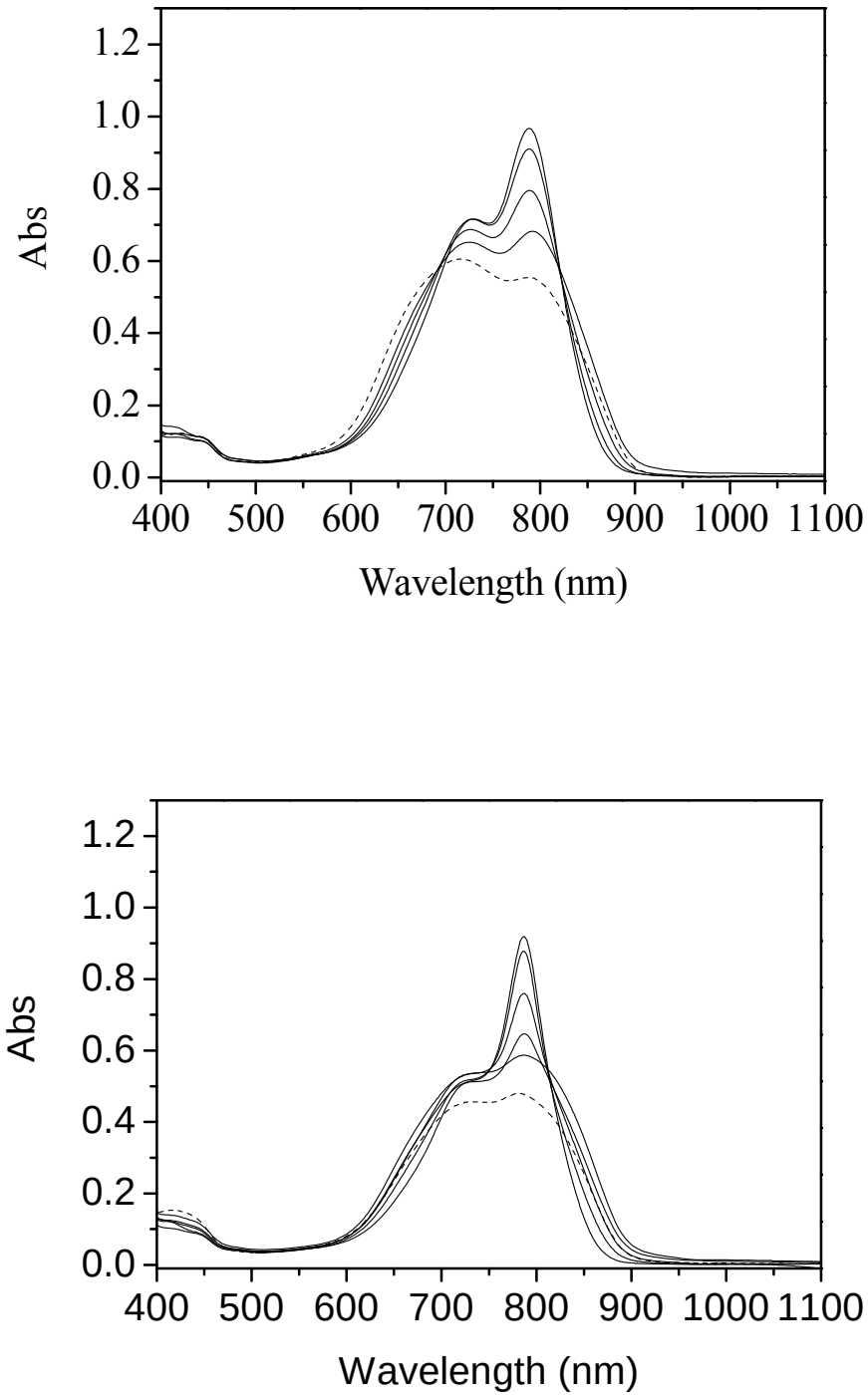

Figure 3.3. B. Absorption of BHmCs (10 μM) in the absence (dotted line) and the presence (solid line) of HSA (0.1 to 100 uM). Upper; BHmC-8, bottom; BHmC-12.

slightly increase while the H-bands slightly decrease compared to BHmC-4 and -12. There are two possibilities for the formation of the BHmC-6 (or -8)-HSA complex. First, these dyes interact with HSA in their open form. The second suggestion is that the intramolecular H-complex and/or intermolecular H-aggregates are bound to the surface or hydrophobic pocket of HSA without opening up the clamshell form. Further studies are needed to determine the actual conformations.

In BHmC-6, there is a small spectral change on the M-band compared to BHmC-4. As mentioned above, two binding modes are possible. However, there are three isosbestic points that can be used to estimate the spectral behavior upon interaction with HSA. It should be noted that the isosbestic point indicates the intermediate of two species between free and bound dyes. The first isosbestic point at 677 nm shows that upon the increase in concentration of HSA, H-aggregates are opening up to 30 μM. Consistently with the second isosbestic point (at 767 nm), there seems to be opening up of BHmC-6 at high HSA concentration. During this process, H-dimer (or aggregate) characterized by a band at 721 nm is important since this band decreases in intensity at higher concentrations. It can be inferred that at HSA concentration of more than 50 μM, the HSA expels the H-dimer (or H-aggregates) bound on the surface of HSA. More interestingly, as judged by the bands around 820 nm, all BHmCs show J-aggregation, meaning that these dyes inherently form H-aggregates and J-aggregates and these aggregates are modified upon the addition of HSA.

In BHmC-8, there are two isosbestic points for H- and J-aggregates. According to Figure 3.3., the ratio between M- and H-band is constantly changing without isosbestic point changes upon the increase in HSA concentration. Also, the M-band keeps increasing up to 100 μM HSA. This can be explained by assuming that BHmC-8 predominantly binds to HSA with its open form, as compared to BHmC-6.

Clearly, as HSA concentration increases, the concentration of the inter- and

intramolecular H-aggregates free in solution decreases and the fraction of the dimeric dye molecules bound to HSA in its clam-shell form also decreases. This indicates that the interactions of open linear form of BHmC-6 and -8 with HSA are less predominant than the interaction for BHmC-4 and -12 because of the presence of intramolecular dimer, even at high HSA concentration. Clearly, binding of BHmC-4 in the open form to HSA is more favorable than those of BHmC-6 and -8.

Fluorescence spectra

The fluorescence emission of the dimeric dyes is very weak in aqueous solutions relative to pure methanol. This is very advantageous for utilizing BHmCs as non-covalent labels because the unbound form of the dye to HSA has much lower quantum yield (Figure 3.2(B)). It should be noted that one of the major drawbacks of using RK780 and similar monomeric dyes as non-covalent labels is the existence of a relatively strong fluorescence of the unbound free form of the non-covalent label.

The emission spectra of the BHmCs at constant concentration of 10 μM with different amounts of HSA added are given in Figure 3.4. Upon an increase in HSA concentration, up to 50 μM, a strong fluorescence enhancement of BHmC-4 and -12 is observed. This can be explained in terms of decreased concentration of weakly fluorescent intra- and intermolecular dye aggregates that are free in solution as the concentration of a highly fluorescent complex of the open linear form of the dye with HSA increases. However, in the spectra of BHmC-6 very small fluorescence changes, even in the presence of HSA, are observed. As can be seen from Figure 3.4., HSA-BHmC-6 complex gives small fluorescence enhancement. While the more rigid intramolecular H-dimer of BHmC-6 partially binds to HSA, BHmC-8 seems to easily open its dimeric form in the presence of HSA, as seen from Figure 3.4.. Therefore, one can assume that in its bound form in the presence of HSA,

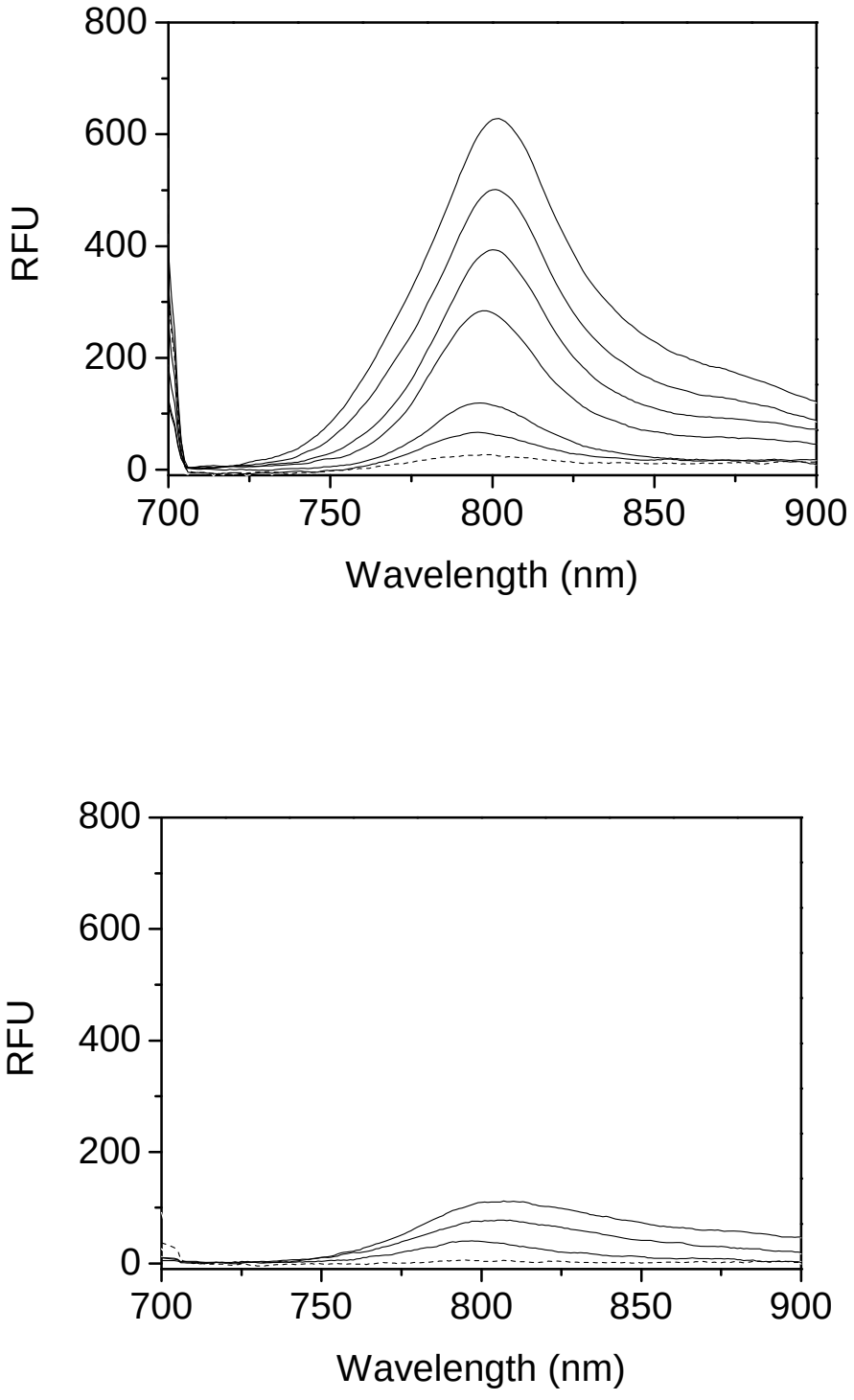

Figure 3.4. A. Fluorescence emission spectra of BHmCs (10 μM) in the absence (dotted line) and the presence (solid line) of HSA (0.1 to 100 uM). Upper; BHmC-4, bottom; BHmC-6.

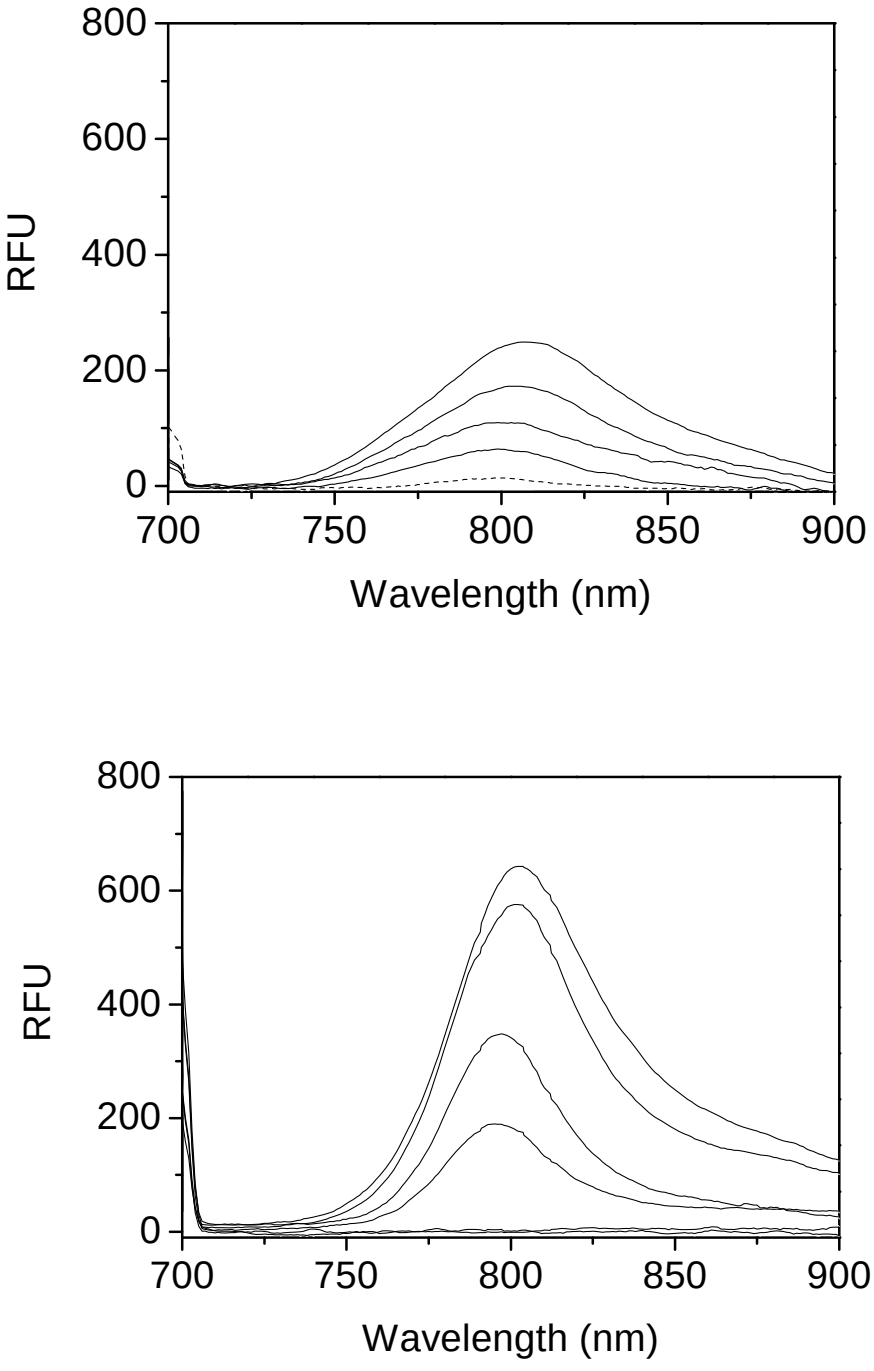

Figure 3.4. B. Fluorescence emission spectra of BHmCs (10 μM) in the absence (dotted line) and the presence (solid line) of HSA (0.1 to 100 uM). Upper; BHmC-8, bottom; BHmC-12.

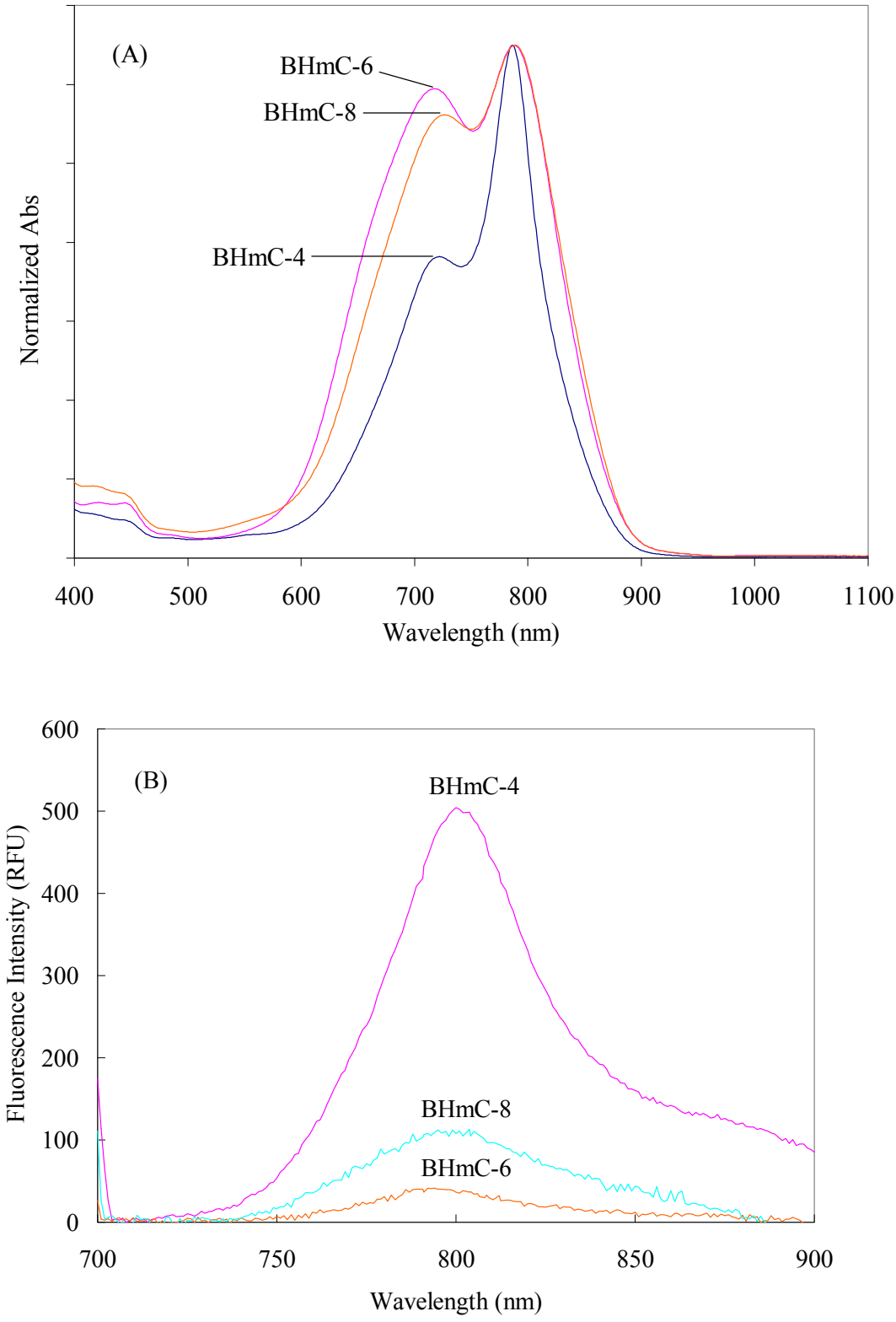

Figure 3.5. Spectral comparison of BHmCs (10 μM) regarding their complexes in the presence of HSA (10 μM).

BHmC-8 behaves like an intermediate state between BHmC-4 and -6. It can be compared with absorption spectra and the ratio between aggregates and monomer bands since fluorescent spectra are dependent on monomer band of the absorption spectra (figure 3.3.).

BHmCs and HSA complexes were studied at 10 μM concentrations. Figure 3.5.(A). shows that BHmC-6 forms strong intramolecular H-dimer and/or intermolecular H-aggregates which give a high and broad H-band relative to the others. It also shows that upon binding to HSA, BHmC-4 and -12 easily open their intramolecular H-dimers (*see* also figure 3.3.). Importantly, these results indicate that for non-covalent labeling the use of BHmC-4 and -12 is more advantageous than the use of the previously synthesized BHmC-10.[14]

3.4. Conclusions

The spectral work outside the range of autofluorescence of biomolecules is the main advantage of using NIR dyes for labeling of the biomolecules. An additional advantage is gained by using BHmCs as the NIR fluorescent labels. More specifically, the background fluorescence signal produced by monomeric NIR dyes is greatly reduced for BHmCs. The hypsochromic shifted band (700 nm) of the BHmCs in phosphate buffer indicate their strong inter- and intramolecular interactions. Due to the strong inter- and intramolecular aggregation, the BHmCs show low extinction coefficient and low fluorescence quantum yield. This fluorescence is negligible in the aqueous environment.

BHmCs exhibit diverse interactions with HSA. BHmC-4 easily dissociates its H-aggregates in the presence of HSA. BHmC-6 has a conformationally rigid structure, and its strong intramolecular H-dimer emits low fluorescence. Upon binding with HSA, the fluorescence of BHmC-6 changes negligibly, that for BHmC-8 shows a slight increase, and the fluorescence of BHmC-4 and -12 is greatly increased. It can be assumed that binding sites of the rigid intramolecular H-dimer of the cationic BHmC-6, in phosphate buffer at pH 7.2,

are the hydrophobic cavities and the negatively charged surface of HSA (pI 4.8). BHmC-8 exists in a more flexible intramolecular form that can readily open up in methanol while strongly associating into H-aggregates in phosphate buffer. It is suggested that BHmC-4 and -12 binds with HSA in the open form exclusively, while the H-type intramolecular interaction in BHmC-6 is mostly retained in the complex with HSA. Bis-cyanine BHmC-4 and -12 may be of significant bioanalytical utility due to its negligible fluorescence in aqueous solution and a strong increase in fluorescence upon binding with a protein.

In summary, these novel bis(heptamethine) cyanine dyes exhibit diverse and favorable characteristics as labels for biomolecules or sensor dyes. Importantly, they seem to be more advantageous than the earlier synthesized BHmC-10. Additional detailed studies are needed to fully develop the analytical utility of these bis-cyanines.

References

1. Welder, F.; Paul, B.; Nakazumi, H.; Yagi, S.; Colyer, C. L., Symmetric and asymmetric squarylium dyes as noncovalent protein labels: a study by fluorimetry and capillary electrophoresis. *J Chromatogr B Analyt Technol Biomed Life Sci* **2003,** 793, (1), 93-105.

2. McCorquodale, E. M.; Colyer, C. L., Indocyanine green as a noncovalent, pseudofluorogenic label for protein determination by capillary electrophoresis. *Electrophoresis* **2001,** 22, (12), 2403-2408.

3. Moody, E. D.; Viskari, P. J.; Colyer, C. L., Non-covalent labeling of human serum albumin with indocyanine green: a study by capillary electrophoresis with diode laser-induced fluorescence detection

Journal of Chromatography, B: Biomedical Sciences and Applications

1999, 729, (1 + 2), 55-64.

4. Colyer, C. L., Noncovalent labeling of proteins in capillary electrophoresis with laser-induced fluorescence detection. *Cell Biochemistry and Biophysics* **2000,** 33, 323-337.

5. Ogulchansky, T. Y.; Losytskyy, M. Y.; Kovalska, V. B.; Lukashov, S. S.; Yashchuk, V. M.; Yarmoluk, S. M., Interaction of cyanine dyes with nucleic acids. XVIII. Formation of the carbocyanine dye J-aggregates in nucleic acid grooves. *Spectrochim Acta A Mol Biomol Spectrosc* **2001,** 57, (13), 2705-15.

6. Ogul'chansky, T.; Losytskyy, M.; Kovalska, V. B.; Yashchuk, V. M.; Yarmoluk, S. M., Interactions of cyanine dyes with nucleic acids. XXIV. Aggregation of monomethine cyanine dyes in presence of DNA and its manifestation in absorption and fluorescence spectra. *Spectrochim Acta A Mol Biomol Spectrosc* **2001,** 57, (7), 1525-32.

7. Ogul'chansky, T.; Yashchuk, V. M.; Losytskyy, M.; Kocheshev, I. O.; Yarmoluk, S. M., Interaction of cyanine dyes with nucleic acids. XVII. Towards an aggregation of cyanine

dyes in solutions as a factor facilitating nucleic acid detection. *Spectrochim Acta A Mol Biomol Spectrosc* **2000,** 56, (4), 805-14.

8. Patonay, G.; Kim, J. S.; Kodagahally, R.; Strekowski, L., Spectroscopic study of a novel bis(heptamethine cyanine) dye and its interaction with human serum albumin. *Appl Spectrosc* **2005,** 59, (5), 682-90.

9. Kim, J. S.; Kodagahally, R.; Strekowski, L.; Patonay, G., A study of intramolecular H-complexes of novel bis(heptamethine cyanine) dyes. *Talanta* **2005,** 67, (5), 947-954.

10. Tatikolov, A. S.; Costa, S. M., Complexation of polymethine dyes with human serum albumin: a spectroscopic study. *Biophys Chem* **2004,** 107, (1), 33-49.

11. Schaberle, F. A.; Kuz'min, V. A.; Borissevitch, I. E., Spectroscopic studies of the interaction of bichromophoric cyanine dyes with DNA. Effect of ionic strength. *Biochim Biophys Acta* **2003,** 1621, (2), 183-91.

12. Sowell, J.; Parihar, R.; Patonay, G., Capillary electrophoresis-based immunoassay for insulin antibodies with near-infrared laser induced fluorescence detection. *J Chromatogr B Biomed Sci Appl* **2001,** 752, (1), 1-8.

13. Sowell, J.; Agnew-Heard, K. A.; Christian Mason, J.; Mama, C.; Strekowski, L.; Patonay, G., Use of non-covalent labeling in illustrating ligand binding to human serum albumin via affinity capillary electrophoresis with near-infrared laser induced fluorescence detection. *Journal of Chromatography, B: Biomedical Sciences and Applications* **2001,** 755, (1-2), 91-99.

14. Sturmer, D. M. a. H., D. W., *The Theory of the Photographic Process*. 4th ed ed.

15. Zollinger, H., *Color Chemistry: Syntheses, Properties, and Applications of Organic Dyes and Pigments*. 2nd ed. ed.; VCH Publishers: New York, 1991.

Chapter 4. Capillary electrophoresis for dye applications

4.1. Introduction

Separation science is very important technique that separates individual components in a complex mixture. Due to the complexity in chemical and biological sciences, a number of separation techniques have been developed and applied to isolate complicated samples. As one of the universal separation methods, capillary electrophoresis has been extensively studied and developed.[1-5] This chapter introduces the basic instrumentation and applications capillary electrophoresis (CE) and discuses detailed capillary electrophoresis (CE) with near-infrared laser induced fluorescence (NIR-LIF) detection.

Capillary electrophoresis (CE) applies an electric field to separate sample mixtures based on their size and charge. It is one of the electrophoresis techniques that apply electric field to capillary. Electrophoresis was first introduced by Tiselius in 1937 to separate protein mixtures.[2, 3] In 1967, capillaries with i.d. 1 to 3 mm were induced by [6]. Since then, Virtanen[7] used glass capillary with i.d. 200 to 500 um and few years later, Mikkers et al. performed electrophoresis with Teflon capillary electrophoresis.[8-10] In early 1980, Jorgenson and Lukacs developed fused-silica capillary with i.d. 75 um.[11, 12] Capillary electrophoresis contains the advantages of electrophoresis and liquid chromatography in a method that provides high efficiency, fast analysis, and small sample consumption. Capillary electrophoresis has been recently applied to many analytical areas, such as marcrobiomolcule analysis, amino acid, chiral compound, protein etc.[1, 4, 13-17] Since 1988, CE related research has performed in both bioanalytical and pharmaceutical areas.

4.2. Capillary electrophoresis

The separation in capillary electrophoresis occurs as a result of the differential migration of sample mixtures in electric field. CE uses small internal diameters (20 to 100 um) of fused-silica capillaries, and the capillary is filled with buffers (Figure 4.1). Use of a

thin capillary offers several advantages, especially prevention of joule heating. Due to the high electric resistant of the capillary, high electric field (100 to 500 V/cm) with minimum joule heating can be applied, and due to a greater surface-to-volume ratio, it allows effective dissipation of heat.[1] In addition, the application of a high voltage applied results in short analysis time, improved efficiency, and resolution (Figure 4.2). The plug profile of electroosmotic flow (EOF) leads the whole flow of solution in CE, resulting in high theoretical plates over 10^5. The EOF is not related to charge, thus all solutes can be analyzed simultaneously. Also, CE is a separation technique that is rapidly developing due to the possibilities of minute sample consumption (1 to 10 nl), on-capillary detection, and qualitative and quantitative analysis.

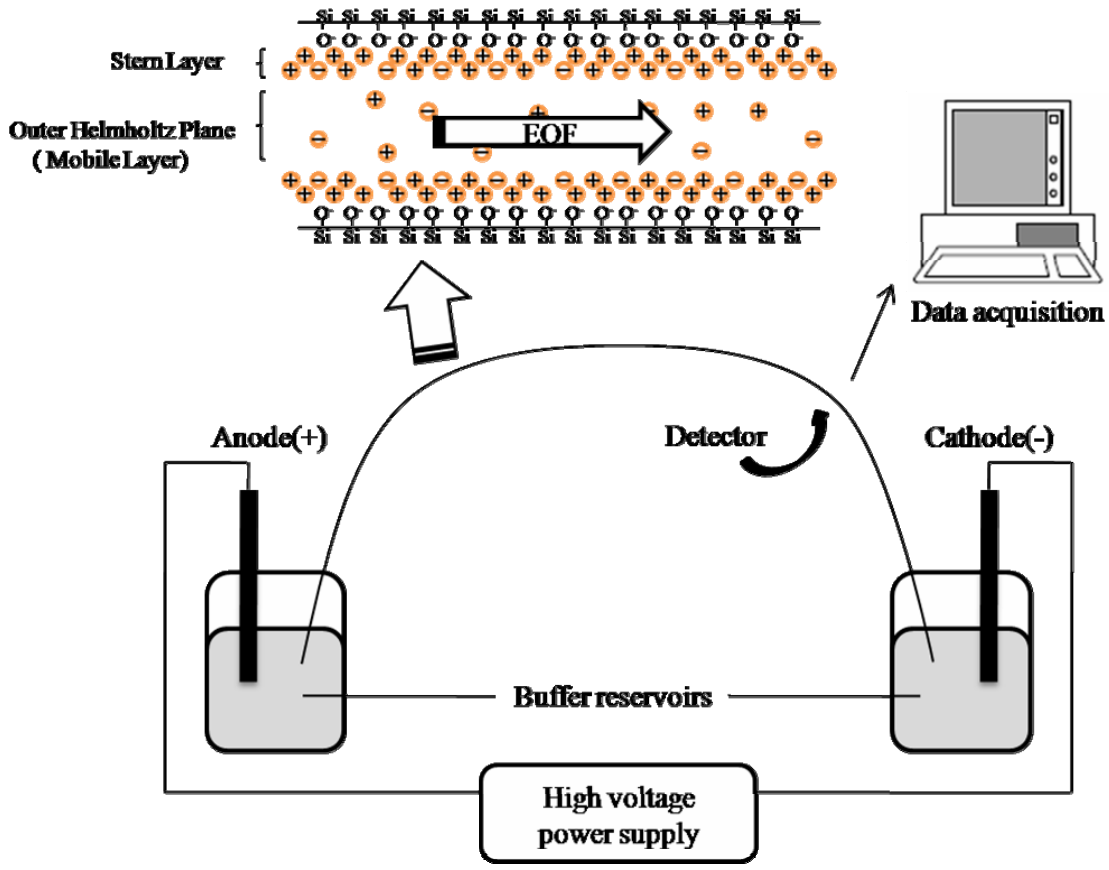

Figure 4.1. Basic configuration of capillary electrophoresis and representation of electroosmotic flow in CE.

Electrophoretic flow. Electrophoretic flow defines that a charged particle in electric field moves to electrode oppositely charged. The velocity, v_e, is expressed

$$v_e = \mu_e \times E = \mu_e \times V / L \quad (1)$$

where μ_e is the particle mobility, E is the applied field, V is the applied voltage, and L is the length of capillary. The separation of particle can be given by different velocity in capillary and the particle mobility is

$$\mu_e = \frac{q}{6\pi\eta r} \quad (2)$$

q represents the effective charge of ionized solute, η is the viscosity of the buffer, r is the Stockes radius of the ion. This equation explains that a small molecule, highly charged particle will have higher mobility than a large molecule, minimally charged species.

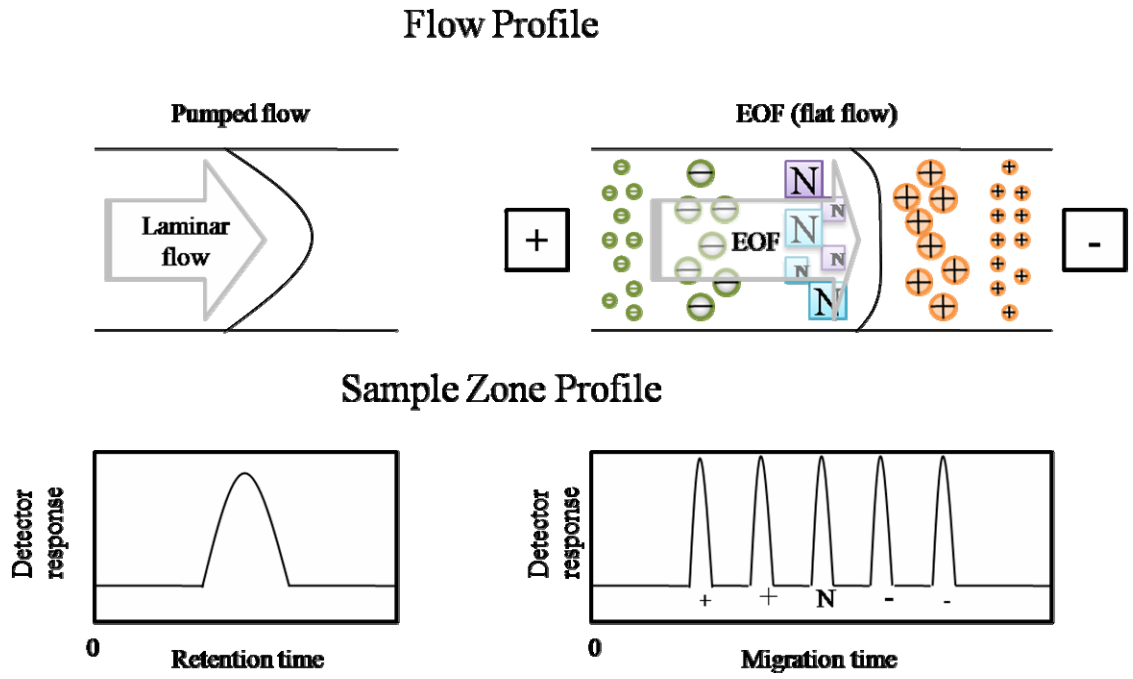

Figrue 4.2. Comparison of electroosmotic flow (CE) and pressure driven flow profiles (HPLC), and differential solute migration in capillary zone electrophoresis.

Electroosmotic flow. There is an electroosmotic flow (EOF) that leads all the fluid to one side with constant rate and direction and plays a role as a powerful force for separation.[1, 3] The EOF is determined by the surface charge of the capillary wall. Generally, the inner surface of fused-silica capillary has Si-OH groups, and it changes into $Si\text{-}O^-$ in a solution at pH >3. The ionized $Si\text{-}O^-$ pulls the cations of buffer and forms cation-layers. These cations generate more cation-layers since they cannot neutralize the nagatively charged capillary wall. The former formed layer is called static layer, or Stern layer or Inner Helmholtz layer and the later layer on the Stern layer is called mobile layer or Outer Helmholtz Plane. Both layers are called diffusion double layer (Figure 4.1). Under an applied field, the cations in Outer Helmholtz Plane migrate in the direction of the cathode. Because these cations are hydrated, bulk buffers are pulled toward the cathode, generating electroosmotic flow toward the cathode.

This EOF can be expressed by an equation below.

$$v_{eo} = \mu_{eo} \times E = \left(\frac{\varepsilon\zeta}{4\pi\eta} \right) \times E \qquad (3)$$

where the υ_{eo} is the velocity of EOF, ε is the permittivity of the solution, η is the viscosity, and ζ is the zeta potential at the capillary and solution interface. The character of EOF is flat flow in capillary as show in Figure 4.2. Because of the flat flow, the sample zone is concentrated and peak broadening is reduced, resulting in high resolution. This can be compared with the peak broadening in HPLC which shows laminar flow or parabolic flow due to the resistance of the flow by a pump in HPLC column.

The velocity of a sample in an electric field can be presented as the sum of electrophoretic flow and EOF. Thus, the mobility of a sample in a capillary differs based on charge, i.e. cation, neutral, or anion, and sequence. In the aspect of size of a sample, a highly charged small molecule elutes first, and a neutral and a less charged large molecule elutes

later. Figure 4.2. shows the elution order.

4.3. Separation parameters

Measurement of EOF. The simple way to measure the electroosmotic flow is loading a neutral marker. When the retention time and the length of capillary to detector are known, electroosmotic velocity can be obtained. The EOF has units of cm/sec, and can be expressed

$$\nu_{EOF} = \frac{l}{t_{nm}} \tag{4}$$

t_{nm} represents retention time (s) and l is the effective length (cm). From Eq 2, the electroosmotic mobility can be derived as following

$$\mu_{EOF} = \frac{\nu_{EOF}}{E} \tag{5}$$

The typical values for μ_{EOF} are 10^{-5} to 10^{-4} $cm^2/V.s$ and the common neutral molecules are benzene, pyridine and methanol, etc.

Efficiency. In electric mobile systems, efficiency is calculated in terms of the number of theoretical plates, N. N can be obtained from one of following equations.

$$N = 16\left(\frac{t}{w}\right)^2 \tag{6}$$

$$N = 5.54\left(\frac{t}{w_{1/2}}\right)^2 \tag{7}$$

t is the retention time, w is the peak width at base line and $w_{1/2}$ is the peak width at half height. Due to the longitudinal diffusion, sample zone broadening occurs, so the efficiency is also related to molecular diffusion.

$$\sigma^2 = 2Dt = \frac{2Dl}{\mu_e E} \tag{8}$$

D is diffusion coefficient and *l* is the effective length of capillary. Since $N = \left(\frac{l}{\sigma}\right)^2$, N can be presented by

$$N = \frac{\mu_e El}{2D} = \frac{\mu_e V}{2D} = \frac{(\mu_e + \mu_{eo})V}{2D} \quad (9)$$

Because μ and D are constant in a same molecule, N is proportional to the applied voltage.

Resolution. Resolution (R) represents the degree of the separated two peaks and can be defined by,

$$R_s = \frac{2(t_2 - t_1)}{w_1 + w_2} = \frac{t_2 - t_1}{4\sigma} \quad (10)$$

This equation shows the relation of different retention times and the process of the separation of two molecules. σ is the standard deviation and 1 and 2 are the elution order for the molecules, respectively. The degree of the separation for two molecules can be also related to efficiency.

$$R_s = \frac{1}{4} N^{1/2} \left(\frac{\Delta\mu}{\bar{\mu}}\right) \quad (11)$$

Here, $\Delta\mu$ is μ_2-μ_1 and $\bar{u}$ is $(\mu_2+\mu_1)/2$.

4.4 CE modes

The basic CE modes include capillary zone electrophoresis (CZE), micellar electrokinetic capillary chromatography (MEKC), capillary isoelectric focusing (CIEF), and capillary gel electrophoresis (CGE), etc. Most of the modes can be readily modified and handled depending on separating buffers. Moreover, the modes are complementary because they have

different separation mechanism.

Table 4.1. Mode of Capillary Electrophoresis for Different Classes of Analytes.[1]

Small Ions	Small Molecules	Peptides	Proteins	Oligonucleotides	DNA
CZE ITP	MECC CZE ITP	CZE MECC IEF CGE ITP	CZE CGE IEF ITP	CGE MECC	CGE

Capillary zone electrophoresis (CZE). CZE is the simplest mode filling with only run buffer. In CZE, solutes moves with different mobility in sample zone.[18-20] In this separation, selectivity of the solutes is easily varied by changing pH of buffer and mixing additives, such as surfactants and chiral selectors. Also, since EOF in CE is very sensitive to electrolytes, the selection of the electrolytes is important and running buffer that maintains pH during separation should be considered.

Micellar electrokinetic capillary chromatography (MEKC). MEKC is a form of the combination of electrophoresis and chromatography.[21-24] In 1984, Terabe introduced this mode. Since then, it became one of the universal modes because MEKC can separate not only ionic compounds but also nonionic neutral compounds. The separation can be performed by adding surfactants in running buffers. At a critical micelle concentration, individual surfactants aggregate to form a micelle, and this micelle under a certain environment follows the same or opposite direction of EOF. Because EOF is faster than micelle migration in neutral or basic solution, the apparent direction of micelle migration is same as that of EOF. While the micelle moves, it has hydrophobic and/or electrostatic interactions with solutes, as

in the stationary phase in chromatography, and then the nonionic solutes can be separated by the interaction with micelle.

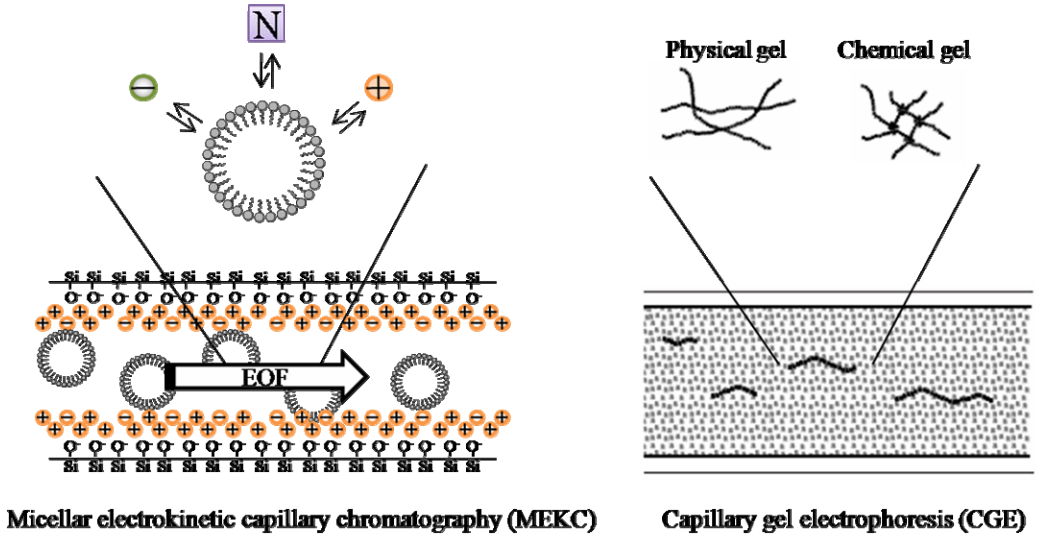

Figure 4.3. Micellar electrokinetic capillary chromatography (MEKC) and Capillary gel electrophoresis (CGE).

Capillary gel electrophoresis (CGE). CGE separates molecules based on size in a capillary filled with gel (Figure 4.3). This mode has been used in bioscience to separate macromolecules such as proteins and nuclei acids.[1, 25] Polyacrylamide is a universal gel and it can be used as chemical (uses polymerization in capillary) and physical (adds the polymer in run buffer) gel dependent on uses. This mode is similar to slab gel electrophoresis separation.

Capillary isoelectric focusing (CIEF). CIEF uses the difference of isoelectric points (pI) of protein or peptide. In this mode, pI can be estimated by the addition of ampholyte to the running buffer. After injecting the ampholyte and sample, and applying voltage, a pH

gradient is generated and the samples at a certain pH region are fixed, indicating the pI of the samples. After that, pressure or salt of the electrolyte is used to give the mobility.

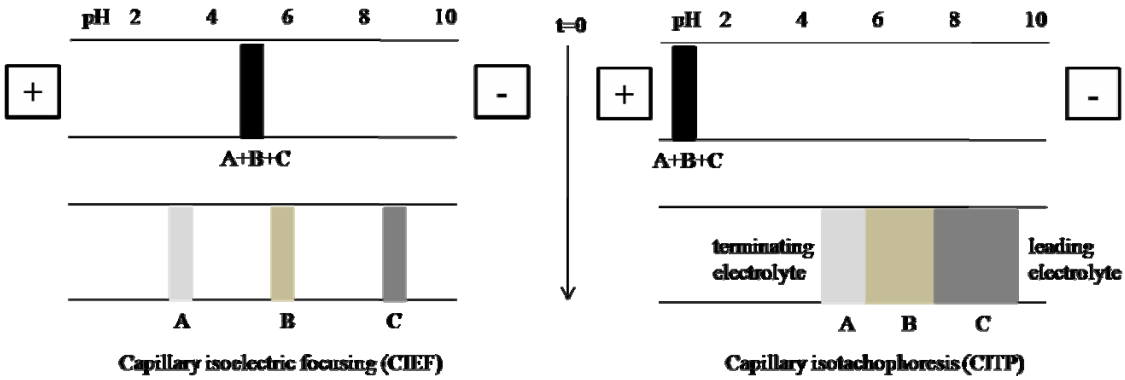

Figure 4.4. Capillary isoelectric focusing (CIEF) and capillary isotachophoresis (CITP).

Capillary isotachophoresis. (CITP). CITP uses two different buffers, and a sample is placed between the front buffer (leading electrolyte) and the rear buffer (terminating electrolyte).[1-3] In this mode, the electric field applied to the capillary maintains a constant mobility of the solutes. The mobility of the solute presents the relation of mobility and electricity, thus the sample zone with higher mobility has low electric field. This mode is applied to concentrate a sample and uses relatively large inner diameter of capillary.

4.5. Detection methods

The wide range of detection methods is available with capillary electrophoresis, such as UV/visible absorbance, fluorescence, conductivity, mass spectrometry, refractive index and electrochemical detection. The advantage of capillary electrophoresis over HPLC is that on-column detection is possible. This eliminates the band broadening cased by the detector coupling to the HPLC column. However, the small volume of sample injected and the small detection window requires highly sensitive detection systems. A brief description of available

detectors is presented in the section. Table 4.2. shows the lists of possible detection methods and their characters.

UV/Visible absorbance. Uv/vis detector is a universal method because the detection range is broad for common samples.[1, 2] The use of fused silica capillary makes it possible to use most of visible ray from 200 nm. The efficiency in CE is relatively high because the broadness by the mixture of individual samples is not existed. For the most of optical detectors, this region for detection range should be narrow to obtain higher resolution. Of the Uv/vis detectors, fixed-wavelength Uv/vis detector and photodiode are the examples of the detector. When using DAD, several wavelengths can be monitored simultaneously and the spectrum for each component can be readily observed, providing easy analysis. It is possible to find the optimum wavelength and confirm the purity of the peak and the quantity of the overlapped peaks. Moreover, peak identification is possible by comparing the spectrum of a sample with that of known compounds.

Fluorescence. Fluorescence detector in capillary electrophoresis greatly improves sensitivity (about 10^{-15}-10^{-17}) since the fluorescence is measured against zero background signal.[1, 26] However, the intrinsic fluoresce of the number of compounds are limited. Thus, the detection frequently requires a fluorophore as a label. The fluorescent signal is often collected at 90° degree to excitation source and can be discriminated by using filters or gratings. Laser induced fluorescence (LIF) further provides a superior approach to improving detection limits (about 10-18-10-20). A laser used in LIF detection concentrates high power monochromatic light and excites fluorophores in a small detection area, resulting in low limit of detection (LOD). Thus, it is an ideal detector for capillary electrophoresis measurement. In section 4.6, detailed instrumentation and applications of CE-LIF are introduced.

Table 4.2. Methods of detection in CE. Cited from Beckman coulter's tutoring material.

Method	Mass detection limit (moles)	Concentration detection limit (molar)	Advantages/ disadvantages
UV- Vis	10^{-13} - 10^{-16}	10^{-5} - 10^{-8}	• Universal • Diode array offers spectral information
Fluorescence	10^{-15} - 10^{-17}	10^{-7} - 10^{-9}	• Sensitive • Usually requires derivitisation
Laser induced fluorescence	10^{-18} - 10^{-20}	10^{-14} - 10^{-16}	• Extremely sensitive • Usually requires derivitisation • Expensive
Amperometry	10^{-18} - 10^{-19}	10^{-10} - 10^{-11}	• Sensitive • Selective but useful only for electroactive analytes • Requires special electronics and capillary modifications
Conductivity	10^{-15} - 10^{-16}	10^{-7} - 10^{-8}	• Universal • Requires special electronics and capillary modifications
Mass spectrometry	10^{-16} - 10^{-17}	10^{-8} - 10^{-9}	• Sensitive and offers structural information
Indirect UV, fluorescence, amperometry	10 - 100 times less than direct method		• Universal • Lower sensitivity than direct methods

Mass spectrometry. Another suitable detection for capillary electrophoresis is mass spectrometry that can measure the molecular weight of an analyte.[1, 2] The ionized and broken fragments are separated based on their mass to charge ratio. The spectrum contains information on the mass and relative abundance of the ion fragments. Thus, the detection

provides both qualitative and quantitative analysis in samples. Low limit of detection is also possible with mass spectrometry (about 10^{-16}-10^{-17}).

Conductivity detector. A conductivity detector is less sensitive than the detectors that directly detect the physical properties of molecules.[1] However, it is obvious that a conductivity detector is useful for the analysis of some sorts of materials including metallic ions, organic acids and inorganic acids, etc. The limit of detection (LOD) for a conductivity detector is dependent on the mobility between individual molecules and electrolyte ions.

Radioactive detection. Radiocapillary electrophoresis is also a sensitive detection scheme that monitors the sensitivity and selectivity of radioactive isotopes.[1] Altia et al. explained the separation and detection of capillary electrophoresis with γ emitter. Recently, an on-line radioactive detector has been developed for ^{32}P-labeled molecule separated by capillary electrophoresis. The detector is located near the outlet of the capillary and is consisted of a small semiconductor of CdTe that directly detects β particle emitted. This work shows as low as 10^{-9} M LOD.

4.6. Capillary electrophoresis with near-infrared laser induced fluorescence (CE-NIR-LIF)detection

Capillary electrophoresis with laser induced fluorescence (CE-LIF). The most sensitive detection method available for capillary electrophoresis is laser induced fluorescence.[1, 27] Some problems encountered with laser induced fluorescence detection. One of the problems is the incident light reflected by the capillary wall. This light scatter can be greatly reduced by the use of post-column detection that used a sheath-flow arrangement. However, it requires complicated apparatus and is not commercially available. Another disadvantage is that most

analytes require a fluorophore as a label due to lack of native fluorescence. This complicates chemistry to find a suitable label. Despite of the problems associated with laser induced fluorescence, there are numerous applications for trace analysis. For instant, it is ideal to a minute sample having a particular functional group. In this case, a suitable fluorophore can be labeled the functional group, resulting in increasing fluorescence for the target molecules. Many biomolecules including peptide, amino acids, protein, carbohydrates, oligonucleotides, and DNA are applied with capillary electrophoresis with laser induced fluorescence.

Capillary electrophoresis with near-infrared laser induced fluorescence (CE-NIR-LIF). The most applications of capillary electrophoresis with laser induced fluorescence uses the visible region of the spectrum and requires visible dyes as a label.[1] The use of near-infrared regions (650-1100 nm) with NIR dyes offers distinct advantages for bioanalytical applications.[27, 28] First of all, the scatter noise and matrix autofluorescence can be minimized in NIR region due to the fact that noise resulting in from scatter is related to the wavelength of detection by $1/\lambda^4$, and only few molecules possess fluorescence in NIR region. As can be seen in table 1.2., detection at 820 nm versus 520 nm results in more than 6-fold reduction in scatter noise. Second, the advances of semiconductor technology and fiber optic technology provide fast and sophisticated signal processing and offer low cost, long usable life time, stable output and compact size in NIR region, compared to an argon ion laser in visible region (table 1.1). Also, when looking at detectors, silicon avalanche photodiodes (APD) has advantages in NIR region. Compared to the commonly used photomultiplier tube (PMT), avalanche photodiode costs less than $ 50 with high quantum efficiency and extended life time. It also lowers noises and power consumption. The use of NIR dyes with near-infrared technology take full advantage due to the high molar absorptivities and quantum yields. Also, the various functionalities of NIR dyes facilitate the biomolecule analysis.

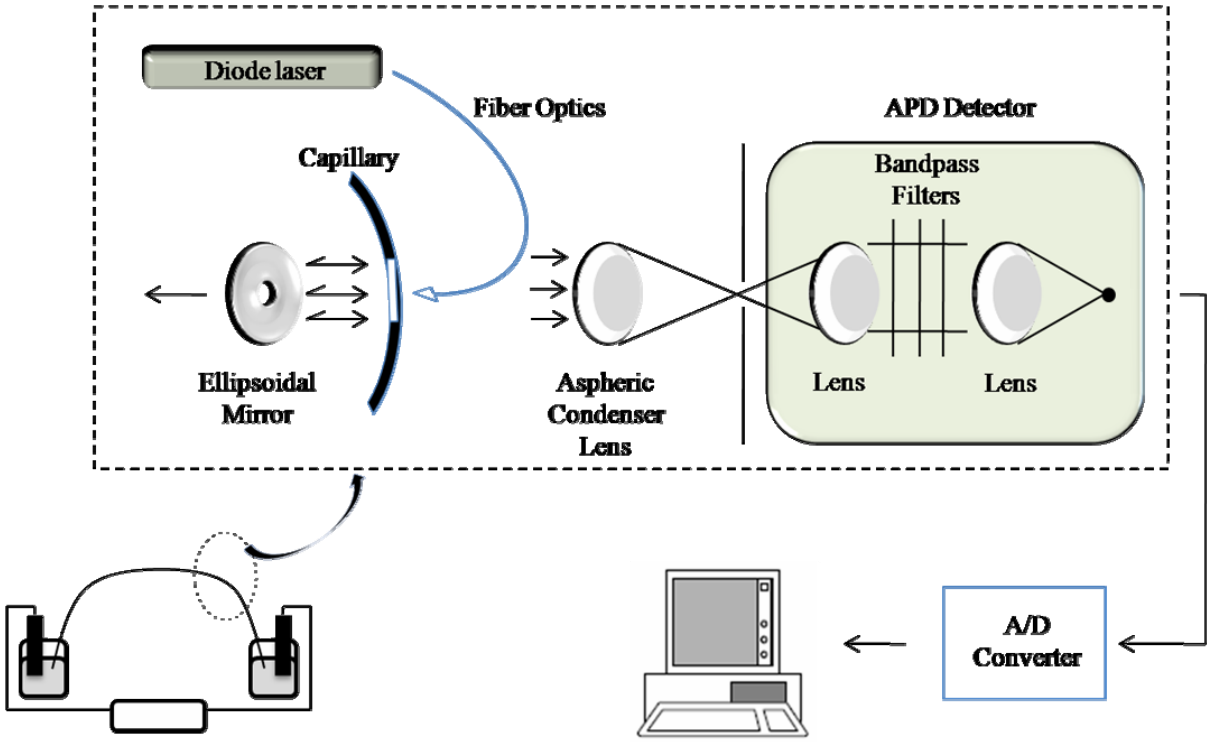

Figure 4.5. Schematic of CE-NIR-LIF detection.

References

1. Landers, J. P., *Handbook of Capillary Electrophoresis* 2nd ed.; CRC press: Boca Raton, FL, 1997.

2. H. Shintani, J. P., *Handbook of Capillary Electrophoresis Applications*. Blackie Academic & Professional: 1997.

3. Baker, D. R., *Capillary Electrophoresis*. John Wiley & Sons, Inc.: 1995.

4. He, X.; Ding, Y.; Li, D.; Lin, B., Recent advances in the study of biomolecular interactions by capillary electrophoresis. *Electrophoresis* **2004,** 25, (4-5), 697-711.

5. de Jong, E. P.; Melanson, J. E.; Lucy, C. A., Noncovalent labeling of myoglobin for capillary electrophoresis with laser-induced fluorescence detection by reconstitution with a fluorescent porphyrin. *Electrophoresis* **2004,** 25, (18-19), 3153-3162.

6. Hjerten, S., Free zone electrophoresis. *Chromatogr Rev* **1967,** 9, (2), 122-219.

7. Virtanen, R., Zone electrophoresis in a narrow-bore tube employing potentiometric detection. A theoretical and experimental study. *Acta Polytechnica Scand* **1974,** 123, 1.

8. Mikkers, F.; Ringoir, S.; De Smet, R., Analytical isotachophoresis of uremic blood samples. *J Chromatogr* **1979,** 162, (3), 341-50.

9. Oerlemans, F.; Verheggen, T.; Mikkers, F.; Everaerts, F.; de Bruyn, C., Analysis of serum purines and pyrimidines by isotachophoresis. *Adv Exp Med Biol* **1979,** 122B, 429-33.

10. Oerlemans, F.; Verheggen, T.; Mikkers, F.; Everaerts, F.; de Bruyn, C., Determination of uric acid in serum: comparison of a standard enzymatic method and isotachophoresis. *Adv Exp Med Biol* **1979,** 122B, 435-40.

11. Jorgenson, J. W.; Lukacs, K. D., Free-zone electrophoresis in glass capillaries. *Clin Chem* **1981,** 27, (9), 1551-3.

12. Jorgenson, J. W.; Lukacs, K. D., Zone electrophoresis in open-tubular glass capillaries. In 1981; Vol. 53, pp 1298-1302.

13. Yan, W.; Colyer, C. L., Investigating noncovalent squarylium dye-protein interactions by capillary electrophoresis-frontal analysis. *Journal of Chromatography, A* **2006,** 1135, (1), 115-121.

14. Schou, C.; Heegaard, N. H., Recent applications of affinity interactions in capillary electrophoresis. *Electrophoresis* **2006,** 27, (1), 44-59.

15. Ostergaard, J.; Heegaard, N. H., Bioanalytical interaction studies executed by preincubation affinity capillary electrophoresis. *Electrophoresis* **2006,** 27, (13), 2590-608.

16. Kraly, J.; Fazal, M. A.; Schoenherr, R. M.; Bonn, R.; Harwood, M. M.; Turner, E.; Jones, M.; Dovichi, N. J., Bioanalytical applications of capillary electrophoresis. *Anal Chem* **2006,** 78, (12), 4097-110.

17. Lacroix, M.; Poinsot, V.; Fournier, C.; Couderc, F., Laser-induced fluorescence detection schemes for the analysis of proteins and peptides using capillary electrophoresis. *Electrophoresis* **2005,** 26, (13), 2608-21.

18. Dolnik, V., Recent developments in capillary zone electrophoresis of proteins. *Electrophoresis* **1999,** 20, (15-16), 3106-15.

19. Kraak, J. C.; Busch, S.; Poppe, H., Study of protein-drug binding using capillary zone electrophoresis. *J Chromatogr FIELD Full Journal Title:Journal of chromatography* **1992,** 608, (1-2), 257-64.

20. Dette, C.; Ebel, S.; Terabe, S., Neutral and anionic cyclodextrins in capillary zone electrophoresis: enantiomeric separation of ephedrine and related compounds. *Electrophoresis* **1994,** 15, (6), 799-803.

21. Wang, J.; Warner, I. M., Chiral Separations Using Micellar Electrokinetic Capillary Chromatography and a Polymerized Chiral Micelle. In 1994; Vol. 66, pp 3773-3776.

22. Nishi, H.; Tsumagari, N.; Kakimoto, T.; Terabe, S., Separation of beta-lactam antibiotics by micellar electrokinetic chromatography. *J Chromatogr* **1989,** 477, (2), 259-70.

23. Nishi, H.; Fukuyama, T.; Matsuo, M.; Terabe, S., Separation and determination of the ingredients of a cold medicine by micellar electrokinetic chromatography with bile salts. *J Chromatogr* **1990,** 498, (2), 313-23.

24. Nishi, H.; Terabe, S., Application of micellar electrokinetic chromatography to pharmaceutical analysis. *Electrophoresis* **1990,** 11, (9), 691-701.

25. Williams, D. C.; Soper, S. A., Ultrasensitive near-IR fluorescence detection for capillary gel electrophoresis and DNA sequencing applications. *Anal Chem FIELD Full Journal Title:Analytical chemistry* **1995,** 67, (19), 3427-32.

26. Benito, I.; Marina, M. L.; Saz, J. M.; Diez-Masa, J. C., Detection of bovine whey proteins by on-column derivatization capillary electrophoresis with laser-induced fluorescence monitoring. *J Chromatogr A* **1999,** 841, (1), 105-14.

27. Baars, M.; Patonay, G., Ultrasensitive detection of closely related angiotensin I peptides using capillary electrophoresis with near-infrared laser-induced fluorescence detection. *Anal Chem* **1999,** 71, (3), 667-71.

28. Sowell, J.; Parihar, R.; Patonay, G., Capillary electrophoresis-based immunoassay for insulin antibodies with near-infrared laser induced fluorescence detection. *J Chromatogr B Biomed Sci Appl* **2001,** 752, (1), 1-8.

Chapter 5. Investigation of Noncovalent Biomolecule Labeling with Near-infrared Bis(heptamethine cyanine) Dyes by Capillary Electrophoresis with Near-infrared Laser Induced Fluorescence Detection

5.1. Introduction

Capillary electrophoresis with near-infrared laser induced fluorescence detection (CE-NIR-LIF) has recently been used for various applications.[1-10] CE has the advantages of minimal reagent consumption, high efficiency, high selectivity, and rapid separations for complicated mixtures. The use of near-infrared laser induced fluorescence (NIR-LIF) detection allows high sensitivity and reduction of possible background interference due to few molecules possessing intrinsic fluorescence in the NIR region of spectrum. The combination of CE and NIR-LIF has other advantages in the aspects of operation lifetime and maintenance costs. Moreover, very low detection limits can be achieved using NIR fluorescence because of high molar absorptivity and high quantum yield of NIR dyes as well as the virtually non-existent background interference and high efficiency of semiconductor laser and detection systems.[10]

This chapter introduces NIR cyanine dyes with CE-NIR-LIF detection for further non-covalent labeling investigation. First, different chemical structures of NIR cyanine dyes are studied in order to exam the influence of the structural dependency on protein labeling. RK780, JCM783 and JCM793 with different functionality are used for the purpose. Second, by modifying BCAII with acetic anhydride (AA) and succinic anhydride (SA), the influence of different hydrophobicity of a protein on non-covalent labeling is investigated. Since most of NIR dye-protein labelings rely on hydrophobic-hydrophobic interaction, labeling efficiency can be increased by the modification. In addition, the non-covalent strategies with CE-NIR-LIF detection is introduced; pre-column and on-column labeling.[3, 11-14] In pre-cluomn labeling a sample mixture is simply loaded to a capillary, and the separation is dependent on charge to size ratio of the mixture. On-column labeling obeys same rule except that the sample mixture is prepared separately; i.e., the label is an additive in run buffer.

This chapter discusses applications of novel carbocyanines with CE-LIF detection,

which open up powerful new analytical applications that are not only unavailable using visible fluorophores but also take advantage of the low interference of this spectral region.

5.2. Experimental

Instrumentation. Absorption measurements were acquired on a Perkin-Elmer Lambda UV/VIS/NIR (Lambda 50) spectrophotometer (Norwalk, CT). Fluorescence emission spectra were taken using a K2 spectrofluorometer (ISS, Champaign, IL) equipped with a R928 Hamamatsu photomultiplier tube (Bridgewater, NJ). Commercial GaAlAs laser diodes (Laser Max, Rochester, NY) were used as the excitation source at 690 nm. The spectral bandpass was 16 nm and the integration time was 3 s. All absorption and fluorescence measurements were taken in a 1 cm cuvette.

A modified P/ACE 5000 capillary electrophoresis instrument (Beckman Instruments, Fullerton, CA, USA) was used for all separation. The instrument was interfaced with a proprietary microscope and laser obtained from LI-COR (Lincoln, NE, USA). The laser assembly consisted of a GaA1As laser diode emitting at 785 nm, modulated with a 50% duty cycle. The laser was focused directly onto a fiber optic cable. The arrangement gave an average of 4 mW of power at the capillary interface. Detection was accomplished through the use of a Peltier cooled, three stage avalanche photodiode (APD). In order to reduce background noise, three 820 nm (+/– 10 nm) bandpass filters were used. The APD signal was demodulated by a lock in amplifier. The signal is filtered before it arrives at a Beckman 406 A/D converter. A personal computer was used to collect the signal from the A/D converter. A detailed description of the instrument is available elsewhere.[9, 10]

Other materials and Solvents. Fatty acid free HSA (≥96% purity) was obtained from Sigma (St. Louis, MO). Sodium phosphate monobasic (monohydrate) and sodium phosphate dibasic

(monohydrate) were purchased from Fisher Scientific (Fair Lawn, NJ). Water was Nanopure grade (Barnstead model D4751 ultrapure water system). Alkyl alcohol series were obtained from the Aldrich Chemical Company (Milwaukee, WI) in HPLC grade.

Methods. Stock solutions of all BHmCs series (1 mM) in methanol were stored in the dark at 4 °C. The 10 uM stock solution of HSA (≥96% purity, Sigma, St. Louis, MO) was prepared in 100 mM borate buffer at pH 9.0. Stock solution of HSA was prepared fresh daily. For spectrum study, the dye–HSA mixture was vortexed for 30 s. All working solutions contained only 1% (v/v) methanol to facilitate dye dissolution but to avoid denaturation of HSA. All spectra measurements were performed at room temperature. Some special other sample treatments were mentioned in each case.

Separations were performed at 23 °C. All buffers used were filtered and sonicated prior to use. All separations were performed using fused-silica capillaries with a polyimide coating (Polymicro Technologies, Phoenix, AZ, USA). Total capillary length was 57 cm, with an injection to detection length of 50 cm. The capillaries were 50 um inner diameters (i.d.) and 363 um outer diameters (o.d.). Between each run, the capillary was pressure rinsed with 1 N sodium hydroxide for 10 min, followed by 5 min rinses with water and run buffer, respectively. Samples were introduced by pressure injection (0.5 psi) and separated by 30 kV. Separations were carried out in the normal polarity mode and voltage was applied over a 17 s ramp time. For some other purpose, more detailed separation conditions are mentioned in each data, otherwise, those separation conditions above are applied.

5.3. Results and Discussion

Noncovalent labeling

For capillary electrophoresis with near infrared laser induced fluorescence (CE-NIR-

LIF) detection, the detection wavelengths of individual NIR carbocyanine dyes in different solvents were investigated in Table 5.1.. Dye-HSA complexes are also studied in the table. Interestingly, BHmCs in borate buffer exhibit non fluorescence due to H-type complex in the aqueous buffer, but the addition of HSA opens up the complex and enhanced fluorescence. A different behavior can be observed for monomeric carbocyanines of varying hydrophobicity as it can be seen in Figure 5.1.. The less hydrophobic the NIR dye (Dye 3) is, the less it is suitable for non-covalent labeling.

Table 5.1. Spectral properties of NIR dyes in different solvents.

	MeOH		Borate (100 mM, pH 9.0)		HSA (3 uM)	
	λ_{max}^{abs} (nm)	λ_{max}^{em} (nm)	λ_{max}^{abs} (nm)	λ_{max}^{em} (nm)	λ_{max}^{abs} (nm)	λ_{max}^{em} (nm)
Dye 1	780	802	775	800	786	803
Dye 2	783	798	775	793	803	811
Dye 3	789	806	782	806	-	-
BHmC-4	783	811	697, 792	-	792	806
BHmC-6	787	812	707, 801	-	792	809
BHmC-8	781	810	717, 807	-	793	810
BHmC-10	780	810	725, 809	-	791	806
BHmC-12	780	809	736, 800	-	797	809

This is in an interesting contrast to the requirements of covalent labeling, where NIR dyes are required to have significant aqueous solubility for the labeling reaction step. It is most likely that the hydrophobic pocket in HSA contributes the interaction for non-covalent labels. Dye 3 is, however, used for indirect detection by mixing it in run buffer prior to HSA injection. In this case of indirect detection technique, a negative peak for HSA is observed in Figure 5.2.. Since HSA sample zone does not contain dye 3, background base line shows fluorescence and the sample zone shows a vacant peak.

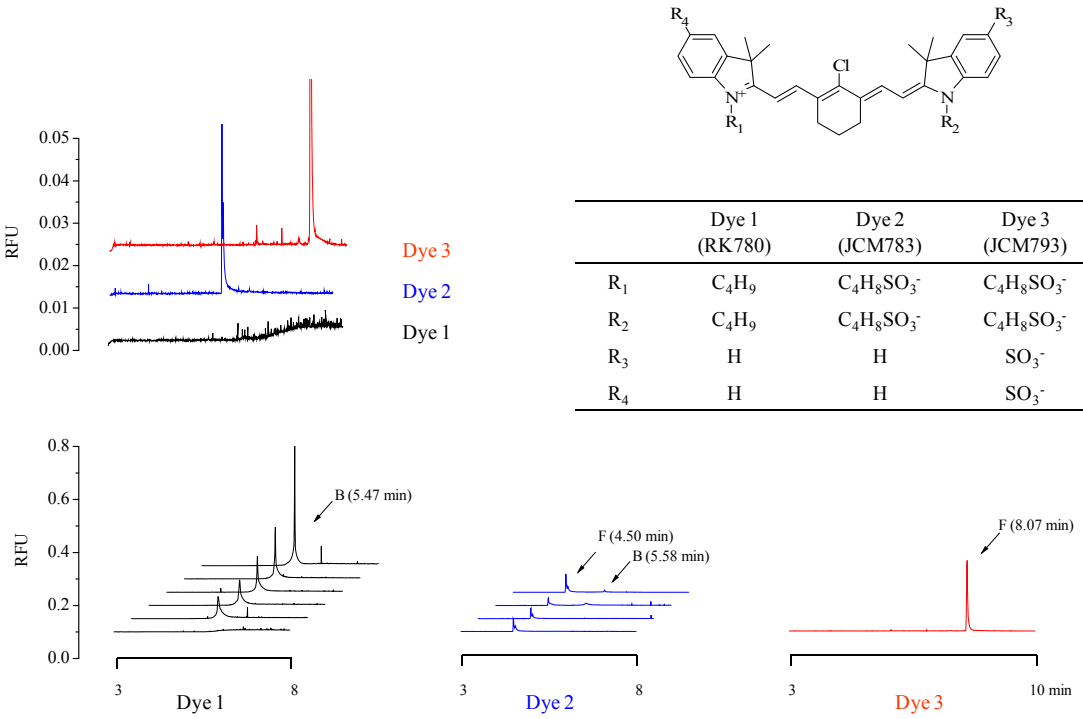

	Dye 1 (RK780)	Dye 2 (JCM783)	Dye 3 (JCM793)
R_1	C_4H_9	$C_4H_8SO_3^-$	$C_4H_8SO_3^-$
R_2	C_4H_9	$C_4H_8SO_3^-$	$C_4H_8SO_3^-$
R_3	H	H	SO_3^-
R_4	H	H	SO_3^-

Figure 5.1. Use of three types of heptamethine cyanine dyes for HSA labeling. 5 uM for each dye was injected in upper-left electropherogram. Prior to sample loading, 5 uM dyes with various concentration of HSA in 100 mM borate at pH 9.0 were mixed and injected for 1s. Three dyes with different substitutes and charges are shown in the table. Instrument condition: capillary; 50 cm to detector and 57 cm to outlet, 30kVs, runbuffer; 100mM borate pH 9.0, pressure; 0.5 psi.

It seems that the hydrophobicity of carbocyanine dyes plays an important role for noncovalent labeling. In figure 5.3., RK 780 (dye 1) and BHmC-12 are applied to find their uses as a noncovalent probe in capillary electrophoresis. In this study, dyes are prepared in run buffer prior to HSA injection. In order to find the optimum concentration of dyes, 0.15 uM of HSA is loaded to a capillary. RK 780 at 0.1 uM shows stable base line, but gives low fluorescent response upon addition of HSA. 10 uM of the dye shows reasonable detection response with HSA. However, due to unstable base line in initial analysis time, it should be incubated at least for 30 min.

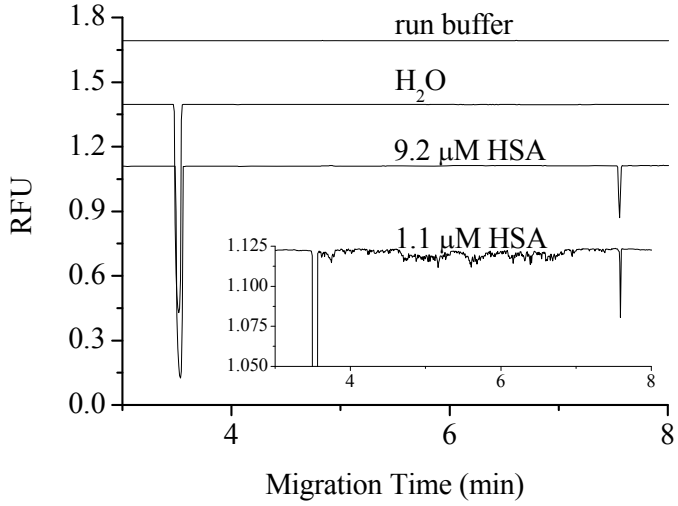

Figure 5.2. Indirect fluorescent detection of HSA. CE conditions: 40 cm x 47 cm, 50 um, 20 kV, 3s injection time. Run buffer contains dye 3 (12.8 uM containing 2 % methanol), and DI water and HSA were injected.

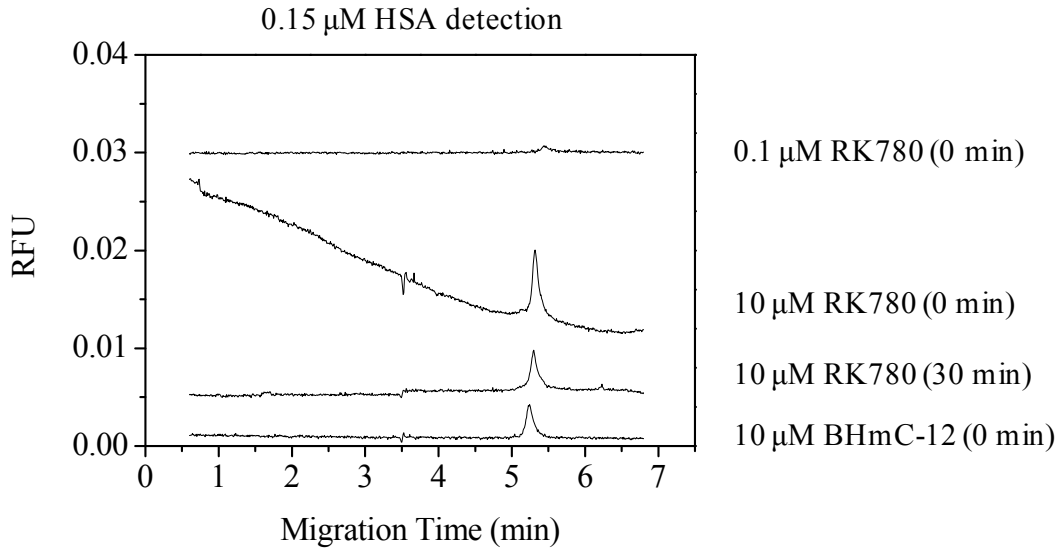

Figure 5.3. Non-covalent dye labeling to HSA. CE conditions: 40 cm x 47 cm, 50 um, 20 kV, 3s injection time. Runbuffers contain different dyes, concentrations having (a, b and d) 0 and (c) 30 min incubation time. a; 0.1 uM Dye 4, b and c; 10 uM dye 4, d; 10 uM BHmC-12. Applied protein concentration was 0.15 uM.

a)

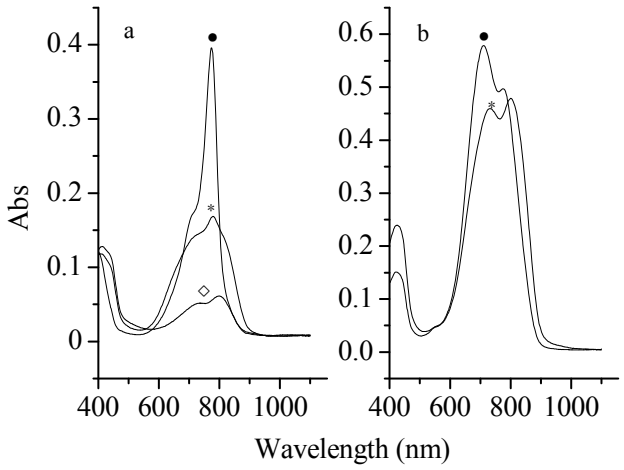

b)

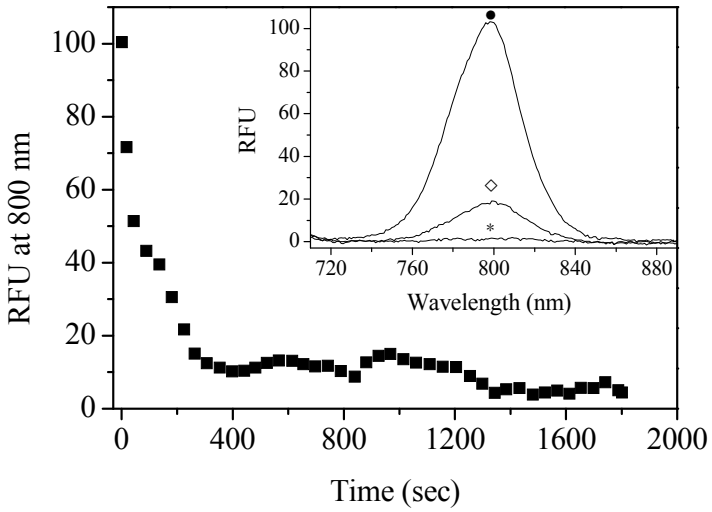

Figure 5.4. a) Spectral properties of Dye 1 (left) and BHmC-12 (right) in different solvents at room temperature. 10 uM dye concentrations were used in (•) H_2O at 0 min, (*) 100 mM borate at pH 9.0 at 0 min and (◦) 100 mM borate ate pH 9.0 after 30 min. b) Tim-dependent fluorescent spectral property of Dye 1 in borate at room temperature. Inset shows (◦) Dye 1 at 0 min, (•) at 30 min and (*) BHmC-12 at 0 min. Dye 1 exhibits low fluorescence after 30 min.

Figure 5.4. presents the optimal incubation time of the dye 1 to lower the background fluorescence for on-column labeling. In the case of BHmC-12, the incubation time is not a need for the labeling since it exhibits non-fluorescence without a sample. It is well compared in the inset in figure 5.4. and chapter 2.

BHmC-12 loaded to capillary does not result in NIR fluorescence signal unless biomolecules are added. HSA was used to illustrate this effect. The negatively charged capillary wall after activating the silanol group generally obstructs biomolecule detection with positively charged dyes. In other words, there may be electrostatic interaction between the negative wall and the positive dye, resulting in dragging the dye in the capillary and showing noises. As can be seen in figure 5.5., this fluorescent noise is significantly higher for the monomeric dye (dye 1). For bis(carbocyanines) the background fluorescence is significantly lowered. It is presumably that there can be intra-H-type dimers, i.e. closed form, and/or aggregates of BHmC-n on the capillary wall and in run buffer. The detection of HSA in CE-LIF shows clear differences between the dyes. BHmCs show the lowered limit of detection (LOD). Compared to other reports regarding non-covalent labeling, the LOD is significant in that the detectable range is less than 0.14 fmole.

Noncovalent labeling can results in CE electropherograms that are easier to analyze as it can be seen in Figure 5.6.. Quantitative analysis can be simple using pre-column labeling due to the linear behavior of this non-covalent labeling approach. As it can be seen, all BHmC-n dyes result in linear calibration curves. The CE results can be directly compared to monomeric dyes. The calibration curve in Figure 5.6. also shows the binding properties of all the BHmCs. Here the relatively strong binding property of BHmC-12 can be compared with its monomeric counterpart, RK780. The rest of BHmCs seemingly shows relatively weak binding to HSA. It seems that their closed forms need more energy to open up and bind to HSA, based on absorbance spectra from previous researches. Table 5.2. shows their LODs

and binding constants with HSA in CE-LIF.

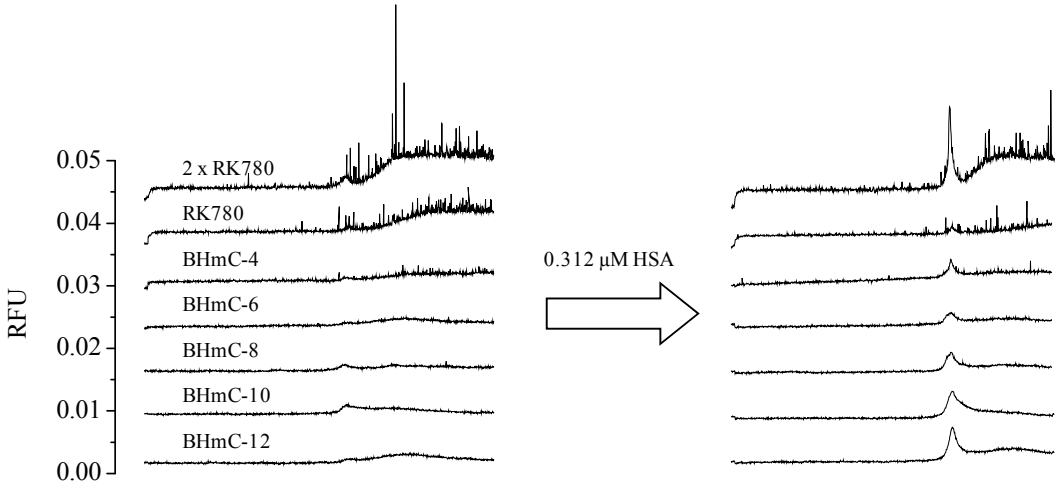

Figure 5.5. Low limit of detection due to intra-H-type dimers and/or aggregates of BHmCs. From top to bottom, 10 uM of RK780 and 5 uM of RK780, BHmC-12, -10, -8, -6 and -4. Left: 1s injection of dyes in MeOH, Right: 1 s injection dyes and 0.312 uM HSA mixture containing 1% MeOH in 100 mM borate pH 9.0. Instrument condition: capillary; 50 cm to detector and 57 cm to outlet, 30kVs, runbuffer; 100mM borate pH 9.0, pressure; 0.5 psi.

Table 5.2. LODs and binding constants of NIR dyes with HSA.

	LOD (fmole)	Binding constant, K_a, (10^5 M^{-1})	Correlation coefficiency, R^2
Dye 1	≥0.14	15.0	0.99
BHmC-4	≤0.14	2.3	0.98
BHmC-10	≤0.14	3.0	0.98
BHmC-12	≤0.14	8.0	0.99

Protein modification for noncovalent labeling.

In this section, the influence of the hydrophobicity of bovine carbonic anhydrase II (BCAII)

on noncovalent labeling is investigated. Generally, when studying noncovalent labeling, hydrophobic and electrostatic interactions play an important role. Thus, this section studies the modified side chains of a sample protein to see their relation to noncovalent interaction. BCAII has been widely studied with capillary electrophoresis because this protein can be readily modified with organic modifiers and shows various peaks based on the number of modified ε-NH_2. Figure 5.7. shows a scheme to modify BCAII with acetic anhydride and presents an electropherogram that shows regulated peaks based on its different charges. In the figure, 18 peaks can be seen because BCAII has 18 lysines on the surface of the molecule.

The mobility of native BCAII was shown in figure 5.8. (left). After addition of 0.039 mM acetic anhydride (AA), peaks near the unmodified BCAII were appeared and at higher concentration of AA, more negative charged BCAIIs were eluted later. Upon addition of different concentration of succinic anhydride (SA), the protein was modified by -2 negative charges and takes more time to elute. On the right-hand side, the modified proteins were mixed with RK780 for fluorescent detection. Here the native protein shows very weak interaction with the dye. However, more modified BCAIIs show higher fluorescent intensity with CE-LIF detection. In the inset picture, different modified protein solutions were mixed with the dye and their fluorescence was taken. It is most likely that the modified charge of ε-NH_2 on the surface of BCAII affects the noncovalent interaction between BCAII and RK780. In the case of succinylated BCAII, it shows little more enhanced fluorescence with RK780. As a result, it can be inferred that the modification of ε-NH_2 of BCAII leads hydrophobic and/or electrostatic interaction.

In figure 5.9., temperature effect on RK780-BCAII is also studied since in most noncovalent labeling, labeling efficiency can be varied dependent on experimental temperature. Generally, applied high temperature partially or completely denatures proteins, and during the process, proteins reforms or aggregates with a ligand or dye and enhances

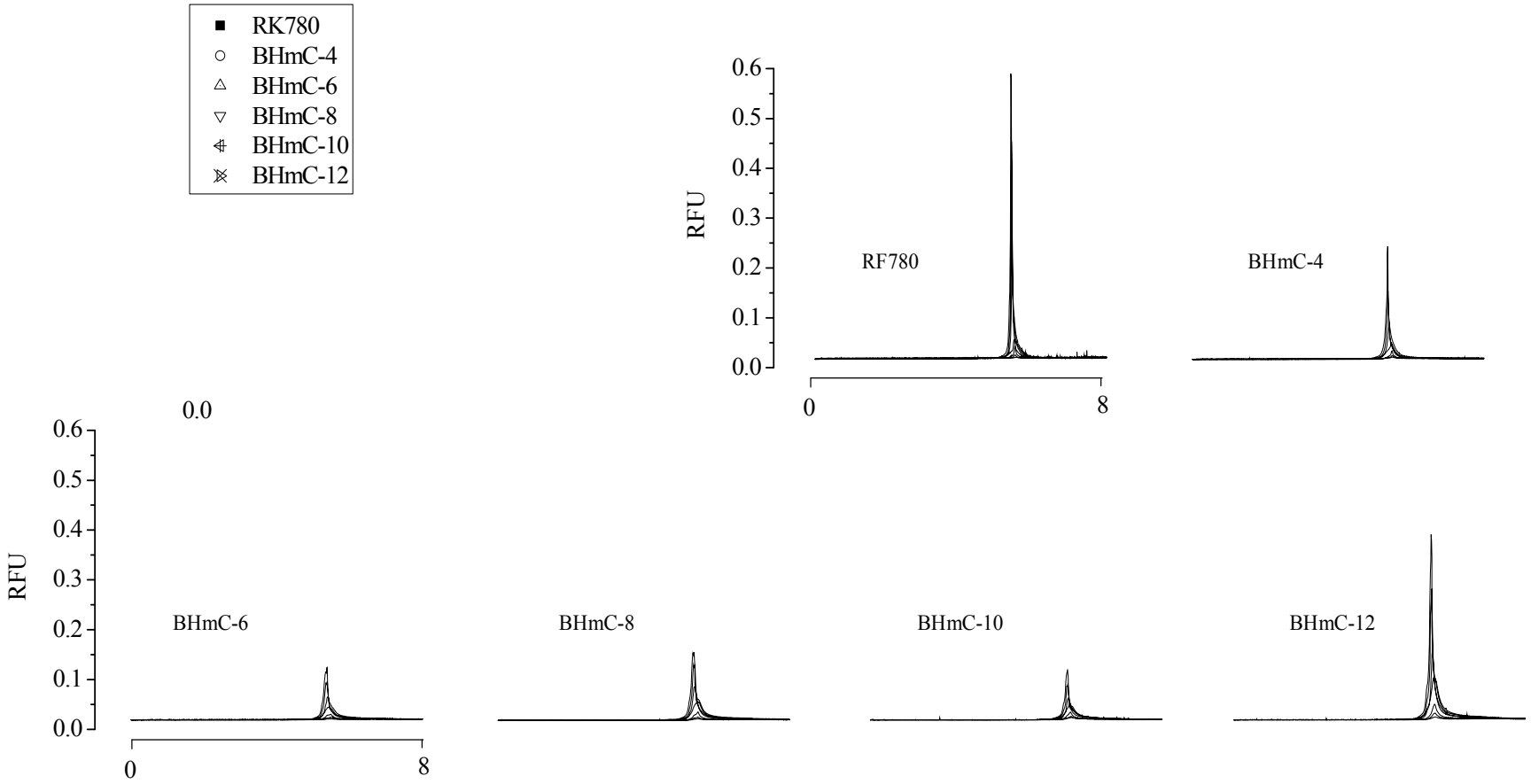

Figure 5.6. Non-covalent labeling HSA with dyes. Dye-HSA mixtures were prepared in 100 mM borate pH 9.0 containing 1 % methanol. Various concentrations, 0.312, 0.625, 1.25, 2.50, 5.0, 10, 20 uM, of HSA were prepared with constant dye concentrations, 5 uM. Experiment conditions were same as in Figure 5. Left-upper: linear calibration curves, y = 4E+06x - 1.2009, R2 = 0.9884 (RK780), y = 2E+06x + 0.2154, R2 = 0.9901 (BHmC-4), y = 2E+06x + 0.3752, R2 = 0.9934 (BHmC-6), y = 2E+06x + 0.4616, R2 = 0.9865 (BHmC-8), y = 1E+06x + 1.0449, R2 = 0.9809 (BHmC-10), y = 4E+06x + 0.746, R2 = 0.9931 (BHmC-12). Dye 3 was used as an internal standard to correct the peak areas of the complex.

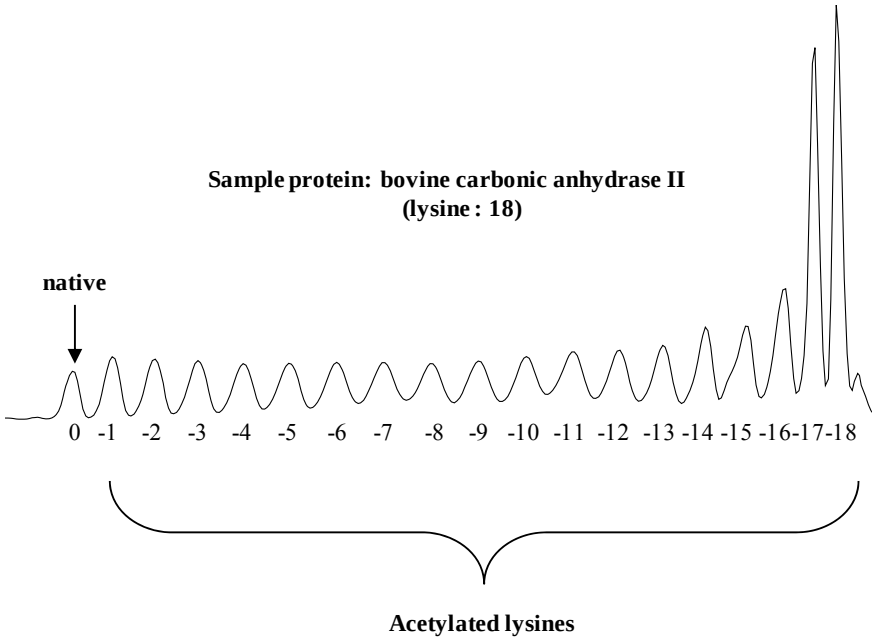

Figure 5.7. Modification of bovine carbonic anhydrase II (BCAII) with acetic anhydride. The number of modified lysines in BCAII appears on electropherogram (charge ladder). CE condition: 25 kV, 70 cm to detector, 77 cm to outlet, 10 sec injection for Uv detection at 214 nm, Tris-Glycine (25mM-192mM, at pH 8.4), 0.5 psi injection pressure.

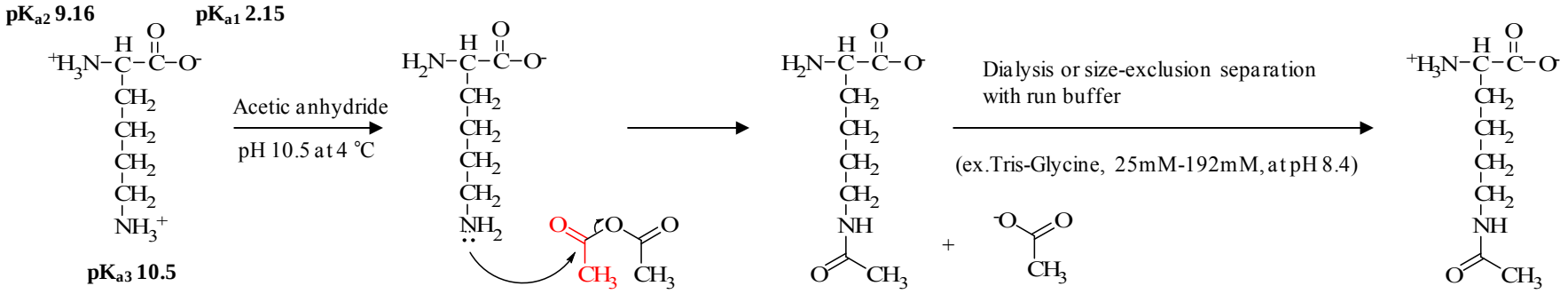

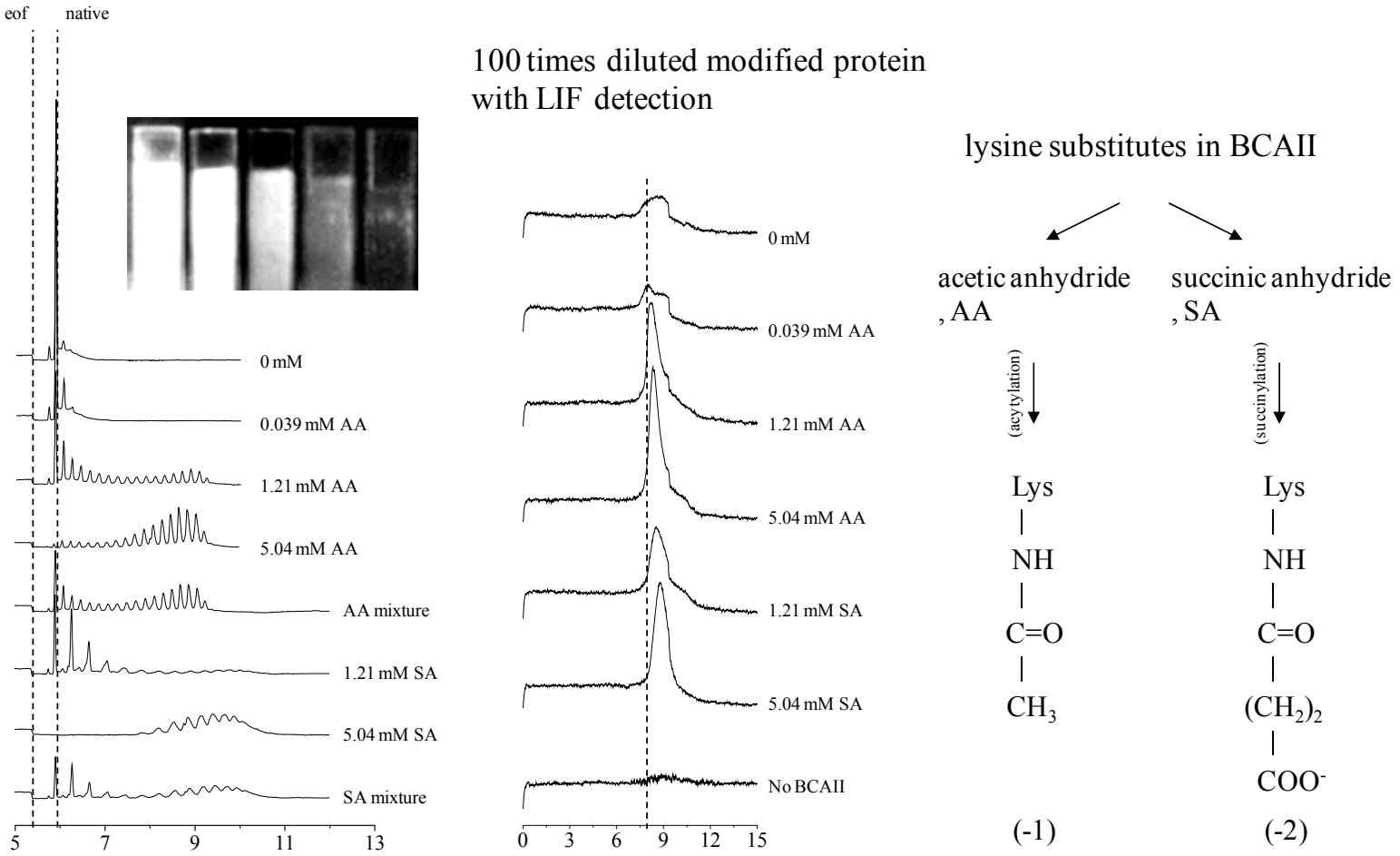

Figure 5.8. Charge ladders with acetic anhydride (AA) and succinic anhydride (SA). Left: various concentration of anhydrides (Uv detection at 218 nm). CE condition: 25 kV, at 214 nm, Right: modified proteins with dye-1 (LIF detection). Picture: from left to right, 5.04 mM AA, 1.21 mM AA, 0.039 mM AA, 0 mM AA, No BCAII (dye-1 was added to the solutions).

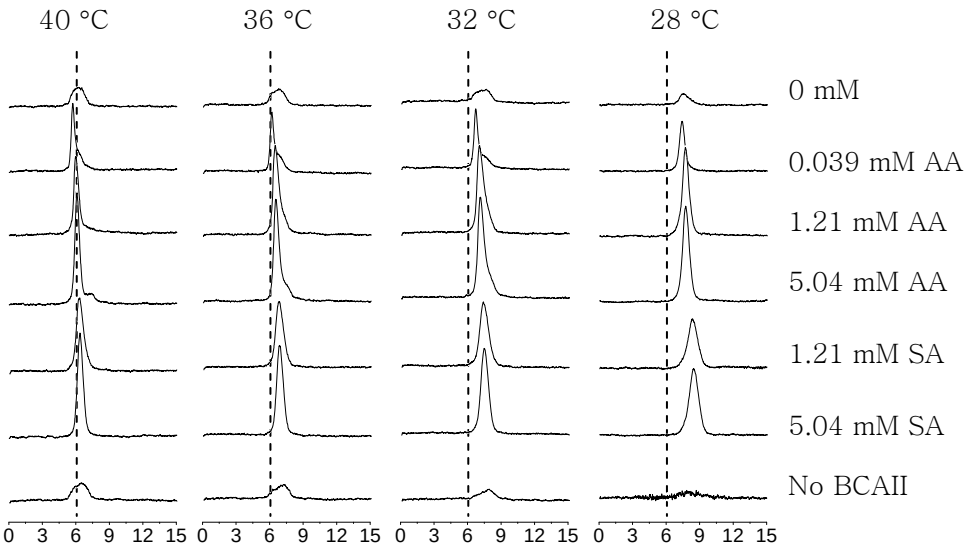

Figure 5.9. Temperature effect on RK780-BCAII complex. The measurement performed at 23 ~ 40 °C at different concentration of anhydrides mixed with RK780 (10 uM). Experimental condition is same as figure 5.8.

fluorescence. It was partially true in this study. When comparing temperature at 28 and 40 °C, improved detection and efficiency were observed.

5.4. Conclusions

The broad range of techniques and their applications in protein identification and quantification studies of a protein by a dye or ligand. The advantageous aspect of covalent method is that a series of identical side chains of amino acids in a protein can be labeled with a probe and this modified protein gives different spectrum response in spectroscopic analysis and different retention time or mobility in chromatographic analysis, and the drawback is that the experimental labeling environment needs to be controlled. In contrast, relatively simple labeling method, non-covalent labeling, is also used the specific binding sites of a protein, and the disadvantage is that the binding parameters need to be considered for a complex. However, it is essential since further applications with this method provide a proper

systematic behavior of this ligand toward a macromolecule, i.e. protein or nucleic acid. Because a protein is a large complicated molecule connected with many differently charged amino acids, its mobility can be easily varied in running buffers having different pH, so that the peaks between a dye and protein cannot be separated in some cases. For that reason, the latter case using non-fluorescent character of a dye will be an ideal case. Also, it should fluorescence upon binding to a target molecule. However, most free dyes fluorescence and the bound dyes require purification in pre-column labeling. In the case of on-column labeling, dyes need to be stored for several minutes so that the background fluorescence is reduced. The BHmCs were the alternative label for the purpose. As explained in chapter 1and 2, the conformationally flexible bis-dye immediately opens up and enhances fluorescence as it interacts with a large molecule and it inherently exhibits negligible fluorescence as it prepared. More interest also focused on its low LOD in CE-NIR-LIF detection. The closed clam-shell form during separation makes it possible to lower the LOD in aqueous solutions where most biomolecules requires for the analysis.

In summary, NIR fluorescence spectroscopy is a significant addition to analytical chemistry by utilizing novel molecular structures and the virtually interference-free NIR region. The advantages discussed in this chapter are not typically available in the shorter wavelength range of the electromagnetic spectrum. In addition, we expect that additional development of complex NIR molecules will open up a revolutionary new area of NIR fluorescence research whose importance can be only compared to advantages of the first NIR applications. By understanding how these molecules interact with the analytes, we can have a blueprint for designing powerful new analytical tools for all area of analytical chemistry by fully taking advantage of the virtually interference-free NIR fluorescence detection as well as specific applications in all areas of biological molecule research.

References

1. Yan, W.; Colyer, C. L., Investigating noncovalent squarylium dye-protein interactions by capillary electrophoresis-frontal analysis. *Journal of Chromatography, A* **2006,** 1135, (1), 115-121.

2. Welder, F.; Paul, B.; Nakazumi, H.; Yagi, S.; Colyer, C. L., Symmetric and asymmetric squarylium dyes as noncovalent protein labels: a study by fluorimetry and capillary electrophoresis. *J Chromatogr B Analyt Technol Biomed Life Sci* **2003,** 793, (1), 93-105.

3. McCorquodale, E. M.; Colyer, C. L., Indocyanine green as a noncovalent, pseudofluorogenic label for protein determination by capillary electrophoresis. *Electrophoresis* **2001,** 22, (12), 2403-2408.

4. Moody, E. D.; Viskari, P. J.; Colyer, C. L., Non-covalent labeling of human serum albumin with indocyanine green: a study by capillary electrophoresis with diode laser-induced fluorescence detection

Journal of Chromatography, B: Biomedical Sciences and Applications

1999, 729, (1 + 2), 55-64.

5. Colyer, C. L., Noncovalent labeling of proteins in capillary electrophoresis with laser-induced fluorescence detection. *Cell Biochemistry and Biophysics* **2000,** 33, 323-337.

6. Patonay, G.; Strekowski, L.; Kim, J. S.; Henary, M., The increasing role of NIR fluorescence spectroscopy in bioanalytical chemistry *NIR news* **2007,** 18, (3), 7-9.

7. Sowell, J.; Parihar, R.; Patonay, G., Capillary electrophoresis-based immunoassay for insulin antibodies with near-infrared laser induced fluorescence detection. *J Chromatogr B Biomed Sci Appl* **2001,** 752, (1), 1-8.

8. Sowell, J.; Mason, J. C.; Strekowski, L.; Patonay, G., Binding constant determination

of drugs toward subdomain IIIA of human serum albumin by near-infrared dye-displacement capillary electrophoresis. *Electrophoresis* **2001,** 22, (12), 2512-2517.

9. Sowell, J.; Agnew-Heard, K. A.; Christian Mason, J.; Mama, C.; Strekowski, L.; Patonay, G., Use of non-covalent labeling in illustrating ligand binding to human serum albumin via affinity capillary electrophoresis with near-infrared laser induced fluorescence detection. *Journal of Chromatography, B: Biomedical Sciences and Applications* **2001,** 755, (1-2), 91-99.

10. Baars, M.; Patonay, G., Ultrasensitive detection of closely related angiotensin I peptides using capillary electrophoresis with near-infrared laser-induced fluorescence detection. *Anal Chem* **1999,** 71, (3), 667-71.

11. Zhang, Z.; Carpenter, E.; Puyan, X.; Dovichi, N. J., Manipulation of protein fingerprints during on-column fluorescent labeling: protein fingerprinting of six Staphylococcus species by capillary electrophoresis. *Electrophoresis* **2001,** 22, (6), 1127-32.

12. Benito, I.; Marina, M. L.; Saz, J. M.; Diez-Masa, J. C., Detection of bovine whey proteins by on-column derivatization capillary electrophoresis with laser-induced fluorescence monitoring. *J Chromatogr A* **1999,** 841, (1), 105-14.

13. Bardelmeijer, H. A.; Lingeman, H.; De Ruiter, C.; Underberg, W. J. M., Derivatization in capillary electrophoresis. *Journal of Chromatography, A* **1998,** 807, (1), 3-26.

14. Williams, D. C.; Soper, S. A., Ultrasensitive near-IR fluorescence detection for capillary gel electrophoresis and DNA sequencing applications. *Anal Chem FIELD Full Journal Title:Analytical chemistry* **1995,** 67, (19), 3427-32.

Chapter 6. A Study of Distinct Conformations of Bis-Cyanine Dyes and Their Efficient Separation via Capillary Electrophoresis

6.1. Introduction

Conformational isomers of Bis(heptamethine) cyanine (BHmC) dye linked by flexible bridge are separated and properly evaluated via capillary electrophoresis using near infrared laser induced fluorescence (CE-NIR-LIF) detection and spectroscopic analysis. Since aggregation of cyanine dyes is dependent on various environment and the formation and slippage of the aggregates change their energy level, CE that uses various aqueous running buffers facilitates the formational or conformational isomers and allows the study of conformational-dependent mobilities on aggregates. Based on the knowledge of their properties obtained by CE, they have been utilized for the fluorescent enhancement upon interaction with human serum albumin (HSA) and acridine orange (AO).

In previous chapters, BHmC dyes are utilized for protein analysis.[1, 2] Compared to their monomeric counterpart, these dimeric dyes exhibit negligible fluorescence in phosphate buffer, and the absorbance spectra of their aggregates are very similar to that of monomer band. It is noteworthy that the heptamethine bridge in these dyes is rigid, whereas the alkyl linker arms between counterparts are very flexible so that intra-dimers are readily formed and possible overlapping regarding intra-dimer to monomeric band could be observed. These dyes seemed to have stable isoforms dependent on the length of alkyl bridge and solvent. Here we have studied their separation between open and closed clamshell form whether or not J-type intra-dimer, *i.e.* isoform of BHmC-O_3, exists under some various solvent environments. In doing so, CE was a very good candidate for their separation. In CE, some of aqueous and organic solvents in running buffer and/or sample solution are commonly applied for separation.[3, 4] It provides the separation of aggregates and observes their behavior under similar solvent condition.

Use of CE in characterization of dye aggregation. The electrophoretic mobility is the

important parameter to specify the motion of charged molecules in electrophoresis. It is well known that the separation of molecules in CE is dependent on the net charge and size of molecules, but the detailed shape dependence of mobility is still unclear because of lacking for molecules with the complexity of shape and charge distribution.[3, 4] In order to explain the influence of molecular shape, many researchers have studied the shape-dependent on mobility by using diverse peptides and proteins, and applied three different relationships.[5-8]

Stoke's law (radius, nonconducting media)[9-11] :

$$\mu = kZM^{-1/3} \qquad \text{- (1)}$$

Classical polymer (chain length, radius of gyration)[12-15] :

$$\mu = kZM^{-1/2} \qquad \text{- (2)}$$

Offord's model (surface area)[5-8, 16] :

$$\mu = kZM^{-2/3} \qquad \text{- (3)}$$

μ represents the electrophoretic mobility, k is a constant, Z is the charge of molecules, M is the molecular weight, and the values, 1/3, 1/2 and 2/3, are a constant related to molecule shape. For Stoke's law, the radius of molecules in nonconducting media is considered. Classical polymer model relates the radius of gyration caused by different chain lengths. Offord's model suggests that the frictional force be considered as a function of the surface area of the molecule and $M^{2/3}$. According to the results reported from the various suggestions, Offord's model is the most appropriate value for proteins and smaller molecules.[8] This is the simple fundamental model for the electrophoresis of a spherical, rigid, and insulating particle for small peptides. However, no relation including Offord's explains flexible molecules.

Recently, Miklós Idei *et al*. have investigated the influence of organic solvent containing background electrolytes (BGEs) on anti-tumor peptides, S-218, S-220, S-228, S-232, S-248, and S-250.[17] According to their report, the addition of organic modifier in BGEs led to alteration of the hydrodynamical size of the peptides and changed their mobilities.

Their report explains that more compact structure, less resistance, and, therefore, higher mobility in CE. When considering this shape-dependent mobility in CE, it was possible to understand the mobility changes of clamshell-like-dimeric cyanine dyes since they have characteristic conformations dependent on environmental changes.

In this report, considering the flexibility of BHmC-O_3 and its solvent-dependent conformation in aqueous solution, we determined the mobility of this unique molecule for each conformational isomer.

6.2. Experimental

Instrumentation. Absorption measurements were acquired on a Perkin-Elmer Lambda UV/VIS/NIR (Lambda 50) spectrophotometer (Norwalk, CT). Fluorescence emission spectra were taken using a K2 spectrofluorometer (ISS, Champaign, IL) equipped with a R928 Hamamatsu photomultiplier tube (Bridgewater, NJ). Commercial GaAlAs laser diodes (Laser Max, Rochester, NY) were used as the excitation source at 780 nm. The spectral bandpass was 16 nm and the integration time was 3 s. All absorption and fluorescence measurements were taken in a 1 cm cuvette.

A modified P/ACE 5000 capillary electrophoresis instrument (Beckman Instruments, Fullerton, CA, USA) was used for all separations. The instrument was interfaced with a proprietary microscope and laser obtained from LI-COR (Lincoln, NE, USA). The laser assembly consisted of a GaA1As laser diode emitting at 785 nm, modulated with a 50% duty cycle. The laser was focused directly onto a fiber optic cable. The arrangement gave an average of 4 mW of power at the capillary interface. Detection was accomplished through the use of a Peltier cooled, three stage avalanche photodiode (APD). In order to reduce background noise, three 820 nm (+/– 10 nm) bandpass filters were used. The APD signal was demodulated by a lock in amplifier. The signal is filtered before it arrives at a Beckman 406

A/D converter. A personal computer was used to collect the signal from the A/D converter. A detailed description of the instrument is available elsewhere.[18]

Other materials and Solvents. Fatty acid free HSA (≥96% purity) and 3,6-Bis(Dimethylamino)acridine, aka Acridine Orange base (AO), were obtained from Sigma (St. Louis, MO). Sodium phosphate monobasic (monohydrate) and sodium phosphate dibasic (monohydrate) were purchased from Fisher Scientific (Fair Lawn, NJ). Water was Nanopure grade (Barnstead model D4751 ultrapure water system). Alkyl alcohol series were obtained from the Aldrich Chemical Company (Milwaukee, WI) in HPLC grade.

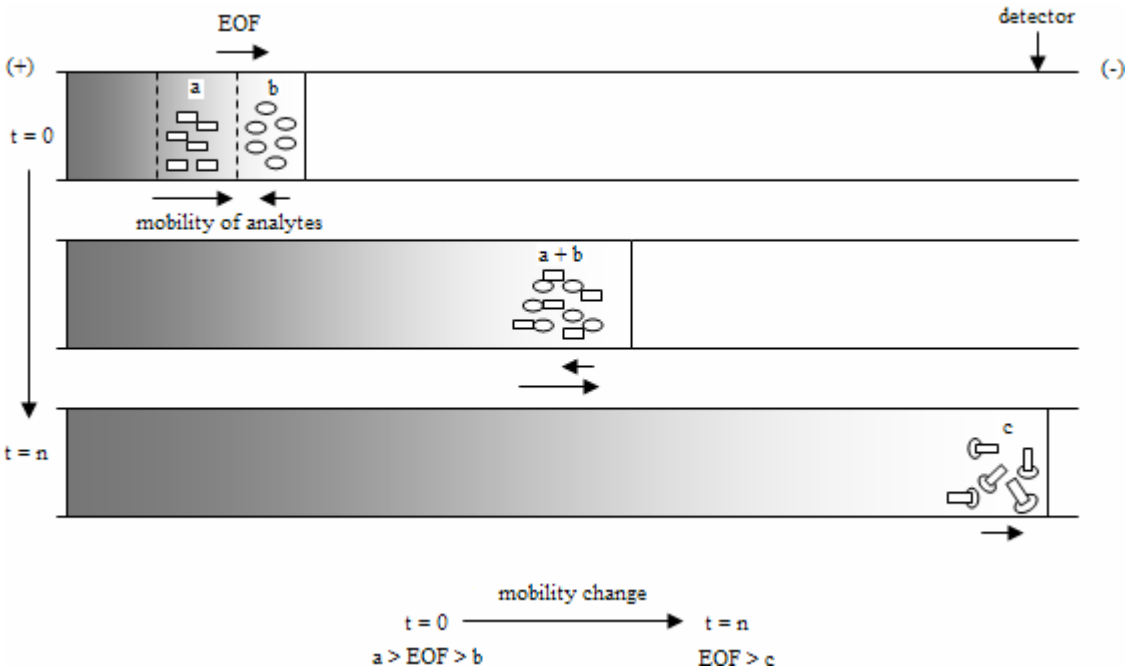

Figure 6.1. Sample handling scheme. For convenience, BHmC-O_3 drew as a regular single molecule, not open or closed clamshell form. a): BHmC-O_3, b): HSA or AO and c): complex of a) and b). Injection times for each sample are 3 s (a) and 2 s (b).

Methods. Stock solutions of all BHmC-Os series (1 mM) in methanol were stored in the dark at 4 °C. The 10 uM stock solution of HSA was prepared in 20 mM phosphate buffer at pH 7.2. Stock solutions of HSA were prepared fresh daily. The individual sample for CE separation was loaded and mixed according to the mobility of individual sample to avoid sample consumption and allow for equilibration. Figure 6.1. represents a basic separation technique considering the mobility of analytes. As increasing separation time t=0 to t=n, BHmC-O_3 having fast mobility binds to HSA. Consequently, the complex for these two molecules causes the decrease of net mobility relative to electroosmotic flow (EOF) in CE. The study of AO interaction to BHmC-O_3 also applies this scheme. For spectral study, the dye–HSA mixture was vortexed for 30 s. All working solutions contained only 1% (v/v) methanol to facilitate dye dissolution but to avoid denaturation of HSA. All spectra measurements were performed at room temperature. Some special other sample treatments were mentioned in each case.

Separations were performed at 25 °C. All buffers used were filtered and sonicated prior to use. All separations were performed using fused-silica capillaries with a polyimide coating (Polymicro Technologies, Phoenix, AZ, USA). Total capillary length was 57 cm, with an injection to detection length of 50 cm. The capillaries were 75 um inner diameter (i.d.) and 363 um outer diameter (o.d.). Between each run, the capillary was pressure rinsed with 1 N sodium hydroxide for 10 min, followed by 5 min rinses with water and run buffer, respectively. Samples were introduced by pressure injection (0.5 psi) and separated by 23 kV. Separations were carried out in the normal polarity mode and voltage was applied over a 17 s ramp time. For some other purpose, more detailed separation conditions are mentioned in each data, otherwise, those separation conditions above are applied.

6.3. Results and discussion

6.3.1 Characteristic conformation of BHmC-O_3.

Recently, Armitage, B. A. *et al*.[19] and some other groups[20] have studied dye aggregates by restricting DNA template to fit on dye dimer and explained fundamental energy level scheme for H- and J-aggregates of cyanine dyes, $DiSC_2$ (5), $DiSC_{3+}$ (5) and PIC. According to them, H- and J-dimers are close to monomer band compared to aggregates and aggregates are represented as high and low every level for H- and J-aggregates, respectively. However, their group and other research groups have not reported the possibility of overlap of dye dimer and aggregates to monomer band. The reason is presumably that the efforts for the separation of dye aggregates have not been attempted and general cyanine dyes show significant different energy level. In this aspect, our BHmCs synthesized for DNA application reveal the possible separation dependent on their conformations. The separation of BHmC-Os aggregates in CE, which can use similar aqueous solutions for aggregation, would be meaningful for further understanding of dye aggregates on their conformation dependent mobility.

For their chemical and physical properties on aggregation, three different BHmC-Os were evaluated under constant CE condition (Fig. 6.2.). Unlike other cyanine dyes, BHmC-Os are relatively large molecule linked by three different bridges. This produces characteristic spectra and mobilities, especially in case of BHmC-O_3. CE separation, which can adapt various aqueous solutions that facilitate dye aggregation, allows us to understand those properties. Figure 6.3. depicts the possible conformation of BHmC-Os, their energy level and mobility. It is noteworthy that J-type di-, tri-, or polymers are red-shifted relative to their monomer band and exhibit sharp and strong fluorescence.[15,34,35] In contrast, H-aggregates are blue-shifted and exhibit negligible fluorescence.[20-26] In the aspect of mobility, H-and J-type close forms are faster than the open form due to their compact size and reduced friction in CE.

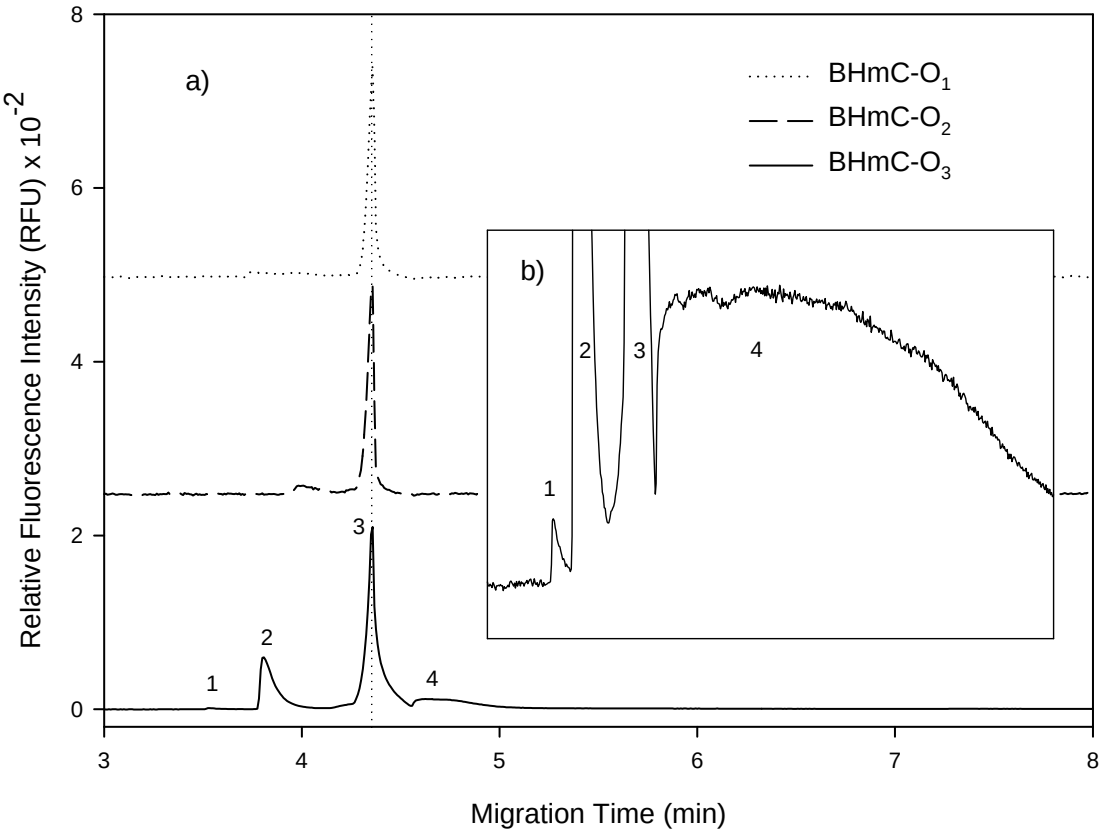

Figure 6.2. Conformational effect of three different bridges in BHmC-Os. a): comparison of three BHmC-Os in CE. b): zoomed window for BHmC-O_3. peak 1 and 2: J-type intra-dimer (closed clamshell form), peak 3: open forms of BHmC-Os, peak 4: J-type aggregate. Condition: 3 second pressure injection (0.5 psi), 23 kV applied voltage, 75 um x 57 cm capillary; 100 mM borate at pH 9.0. All the concentrations of BHmC-Os are 160 uM in methanol.

However, their aggregates having more viscous and larger size are much slow and dragged in CE. CE having 820 nm detection bandpass filter make it possible to predict shape-dependent mobility. In this study, the monomer, open clamshell form, is emitted at around 820 nm, *see* Figure 6.10.. Consequently, their detection in Figure 6.2. produces higher fluorescence intensity for open form (peak 3) than the other closed forms (peak 1 and 2) or aggregates (peak 4). Regarding peak 1, it is sophisticated to identify whether it is another few populated J-type dimer or negligible fluorescence by H-type dimer since they may have

undistinguishable formation. However, in any cases, it is true that there are overlapped dye conformations at around 820 nm and it was possible to separate them in CE by their formation.

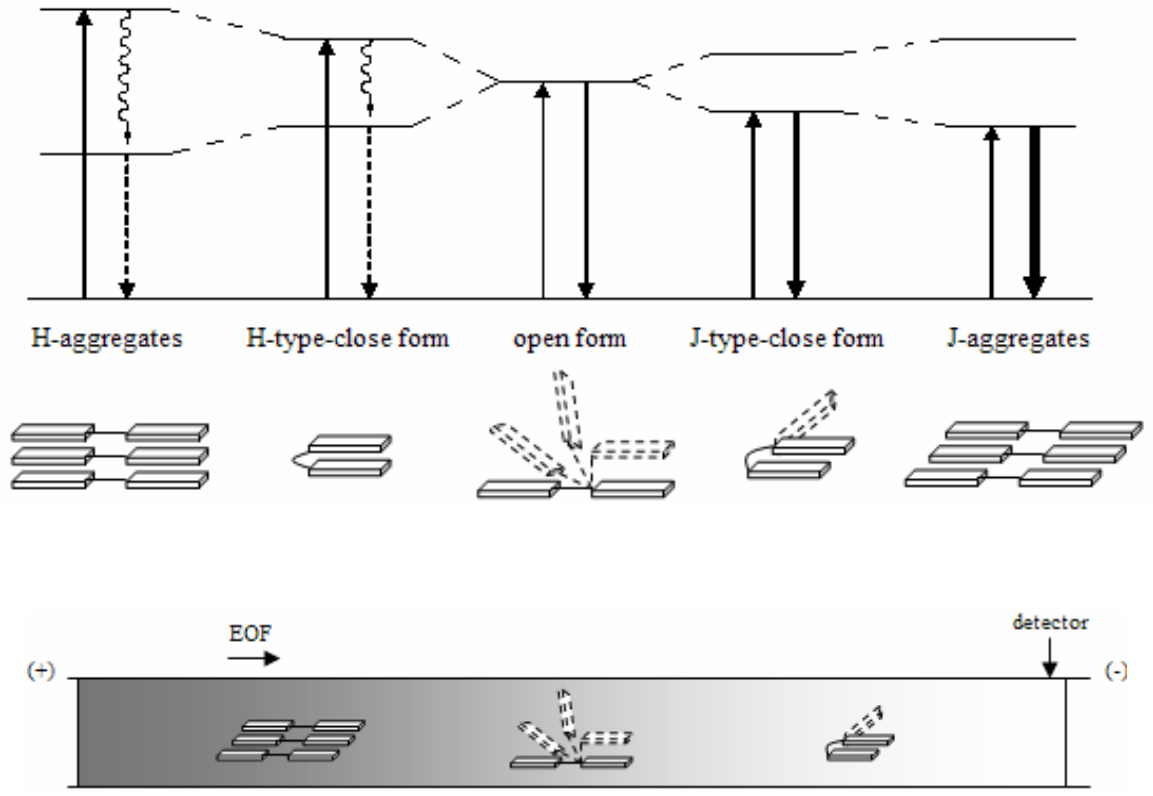

Figure 6.3. Possible conformations for bis(heptamethine) cyanines, and their energy level and mobility in capillary electrophoresis. Dotted and bold arrows in energy level indicate negligible and enhanced fluorescence, respectively. The mobility in capillary drew based on the conformation of BHmC-O_3.

6.3.2 Factors affecting on aggregation.

CE generally uses aqueous running buffer that can promote aggregation. It is well-known that concentration increase of cyanine dyes that aggregate in aqueous solution increases dye aggregation,[27, 28] and they have different formational properties upon

aggregation dependent on the character of individual dye. Moreover, the formational dependence characterizes H- and J-type aggregates. To confirm this dye concentration effect on aggregation, we increased the concentration of BHmC-O_3 in sample solution. Although samples are prepared in methanol, this organic solvent is dispersed to running buffer in CE system.[3, 4] Thus, it results in J-type closed clamshell form and aggregates.

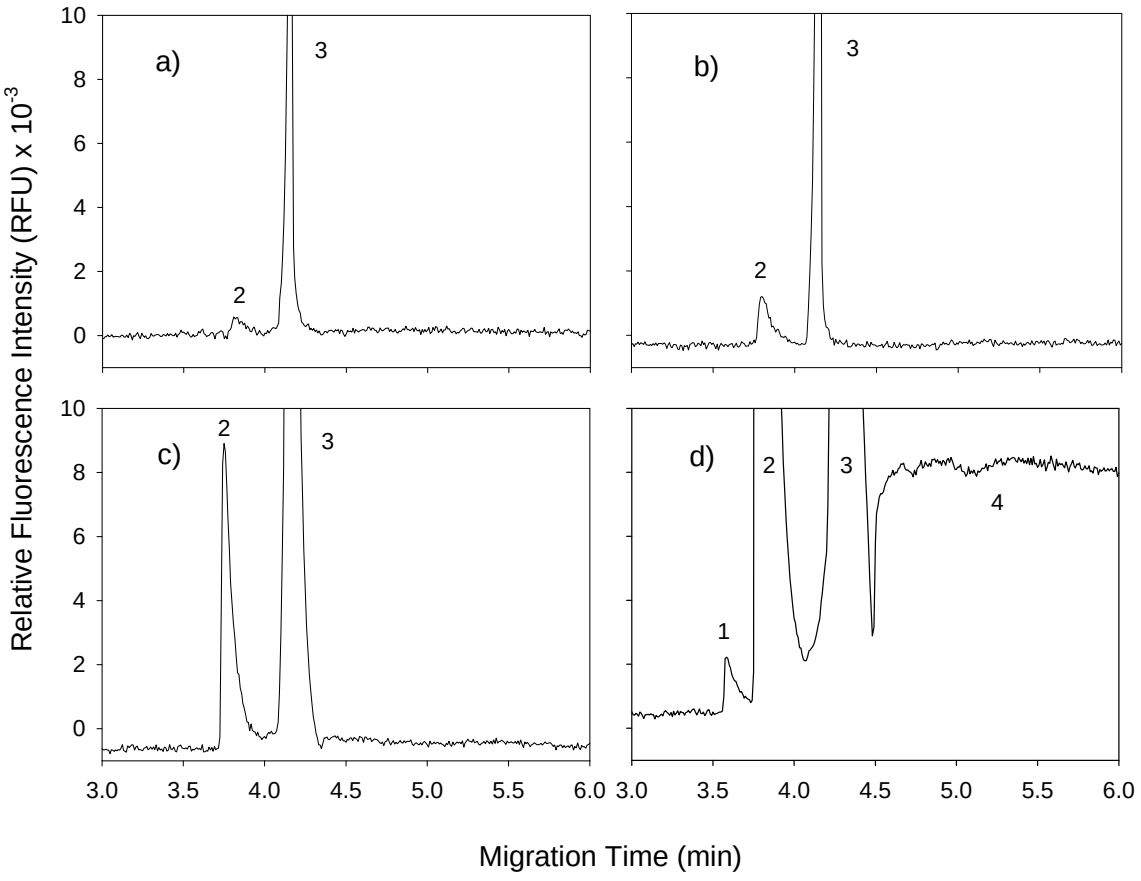

Figure 6.4. Concentration effect on aggregation in CE. BHmC-O_3 in methanol; a) 0.54, b) 3.27, c) 20, and d) 160 uM, respectively. peak 1 and 2: J-type intra-dimer (closed clamshell form), peak 3: open form, peak 4: J-type aggregate. Condition: 3 second pressure injection (0.5 psi), 23 kV applied voltage, 75 um x 57 cm capillary; 100 mM borate at pH 9.0.

Figure 6.4. shows the influence on formation of BHmC-O_3. At low concentration (0. 54 uM), marked peak 3 is observed. Increasing concentration of the dye, the population of peak 2 is enhanced. More interestingly, peak 1 and 4 are appear at 160 uM, meaning that various dye

aggregates exist and their conformations control their mobilities as represented in Figure 6.3..

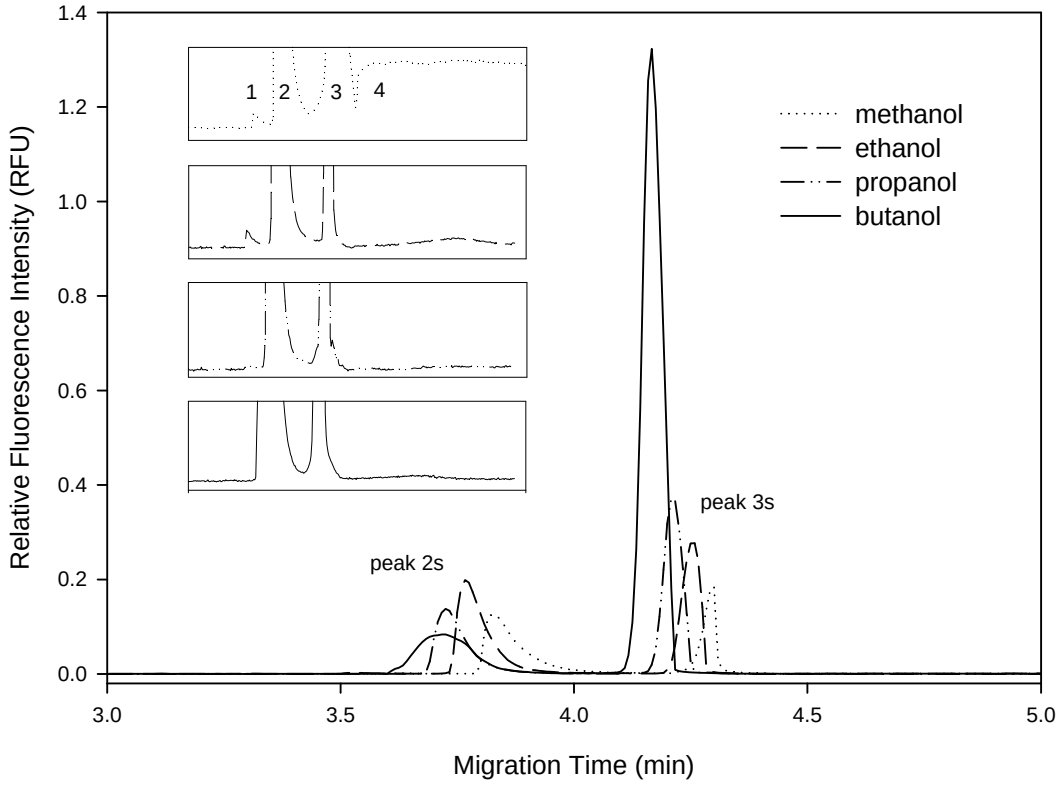

Figure 6.5. Organic solvent composition effect in aspect of dielectric constant and dipole moment. For all sample injections, BHmC-O_3 (160 uM) was dissolved in alkyl alcohol series, methanol, ethanol, propanol and butanol. Small windows indicate zoomed data. peak 1 and 2: J-type intra-dimer (closed clamshell form), peak 3: open form, peak 4: J-type aggregate. Condition: 3 second pressure injection (0.5 psi), 23 kV applied voltage, 75 um x 57 cm capillary; 100 mM borate at pH 9.0.

For solvent effect on aggregation, alkyl alcohols having different dipole moment and dielectric constant are applied in Figure 6.5.. Generally, it is accepted that solvents having higher dipole moment and dielectric constant strongly influence dye aggregation since those solvents have positively charged cyanine dyes distributed and shrink their geometrical conformation.[29-31] In other word, solvents having less polarity facilitate the breakup aggregates. Figure 6.5. shows that the aggregates are broken up upon decrease of dipole moment and dielectric constant.[32] However, these solvents are not strongly influenced

regarding J-type intra-dimer. It is presumably due to similar reason as the study of Chowdhury, A. *et al*. that a dimer has stronger stack coupling than the aggregates.[20] The emission lambda maxes in those four alcohol solvents were slightly different in spectral measurement (data not shown).

	Butanol >	Propanol >	Ethanol >	Methanol >	Water
Dipole moment	1.66	1.68	1.69	1.70	1.85
Dielectric constant	17.8	20.1	24.3	33.0	78.0
	less polarity				high polarity

In mobility aspect, Miklós Idei *et al*. have reported that organic solvents affect the pK of the silanol groups of the capillary and they shift the pK towards higher pH values.[17] This shift results in weaker dissociation of the silanol groups and decrease of the electroosmotic flow (EOF). However, in the study of BHmC-O_3, this phenomenon is reversed since a longer alkyl alcohol prevents the capillary interaction caused by two positive charged BHmC-O_3, resulting in faster mobility in butanol. Moreover, the dielectric constant and dipole moment of butanol open up the closed clam-shell form and increase fluorescence compared to the other alcohols.

We investigated the aqueous solution composition effect on the closed and open form of BHmC-O_3. For this study, all concentrations of individual BHmC-O_3 were maintained at 20 uM in different aqueous solvent ratio of sample solution. As shown in Figure 6..4. and 6.6., this concentration merely has two peaks; peak 2 for closed form and peak 3 for open form. In accordance with organic solvent effect on close clamshell form, these solvent ratio changes affect no conformational modification up to 60 % addition of phosphate, and the fluorescence of open form is decreased. This fluorescence quenching effect is due to formation of H-

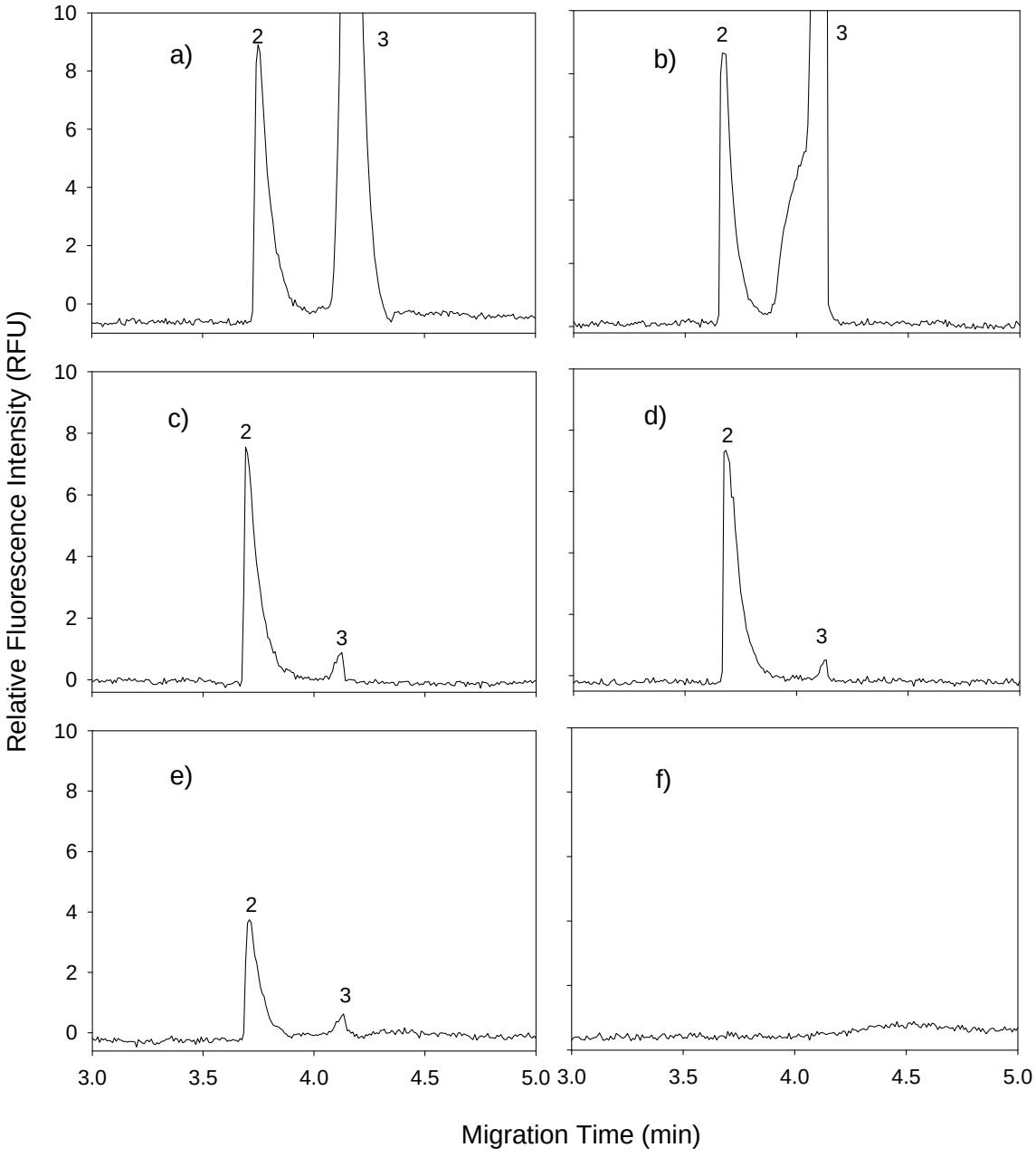

Figure 6.6. Influence of aqueous solvents ratio in sample. 20 uM of BHmC-O_3 are maintained for all measurement. Aqueous solvent compositions with methanol are 0 (a), 20 (b), 40 (c), 60 (d), 80 (e), and 100 (f) % (v/v), respectively. peak 2: J-type intra-dimer (closed clamshell form), peak 3: open form. Condition: 3 second pressure injection (0.5 psi), 23 kV applied voltage, 75 um x 57 cm capillary; 100 mM borate at pH 9.0.

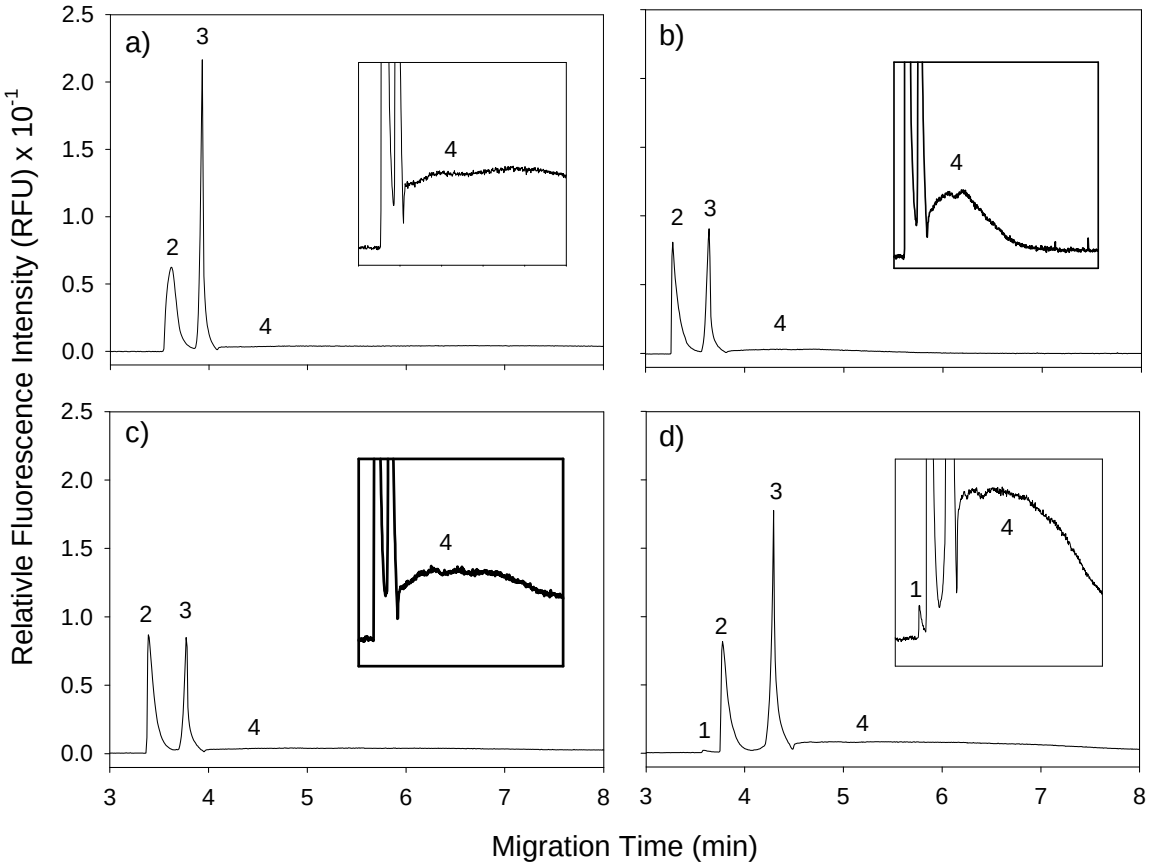

Figure 6.7. Running buffer effect on aggregation. Constant dye concentrations (160 uM) are used. Running buffer: a; 20 mM phosphate (pH 7.2), b; 20, c; 50 and d; 100 mM borate (pH 9.0). peak 1 and 2: J-type intra-dimer (closed clamshell form), peak 3: open form, peak 4: J-type aggregate. Condition: 3 second pressure injection (0.5 psi), 23 kV applied voltage, 75 um x 57 cm capillary.

aggregates of open BHmC-O_3. Finally, in 100 % presence of phosphate, the fluorescence is almost completely quenched.

In order to study possible additional effects on aggregation conditions normally formed in electrophoresis, various running buffers and voltages were applied. The running buffers in CE commonly change the mobilities of sample solutes and provide specific sample stacking zone. The differentiation of running buffer in Figure 6.7.(a) shows that using 20 mM phosphate obtains better resolution, peak symmetry and efficiency, and the other conditions

provide distorted and broadened peaks. Yet, 100 mM borate buffer only provides 4 characteristic peaks (Fig. 6.7d). It is because the other buffers are relatively low ionic strength so that H-type aggregates are facilitated and higher ionic borate buffer (100 mM) produces stronger sample stacking. Meanwhile, voltage influences are studied in Figure 6.8. Resolution is affected but not the change of formation of BHmC-O_3.

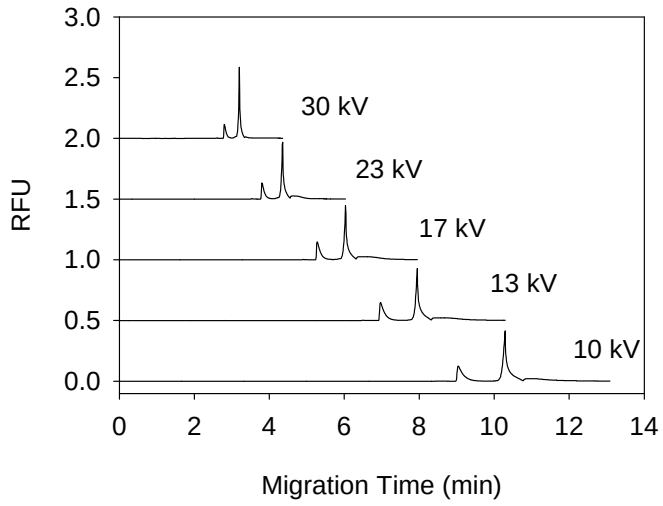

Figure 6.8. Effect of applied voltages. Five different voltages were applied for the separation of BHmC-O3 (160 uM). Condition: 3 second pressure injection (0.5 psi), 75 um x 57 cm capillary; 100 mM borate at pH 9.0.

6.3.3 Fluorescent enhancement of BHmC-O_3 by HSA and AO

Cyanine dyes that aggregate have two distinct photophysical properties, H- and J-aggregates. H-aggregates exhibit negligible fluorescence that makes them possible to use for fluorescent enhancement by interaction with biomolecules, such as DNA, proteins, etc. In contrast, J-aggregates exhibit red-shifted sharp fluorescence that can be used for quenching study. Here we used the character of H-aggregates.

In the previous studies, our group has evaluated the interaction of BHmC-4, -6, -8, -10 and -12 with human serum albumin (HSA).[1, 2] Likewise, HSA-BHmC-O_3 complex was

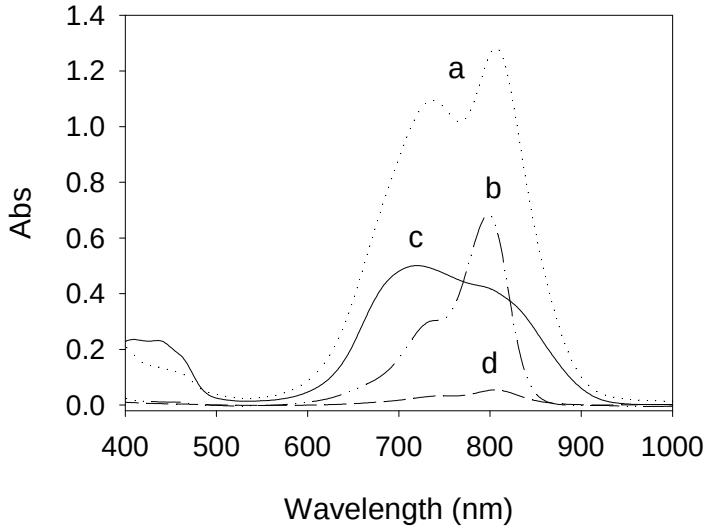

Figure 6.9. Absorbance spectra. a): HSA (10 uM)-BHmC-O_3 (10 uM) complex in 20 mM phosphate, pH 7.2, b): 2 uM BHmC-O_3 in methanol, c): 10 uM BHmC-O_3 in 20 mM phosphate, pH 7.2, d) HSA (1 uM)-BHmC-O_3 (1 uM) complex in 20 mM phosphate, pH 7.2.

prepared in phosphate to evaluate dye interaction with HSA. It can be understood that the net charge of HSA (pI 4.8) in pH 7.2 phosphate is negative, resulting in the interaction of BHmC-O_3 to the surface of HSA. Alternatively, the predominant binding of BHmC-O_3 with hydrophobic cavities of HSA can not be excluded since lysine in HSA predominantly exists relative to other amino acids and the pKa of lysine is 10.4 that promote the repulsion of positively charged BHmC-O_3 from the surface. In the absence of HSA, BHmC-O_3 strongly forms H-type closed conformation or aggregates at around 707 nm (Fig 6.9.) and exhibit negligible fluorescence like other BHmCs. Upon addition of HSA, BHmC-O_3 is open up its aggregates and increases absorptivity for monomer open form, whereas it exhibits similar low fluorescence as BHmC-6, which strongly forms H-type intra-dimer, *see* Figure 6.10. for fluorescence measurement.

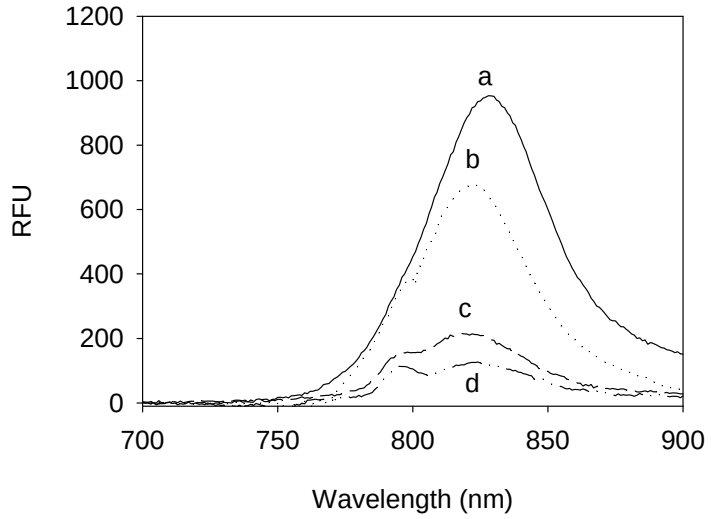

Figure 6.10. Fluorescence spectra. Concentration of BHmC-O_3 in methanol: a); 2, c); 0.4 uM. Concentration of dye-HSA complex in 20 mM phosphate, pH 7.2: c) HSA (10 uM)-BHmC-O_3 (10 uM), d) HSA (1 uM)-BHmC-O_3 (1 uM).

The combination of borate running buffer and dye sample dissolved in phosphate buffer essentially exhibits negligible fluorescence in Figure 6.6. (f). In this study for dye-HSA complex, the same condition was applied since it is possible that background fluorescence from other aqueous solutions can interrupt the further separation of the dye–biomolecule complexes. Generally, it is accepted that high pH and low ionic strength of running buffer prevent protein adsorption to capillary wall.[3, 4] However, as can be seen in Figure 6.11., 100 mM borate running buffer provides better separation efficiency than the others. For the same reason in Figure 6.7., it is owing to the strong sample stacking zone by high ionic strength and pH in capillary. In contrary, no complex peak is detected under phosphate running buffer. It means that the strong dye aggregates formed in phosphate running buffer are hardly deformed upon the addition of HSA.

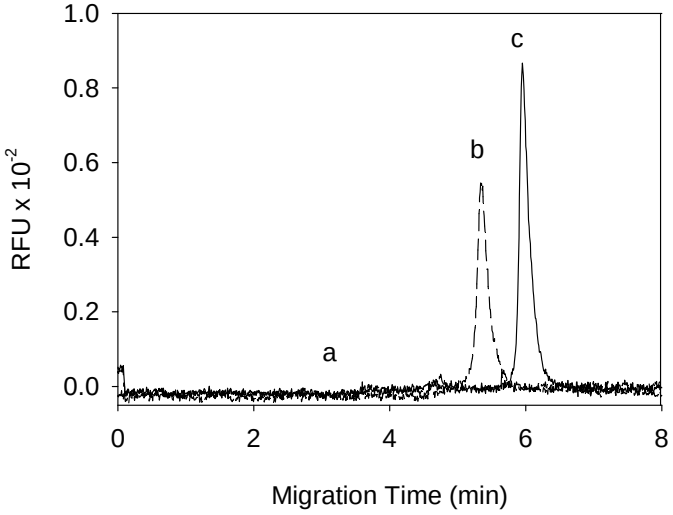

Figure 6.11. Efficient separation of dye-HSA complex. Three different running buffers are used to optimize CE separation for complex; a) 20 mM phosphate, pH 7.2, b) 20 mM borate, pH 9.0, c) 100 mM borate, pH 9.0. Individual injection was applied for on-column interaction of dye and HSA. First sample injection: 10 uM HSA is loaded for 2s (0.5 psi). Second sample injection: 20 uM BHmC-O_3 dissolved in PB is loaded for 3s (0.5 psi). 23 kV applied voltage, 75 um x 57 cm capillary.

Figure 6.12. represents another fluorescence enhancement of BHmC-O_3. For this particular experiment, we hypothesized that addition of flat molecule is able to intercalate to J-type intra-dimer and break up the π-π stacking, resulting in enhanced fluorescence quantum yield. To prove this hypothesis, acridine orange (AO) was added. Since AO is relatively hydrophobic, it was not able to completely rule out that AO can interact with capillary and exterior of the intra-dimer instead of interior. However, the rigid conformation of J-type dimer was not markedly changed its property upon addition of AO, whereas significant changes of mobility and peak area of open form were observed. It is because the running buffer in CE still strongly affects on the conformation of intra-dimer. Moreover, those changes disprove that AO is intercalated into BHmC-O_3 that is not completely open, and higher concentration (11.7 mM) of AO changes the conformation of J-type intra-dimer. The increase of AO concentration significantly changes the migration time and peak area of J-type

intra-dimer, *see* Table 6.1.. Table 6.1. shows the migration time and relative peak area. In Figure 6.13., the ratio of peak area is plotted for individual peak. Since the fluorescence of open BHmC-O_3 is enhanced by lengthening carbon chain in alkyl alcohols, butanol is added for convenient comparison. The dotted square indicates the saturation of AO in BHmC-O_3. indicates the tolerant number of insertion of AO. Under relatively higher concentration (5.8 mM) of AO, peak shapes can be distorted.

Table 6.1. The comparison of migration time and relative peak areas.

	Migration Time (min)			Relative Peak Area [a]		
AO (mM)	peak 1	peak 2	peak 3	peak 1	peak 2	peak 3
0.0	3.75	3.96	4.28	1.00	1.00	1.00
0.7	3.80	3.99	4.35	1.18	1.18	3.28
1.5	3.83	4.03	4.43	1.08	1.22	3.54
3.0	3.84	4.08	4.53	1.20	1.24	3.59
5.8	3.82	4.04	4.72	1.74	1.36	2.63
11.7	3.83	4.05	5.02	1.21	1.42	2.23
butanol	-	3.73	4.18	-	0.92	5.51

[a] BHmC-O_3 in methanol (0 mM AO) was used as a reference sample, and other peak areas of analytes are divided by the reference.

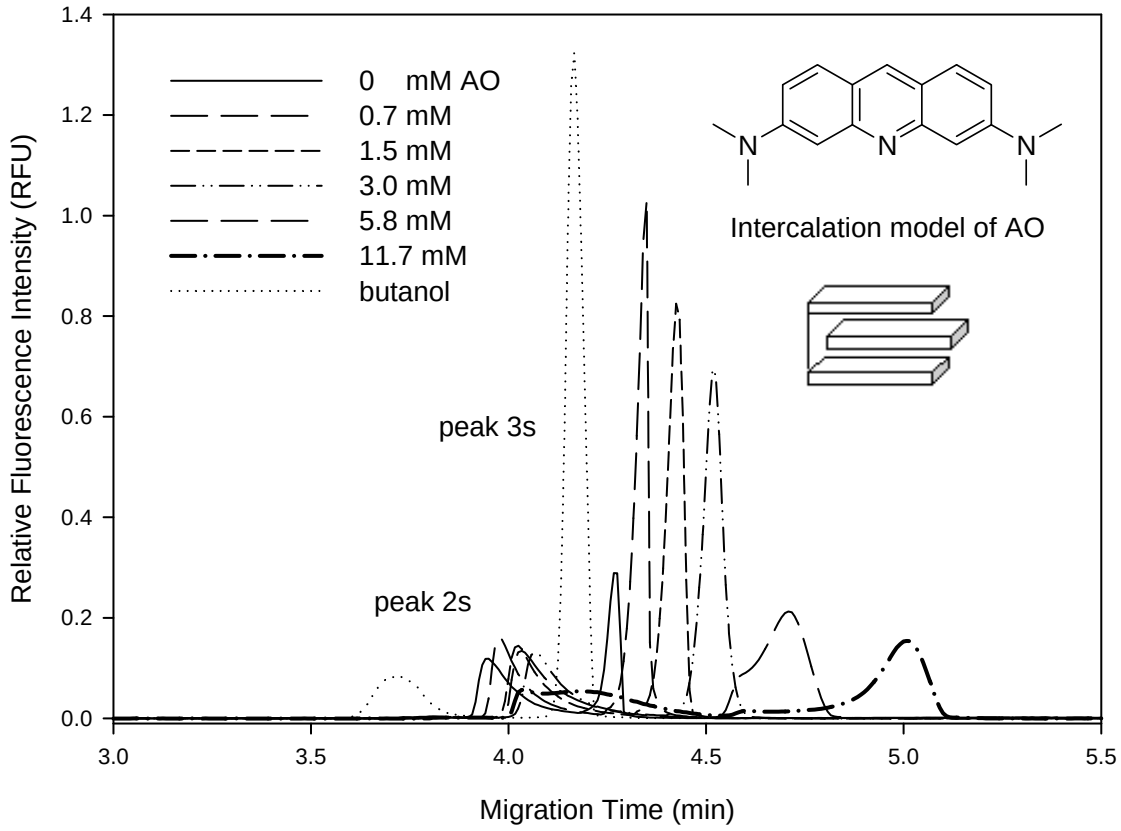

Figure 6.12. Intercalation of acridine orange (AO). Various concentrations of AO were loaded for 2s (0.5 psi), followed by BHmC-O_3 for 3s (0.5 psi). All samples were dissolved in methanol. BHmC-O_3 in butanol is added for the comparison of complete open form with intercalated open form. peak 2: J-type intra-dimer (closed clamshell form), peak 3: open form. Condition: 23 kV applied voltage, 75 um x 57 cm capillary; 100 mM borate at pH 9.0. All the concentrations of BHmC-Os are 160 uM in methanol.

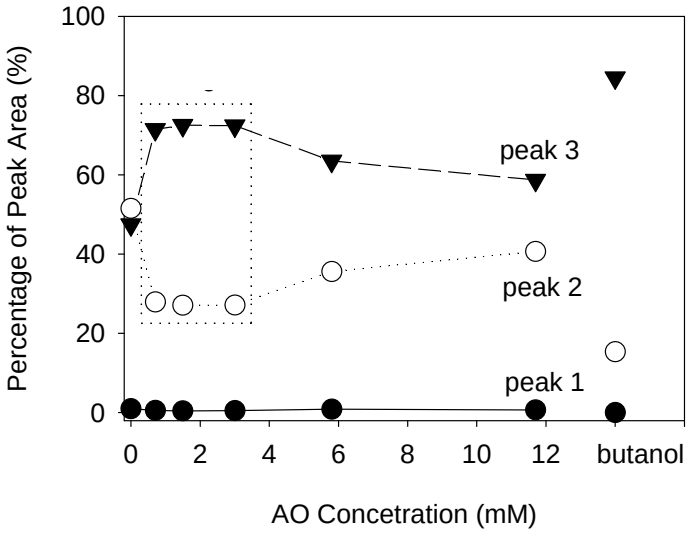

Figure 6.13. Ratio of peak areas. Percentages of peak areas are calculated by the ratio of individual peak. Symbols indicate peak 1 (●), 2 (○) and 3 (▼) in individual peak. Dotted square shows the saturation of AO in BHmC-O_3.

4. Conclusion

Newly synthesized BHmCs have various possibilities to their use as a bioanalytical tool and other environmental influence measurement. By comparing them with their monomeric counterpart, spectral properties were understood in previous reports. In this study, all the solvents used for running buffer and sample solution verify the strong stacking coupling of intra-dimer and they produces other types of aggregates that can be overlapped to open monomer band. CE using aqueous run buffer facilitates their separation depending on conformational mobilities. Moreover, the composition of aqueous buffers provides other interruption generated by intrinsic fluorescence by dye itself or biomolecules. For further application of BHmC-O_3, HSA and AO have been applied and BHmC-O_3 reveals its highly sensitive response on the environmental changes. In case of the addition of HSA, its fluorescence is strongly affected by buffer composition and the study of the insertion of AO

provides the technical merits for the study of micromolecules. So far, there have been some bis-dyes, TOTO-1, YOYO-1 and so on, for DNA intercalation and they have had no significant application for the other studies due to the characters of their relatively small counterparts. However, BHmC-O_3 will arouse one's interest since it has various conformations dependent on environment and can be used for the study of macro- and micromolecules by using its characteristic conformations.

References

1. Patonay, G.; Kim, J. S.; Kodagahally, R.; Strekowski, L., Spectroscopic study of a novel bis(heptamethine cyanine) dye and its interaction with human serum albumin. *Appl Spectrosc* **2005,** 59, (5), 682-90.

2. Kim, J. S.; Kodagahally, R.; Strekowski, L.; Patonay, G., A study of intramolecular H-complexes of novel bis(heptamethine cyanine) dyes. *Talanta* **2005,** 67, (5), 947-954.

3. Landers, J. P., *Handbook of Capillary Electrophoresis* 2nd ed.; CRC press: Boca Raton, FL, 1997.

4. Kitagishi, K., *Handbook of Capillayr Electrophoresis Applications*. Blackie Academic and Professional: London, U. K., 1997.

5. Rickard, E. C.; Strohl, M. M.; Nielsen, R. G., Correlation of electrophoretic mobilities from capillary electrophoresis with physicochemical properties of proteins and peptides. *Anal Biochem* **1991,** 197, (1), 197-207.

6. Basak, S. K.; Velayudhan, A.; Kohlmann, K.; Ladisch, M. R., Electrochromatographic separation of proteins. *J Chromatogr A* **1995,** 707, 69-76.

7. Basak, S. K.; Ladisch, M. R., Correlation of electrophoretic mobilities of proteins and peptides with their physicochemical properties. *Anal Biochem* **1995,** 226, (1), 51-8.

8. Adamson, N. J.; Reynolds, E. C., Rules relating electrophoretic mobility, charge and molecular size of peptides and proteins. *J Chromatogr B Biomed Sci Appl* **1997,** 699, (1-2), 133-47.

9. Overbeek, J. T. G.; Wiersema, P. H., *Electrophoresis, Theory, Methods and Applications*. Academic Press: New York, 1967.

10. Edward, J. T., *Advances in Chromatography*. Marcel-Dekker: New Y.

11. Heimez, P. C., *Principles of Colloid and Surface Chemistry*. Marcel-Dekker: New

York, 1977.

12. Grossman, P. D.; Colburn, J. C.; Lauer, H. H., A semiempirical model for the electrophoretic mobilities of peptides in free-solution capillary electrophoresis. *Anal Biochem* **1989,** 179, (1), 28-33.

13. Grossman, P. D.; Colburn, J. C.; Lauer, H. H.; Nielsen, R. G.; Riggin, R. M.; Sittampalam, G. S.; Rickard, E. C., Application of free-solution capillary electrophoresis to the analytical scale separation of proteins and peptides. *Anal Chem* **1989,** 61, (11), 1186-94.

14. Grossman, P. D.; Soane, D. S., Orientation effects on the electrophoretic mobility of rod-shaped molecules in free solution. *Anal Chem* **1990,** 62, (15), 1592-6.

15. Tanford, C. H., *Physical Chemistry of Macromolecules*. Wiley: New York, 1961.

16. Offord, R. E., Electrophoretic mobilities of peptides on paper and their use in the determination of amide groups. *Nature* **1966,** 211, (5049), 591-3.

17. Idei, M.; Kiss, E.; Dobos, Z.; Hallgas, B.; Meszaros, G.; Hollosy, F.; Keri, G., Separation of anti-tumor peptides by capillary electrophoresis in organic solvent containing background electrolytes. *Electrophoresis* **2003,** 24, (5), 829-33.

18. Baars, M.; Patonay, G., Ultrasensitive detection of closely related angiotensin I peptides using capillary electrophoresis with near-infrared laser-induced fluorescence detection. *Anal Chem* **1999,** 71, (3), 667-71.

19. Seifert, J. L.; Connor, R. E.; Kushon, S. A.; Wang, M.; Armitage, B. A., Spontaneous Assembly of Helical Cyanine Dye Aggregates on DNA Nanotemplates. In 1999; Vol. 121, pp 2987-2995.

20. Chowdhury, A.; Wachsmann-Hogiu, S.; Bangal, P. R.; Raheem, I.; Peteanu, L. A., Characterization of Chiral H and J Aggregates of Cyanine Dyes Formed by DNA Templating Using Stark and Fluorescence Spectroscopies. In 2001; Vol. 105, pp 12196-12201.

21. Zollinger, H., *Color Chemistry: Syntheses, Properties, and Applications of Organic*

Dyes and Pigments. 2nd ed. ed.; VCH Publishers: New York, 1991.

22. Brooker, L. G. S., White, F. L. , Heseltive, D. W. , Keyes, G. H. , Dent, the late S. G. , and Van Lare, E., Spatial configuration, light absorption and sensitizing effects of cyanine dyes. *J. Photogr. Sci.* **1953,** 1.

23. Herz, A. H., Dye-Dye interactions of cyanines in solution and at silver bromide surfaces. *Photogr. Sci. Eng.* **1974,** 18.

24. Eion, G. M.; Michael, K., Enhancement of Phosphorescence Ability upon Aggregation of Dye Molecules. In AIP: 1958; Vol. 28, pp 721-722.

25. Kasha, M., Energy Transfer Mechanisms and the Molecular Exciton Model for Molecular Aggregates. *Radiat. Res.* **1963,** 20.

26. MeRae, E. G.; Kasha, M., *Physical Processes in Radiation Biology*. Academic Press: New York, 1964.

27. Wang, M.; Silva, G. L.; Armitage, B. A., DNA-Templated Formation of a Helical Cyanine Dye J-Aggregate. In 2000; Vol. 122, pp 9977-9986.

28. Daltrozzo, E.; Scheibe, G.; Gschwind, K.; Haimerl, F., On the structure of the J-aggregates of pseudoisocyanine. *Photographic Science and Engineering* **1974,** 18.

29. West, W.; Pearce, S., The Dimeric State of Cyanine Dyes. In 1965; Vol. 69, pp 1894-1903.

30. Valdes-Aguilera O; Neckers D. C., Aggregation phenomena in xanthene. dyes. *Acc Chem Res* **1989,** 22.

31. Neckers, D. C.; Valdes-Aguilera, O., *Photochemistry of the xanthene dyes*. John Wiley & Sons: New York, 1993; Vol. 18.

32. Huang, Y.; Cheng, T.; Li, F.; Luo, C.; Huang, C. H.; Cai, Z.; Zeng, X.; Zhou, J., Photophysical Studies on the Mono- and Dichromophoric Hemicyanine Dyes II. Solvent Effects and Dynamic Fluorescence Spectra Study in Chloroform and in LB Films. In 2002;

Vol. 106, pp 10031-10040.